MOLECULAR FUNCTIONAL ANALYSIS OF THE TUMOR SUPPRESSOR GENE PDCD4

Westfälische Wilhelms-Universität and

International NRW Graduate School of Chemistry

Muenster, Deutschland

Rajeshwari Marikkannu

From

Eriyodu, Tamil Nadu, India

October-2006

Biochemie

MOLECULAR FUNCTIONAL ANALYSIS OF THE TUMOR SUPPRESSOR GENE PDCD4

Inaugural-Dissertation
zur Erlangung des Doktorgrades
der Naturwissenschaften
in der NRW Graduate School of Chemistry
im Fachbereich Chemie und Pharmazie
der Mathematisch-Naturwissenschaftlichen Fakultät
der Westfälischen Wilhelms-Universität Münster

vorgelegt von
Rajeshwari Marikkannu

aus
Eriyodu, Tamil Nadu, Indien

Oktober-2006

Dekan	**: Prof. Dr. F. Ekkehardt Hahn**
Erster Gutachter	**: Prof. Dr. Karl-Heinz Klempnauer**
Zweiter Gutachter	**: Prof. Dr. Hans-Joachim Galla**
Tag der mündlichen Prüfung	**: 15. November 2006**
Tag der Promotion	**: 15. November 2006**

To

the nature.....

the undeniable nature.....

the four seasons.....

the rain in the four seasons.....

the transition between the four seasons.....

the human race, who continuously battle against and constantly falling and raising again.....

There was a bad blot in my day.....

There was a fine blot in my day as well.....

The Metamorphosis.....

M.C Eischer, Dutch,1898-1972

TABLE OF CONTENTS

ABBREVIATIONS

1D	First dimension
2D	Second dimension
2D-SDS-PAGE	Two dimensional sodium dodecyl sulfate polyacrylamide gel electrophoresis
A	Adenine base and the corresponding nucleotide
aa	Amino acid
Ab	Antibody
AKR1	Aldo keto reductases family 1
APS	Ammonium persulfate
AraC	Cytosine arabinoside
ATF	Activating transcription factor
ATP	Adenosine triphosphate
AMP^r	Ampicillin-resistant gene
bp	Base pairs
BSA	Bovine serum albumin
C/EBP	CCAAT/enhancer-binding protein
cAMP	Cyclic adenosine monophosphate
CBB	Coomassie brilliant blue
CK-8	Cytokeratin-8
CK-17	Cytokeratin-17
CMV	Cytomegalovirus
Cpdcd4	Chicken programmed cell death 4 protein
Cpdcd4	Chicken programmed cell death 4 gene
C	Cytosine base and the corresponding nucleotide
dd	Double distilled
DNA	Deoxyribonucleic acid
dNTP	Desoxynucleotide
DTT	1,4-Dithio-DL-threitol
E.coli	*Escherichia coli*
EDTA	Ethylene diamine tetraacetate
eIF	Eucaryotic initiation factor
EMS	Ethyl methane sulphonate
Fig	Figure
GluProRS	Glutamyl prolyl bifunctional tRNA synthetase
G	Guanine base and the corresponding nucleotide
hr	Hour(s)

HBS	HEPES buffered saline
HEPES	4-(2-hydroxyethyl)-piperazin-1-ethansulfonic acid
Hpdcd4	Human programmed cell death 4 protein
Hpdcd4	Human Programmed cell death 4 gene
IEF	Isoelectric focusing
IgG	Immunoglobulin subtype G
IMDM	Iscoves modified Eagles Medium
IPG	Immobiline pH gradient
IPTG	Isopropyl-β-D-thiogalactopyranoside
IRES	Internal ribosome entry site
ITAF	IRES-*trans*-acting factor
JNK	Jun N-terminal kinase
Kb	Kilo basepairs
kDa	Kilo dalton
LB	Luria bertani
M	mole/L
mA	Milli ampere
MA-3	Mouse apoptotic-3 domain
min	minutes
ml	Milli litre
MMC	Mitomycin C
mRNA	Messenger RNA
NES	Nuclear export signal
NLS	Nuclear localization signal
NMD	Nonsense-mediated mRNA decay
NP-40	Nonidet P-40
nt	Nucleotide
OD_{λ}	Optical density at wavelength λ
PAGE	Polyacrylamide gel electrophoresis
PBS	Phosphate buffered saline
Pdcd4	Programmed cell death 4 protein
Pdcd4	Programmed cell death 4 gene
PTGS	Posttranscriptional gene-silencing
RNA	Ribonucleic acid
RNAi	RNA interference
RNAse	Ribonuclease
RNA pol II	RNA polymerase II
rpm	Rotations per minute

rRNA	Ribosomal RNA
RT	Room temperature
sec	Second
SDS	Sodium dodecyl sulfate
siRNA	Small-interfering RNA
SSP	Staurosporine
tRNA	Transfer RNA
TAE	Tris /Acetatic acid / EDTA
Taq	*Thermus aquaticus*
TBE	Tris /Boric acid / EDTA
TEMED	*N,N,N',N'*-tetramethylethylendiamine
TE	Tris/EDTA
TF	Transcription factor
T	Thymine base and the corresponding nucleotide
Tm	Melting temperature
TPA	Tetradecanoyl-phorphol-acetate
Tris	Tris(hydroxymethyl)-aminoethane
U	Units
V	Volt
(v/v)	Volume percentage per total volume
WT	Wild-type
(w/v)	Weight percentage per total volume
X-Gal	5-Bromo-4-chloro-3-indolyl-β-D-galactopyranoside
β-Gal	β-Galactosidase
µl	Micro litre
(-/-)	Double mutant of any gene
(+/-)	Single mutant of any gene

1 SUMMARY

Cancer is one of the major causes of mortality and challenges the human race in the last few decades. Cancer is a disease involving dynamic changes in the genome. The genomes of the cells are constantly altered at multiple sites. Two types of genes are invariably targeted during the tumor development, which are oncogenes and tumor suppressor genes.

The Programmed Cell Death 4 gene (*Pdcd4*) is a novel tumor suppressor gene originally identified as a gene upregulated during apoptosis. It has been shown that Pdcd4 suppresses the tumor promoter TPA induced transformation of keratinocytes. Because Pdcd4 interacts with eucaryotic translation initiation factor eIF4A, it was suggested that Pdcd4 might be involved in controlling the translation of certain, as yet unknown proteins. However, lack of a well-characterized cell system hampers the analysis of molecular functions of Pdcd4.

To study the molecular functions of the Pdcd4 tumor suppressor gene by a reverse genetic approach, a knock-down system was developed. The system was generated by employing the RNAi technology mediated via siRNA directed against the human Pdcd4 gene (*Hpdcd4*) in HeLa cells. Dual luciferase constructs containing different Internal Ribosome Entry Site Elements (IRES) of genes involved in cell growth, cell cycle control and apoptosis were used to study the effect of Hpdcd4 on cap-independent translation and thereby to function as a cell-growth/death regulator. The results obtained show that Pdcd4 acts in an inhibitory manner on several IRES elements under normal physiological conditions.

The 1D-SDS-PAGE analysis showed that the expression of several transcription factors was affected by Hpdcd4. While c-Myc expression was lower, c-Jun and C/EBPβ expression was higher in the absence than in the presence of Hpdcd4. Additionally, in the Hpdcd4 knock-down cells phosphorylation of ATF-2 and c-Jun were less efficient compared to the HeLa wild-type (WT) cells. To identify novel molecular targets of Hpdcd4 in a holistic way, a proteomic approach was performed using 2D-SDS-PAGE followed by mass spectrometry of HeLa WT and Hpdcd4 knock-down cells. Thereby, several novel targets of Hpdcd4 were identified. In the absence of Hpdcd4, cytokeratin-17 (CK-17) as well as Aldo Keto Reductase 1 (AKR1) family members C2 and C3 were overexpressed. In addition, cytokeratin-8 (CK-8) and Glutamyl Prolyl Bifunctional tRNA synthetase (GluProRS) appeared to be biochemically modified in the Pdcd4 knock-down cells compared to the HeLa WT cells. The differential expression of

these target proteins was confirmed by 1D/2D-SDS-PAGE followed by immunoblotting with specific antibodies. The overexpression of CK-17 and the biochemical modification of CK-8 in the absence of Hpdcd4 were reproducible. The identity of AKR1C2 and C3 as well as GluProRS is yet to be assessed and proved as potential targets of HPdcd4.

It was also investigated whether Hpdcd4 has an effect on the mRNA level of CK-17, c-Myc and c-Jun. The mRNA expression level of these genes was consistent with the respective protein expression except for c-Jun. It was further analyzed whether Hpdcd4 is influencing the transcription or the stability of the mRNA transcripts. To analyze the effect of Hpdcd4 on the turn-over of the CK-17 and the c-Myc mRNAs, cells were treated with a transcription-inhibitor actinomycin-D and mRNA levels were analyzed by northern blotting in a time-dependent manner. It appeared that Hpdcd4 is enhancing the degradation of CK-17 and c-Myc mRNA transcripts. In addition to that Hpdcd4 seems to be involved in nonsense-mediated mRNA decay.

In addition to the HeLa knock-down system, in the chicken B-cell line DT40, a Pdcd4 knock-out model has been developed wherein both functional copies of the gene were eliminated by homologous recombination. It was shown that chicken Pdcd4 knock-out cells are viable and grow with the same doubling time as DT40 WT cells. However, there was no difference in the overall rate of protein synthesis between knock-out and WT cells. The two systems developed in the present work will be useful in further elucidating the molecular functions of tumor suppressor Pdcd4 by utilizing the molecular targets identified here.

2 INTRODUCTION

2.1 Cancer

2.1.1 Cancer Statistics

Cancer is the uncontrolled growth and spread of cells that may affect almost any tissue of the body. People are affected by lung, colorectal and stomach cancers which are among the five most common cancers in the world. While men are mostly affected by lung and stomach cancer, breast and cervical cancers are most common among women worldwide (WHO, 2006).

More than 11 million people are diagnosed with cancer every year. It is estimated that there will be 16 million new cases every year by 2020. Cancer causes 7 million deaths every year (12.5%) worldwide (WHO, 2006). The cancer statistics necessitates the inevitability of the focus of scientific research towards cancer aimed at reducing causes and consequences of cancer. Although the causes of cancer are at the genetic level, understanding the cancer cell physiology is also essential to unknot the complexity of cancer. Over the past 25 years cancer research has developed a rich body of information about cancer cell physiology and eventually it has been transferred into knowledge and several rules are made to codify it. The rules are explained in the following section.

2.1.2 Cancer Cell Physiology

A quarter century of rapid advances in cancer research characterized a vast catalog of cancer cell genotypes. However, there are six essential alterations in cell physiology that collectively dictate malignant growth which are: self-sufficiency in growth signals, insensitivity to growth-inhibitory (antigrowth) signals, evasion of programmed cell death (apoptosis), limitless replicative potential, sustained angiogenesis, and tissue invasion and metastasis (Fig.1) (Hanahan and Weinberg, 2000). Almost all types of human tumors share these six capabilities. During tumor development, each of these physiological changes is acquired. The six acquired capabilities of cancer cells are discussed in detail.

Self-Sufficiency in Growth Signals

Normal cells require mitogenic growth signals before they can move from a quiescent state into an active proliferative state. These signals are transmitted into the cell by transmembrane receptors that bind distinctive classes of signaling molecules: diffusible growth factors, extracellular matrix components, and cell-to-cell adhesion/interaction

molecules. Tumor cells generate their own growth signals, thereby largely reducing their dependence for such exogenous growth stimulation. This disrupts the homeostatic mechanisms within the cells and the tissue environment. Although many oncogenes modulate this acquired growth signal autonomy, the SOS-Ras-Raf-MAPK cascade is proved to play a central role.

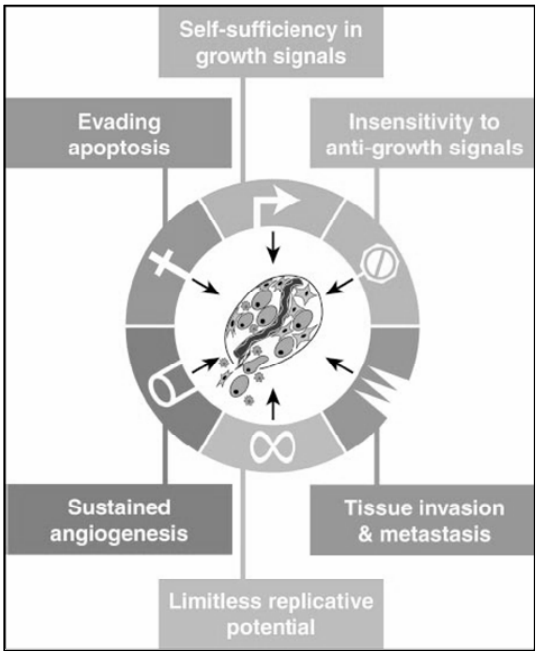

Figure 1: Acquired capabilities of the tumor cells (Hanahan and Weinberg, 2000)

Most of the cancer cells acquire these six functional capabilities through various mechanistic strategies and during various time periods of the tumor development.

Insensitivity to Antigrowth signals

Multiple anti-proliferative signals operate within a tissue to maintain cellular quiescence and tissue homeostasis. These signals include both soluble growth inhibitors and immobilized inhibitors embedded in the extracellular matrix and on the surfaces of nearby cells. These growth-inhibitory signals are received by transmembrane cell surface receptors coupled to intracellular signaling circuits. Antigrowth signals can block proliferation by two distinct mechanisms. They force the cells from the active proliferative cycle into the quiescent (G_0) state. Alternatively, they induce cells to enter into post-mitotic states, usually differentiation. Much of the circuitry that enables normal cells to respond to antigrowth signals is associated with the cell cycle clock. The cancer cells evade these anti-proliferative signals to prosper uncontrollably. Several tumor suppressor genes function at this level. Moreover, all anti-proliferative signals are funneled through the retinoblastoma protein and the related proteins p107 and p130.

Evading Apoptosis

The expansion of tumor cell population is determined not only by the rate of cell proliferation but also by the rate of cell death. Programmed cell death, apoptosis represents a major source for limiting the cell number. Once triggered by a variety of physiologic signals, apoptosis unfolds in a precisely choreographed series of steps. In a span of 30-120 min, cellular membranes are disrupted, the cytoplasmic and nuclear skeletons are broken down, the cytosol is extruded, the chromosomes are degraded, and the nucleus is fragmented. Eventually, the shriveled cell corpse is engulfed by nearby cells in a tissue and disappears, typically within 24 hr (Wyllie et al., 1980).

The apoptotic program can be broadly divided into three classes of components, the signals, sensors and effectors. Apoptotic signals include the survival and death factors influencing the cell from the extra- and intracellular environment. The survival signals are conveyed by the insulin-like growth factor-1 (IGF-1) or IGF-2 and interleukin-3 (IL-3) receptor-ligand pairs, whereas Fas and tumor necrosis factor-α (TNF-α) receptor-ligand pairs mediate the death signals. Most of the signals that elicit apoptosis converge on the mitochondria, which respond to proapoptotic signals by releasing cytochrome c, a potent catalyst of apoptosis (Green and Reed, 1998). The ultimate effectors of apoptosis include an array of intracellular proteases termed caspases (Thornberry and Lazebnik, 1998). Two "gatekeeper" caspases-8 and -9 are activated by death receptors such as Fas or by the cytochrome c released from mitochondria, respectively. These proximal caspases trigger the activation of more than 10 effector caspases that execute the death program, through selective destruction of subcellular structures, organelles, and of the genome.

Resistance to apoptosis can be acquired by cancer cells through a variety of strategies. Firstly, loss of a proapoptotic regulator through mutation involves the p53 tumor suppressor gene which results in the removal of a key component of the DNA damage sensor that can induce the apoptotic effector cascade (Harris, 1996). Secondly, the signals evoked by other abnormalities, including hypoxia and oncogene hyperexpression/activity, are also funneled in part via p53 to the apoptotic machinery; these two are impaired at eliciting apoptosis when p53 function is lost (Levine, 1997).

Limitless Replicative Potential

It was demonstrated that cells in culture have a finite replicative potential (Hayflick, 1997). Once cell populations have progressed through a certain number of doublings, they stop growing, a process termed senescence. Most types of tumor cells that are propagated in culture appear to be immortalized, suggesting that limitless replicative

potential is a phenotype that was acquired *in vivo* during tumor progression and was essential for the development of their malignant growth state (Hayflick, 1997).

From several studies it was evident that telomere maintenance is a major strategy acquired by all the malignant cells to gain limitless replicative potential (Shay, 1997). Telomeres, the ends of chromosomes, are composed of several thousand repeats of a short 6 bp sequence element. DNA polymerases are unable to completely replicate the 3' ends of chromosomal DNA. Thus every chromosome loses 50-100 bp of telomeric DNA from the ends during each S phase. The progressive erosion of telomeres through successive cycles of replication eventually causes them to lose their ability to protect the ends of chromosomal DNA. The unprotected chromosomal ends participate in end-to-end chromosomal fusions; resulting in the death of the affected cell (Counter et al., 1992).

For the maintenance of telomere, almost 85%-90% of the cancer cells upregulate the expression of the telomerase enzyme. This enzyme adds hexanucleotide repeats onto the ends of telomeric DNA (Bryan and Cech, 1999), or activates another mechanism, which appears to maintain telomeres through recombination-based interchromosomal exchanges of sequence information (Bryan et al., 1995). By any one mechanism, telomeres are maintained at a length above a critical threshold, and this in turn permits unlimited multiplication of descendant cells. Both mechanisms seem to be strongly suppressed in most normal human cells in order to deny them unlimited replicative potential.

Sustained Angiogenesis

The supply of oxygen and nutrients by the vasculature to the tissue is crucial for cell function and survival. Angiogenesis, the growth of new blood vessels is carefully regulated. In order to progress to a larger size, incipient neoplasias must develop angiogenic ability (Bouck et al., 1996 and Folkman, 1997). During tumor development, the ability to induce and sustain angiogenesis is acquired in a discrete step, an "angiogenic switch". It is proved to be an early to midstage event in many human cancers. Tumors appear to activate the angiogenic switch by changing the balance of angiogenesis inducers and countervailing inhibitors (Hanahan and Folkman, 1996).

Tissue Invasion and Metastasis

During the development of most types of human cancers, primary tumor masses move out, invade adjacent tissues, and thence travel to distant sites where they may succeed in forming new colonies. These distant settlements of tumor cells, metastases, are the cause of 90% of human cancer deaths (Sporn, 1996). The capability for invasion and

metastasis enables cancer cells to escape the primary tumor mass and colonize new terrain in the body where, at least initially, nutrients and space are not limiting. Like the formation of the primary tumor mass, successful invasion and metastasis depend upon all of the other five acquired hallmark capabilities.

2.1.3 Cancer Cell Genetics

Cancer is a disease involving dynamic changes in the genome. The genomes of the cells are constantly altered at multiple sites; disruptions range from subtle mutations to obvious chromosomal lesions (Kinzler and Vogelstein, 1996). The tumor development proceeds via a process analogous to Darwinian evolution, in which a succession of genetic changes, each conferring a growth advantage, leads to the progressive conversion of normal cells into cancer cells (Foulds, 1974; Nowell, 1976). All cancers must acquire the six capabilities, though the order and means of acquiring them vary significantly. Induction of genetic lesions on several critical genes confers several capabilities. Trillions of potential target cells, each harboring hundreds of susceptible cancer critical genes, are constantly subject to a significant mutation rate in a human life time. These cancer critical genes are divided into two types, which are oncogenes and tumor suppressor genes. These genes and the various types of mutations that affect them are discussed in detail.

Mutations

Mutations are changes in the bases or in the arrangement of the bases that make up a gene. These chromosomal aberrations occasionally produce cells that can escape the normal constraints and flourish as pathological tumors. Hereditary mutations are gene changes that come from a parent, therefore exist in all cells of the body, including reproductive cells and therefore can be passed to every next generation. These are also called germline mutations. This type of mutation is a major cause for 5-10% of cancers. Most cancers are caused by acquired mutations. An acquired mutation occurs when DNA in a cell changes during the person’s life. This can be caused by environmental influences such as exposure to radiation or toxins. Unlike the inherited genes, an acquired mutation starts in one cell of the body and is found only in the offspring of that cell. These are also called sporadic or somatic mutations.

Oncogenes

Oncogenes are genes whose protein products stimulate or enhance the division and viability of cells. This first category also includes genes that contribute to tumor growth by inhibiting cell death. The normal versions of genes in the first group are called proto-oncogenes. Proto-oncogenes are dominant and the mutated versions of these

genes, which are called oncogenes, gain new functions in the cells. The cell growth pathway starts with a growth factor, which binds to a growth factor receptor and the signal from the receptor is sent through a signal transducer. A transcription factor is produced and drives the cell for cell division. If any abnormality is detected, the cell is made to commit suicide by a programmed cell death regulator. More than 100 oncogenes have been identified at all the levels of this cell growth and death pathway and are involved in the multistep process of tumorigenesis (Gronbaek and Guldberg, 2006).

2.1.4 Tumor Suppressor Genes

Tumor suppressor genes either have a dampening or repressive effect on the regulation of the cell cycle or promote apoptosis, and sometimes do both. Mutations in tumor suppressor genes are recessive and these genes undergo bi-allelic inactivation in tumors and thereby loose their function. Tumor suppressor genes regulate diverse cellular activities, including cell cycle checkpoint responses, detection and repair of DNA damage, protein ubiquitination and degradation, mitogenic signaling, cell specification, differentiation and migration, and tumor angiogenesis. Analysis of the tumor suppressor genes is a central part of present cancer research. The functions of tumor suppressor genes can be divided into four major categories (Sherr, 2004) such as 1) Repression of genes that is essential for continuing the cell cycle thereby effectively inhibiting the cell division. 2) Coupling the cell cycle to DNA damage. If the damage can be repaired, the cell cycle can continue. 3) Inducing the programmed cell death. For example, if the DNA damage can not be repaired, the cell usually initiates apoptosis, to remove the threat that it poses for the entire organism. 4) Some proteins involved in cell adhesion prevent tumor cells from dispersing and thereby inhibit metastasis (Hirohashi and Kanai, 2003). About 30 tumor suppressor genes have been well studied, including p53, BRCA1, BRCA2, APC, and RB1. The tumor suppressor gene database contains updated information on 174 identified and putative tumor suppressor genes from human beings and other organisms (Yang, 2003).

2.1.5 Mechanisms of Inactivation of the Tumor Suppressor Genes

Mutations of tumor suppressor genes have been widely found in many cancers. Abnormalities of the p53 gene, in particular acquired mutations have been found in more than 50% of the human cancers, including lung, colorectal and breast cancer as well as many other cancers. Acquired changes in many other tumor suppressor genes also contribute to the development of non-inherited cancers. Although there are many mechanisms operating in the cancer-prone cells to eliminate the tumor suppressor genes, the cells with inherited defect in one copy of a tumor suppressor gene loose

their remaining good copy by six possible ways (Alberts et al., 2002). The normal copy of the gene can be eliminated by point mutation, deletion, gene conversion, mitotic recombination, non dysjunction and duplication, and chromosome loss. The table 1 lists some of the most commonly mutated tumor suppressor genes and the inherited and non-inherited cancers caused by them (ACS, 2005).

Table 1: The Tumor suppressor genes and human cancers

Gene	**Inherited cancer**	**Non-inherited cancers**
RBI	Retinoblastoma	Many different cancers
P53s	Li-Fraumeni syndrome (leukemia & brain tumors)	Many different cancers
INK4a	Melanoma	Many different cancers
APC	Colorectal cancer (with familial polyposis)	Most colorectal cancers
MLH1, MSH2, or MSH6	Colorectal cancer (without polyposis)	Colorectal, gastric, endometrial cancers
BRCA1, BRCA2	Breast & ovarian cancers	Only rare ovarian cancers
WTI	Wilms tumor	Wilms tumors
NF1, NF2	Nerve & brain tumors	Colon cancers and melanomas

In addition to the above mentioned mechanisms a new concept about the mechanism of inactivation of tumor suppressor genes was proposed. Loss of tumor suppressor activity occurs not only through the gene mutation or deletion but also alternatively as a result of altered gene expression (Macleod, 2004; Quon et al., 2001). An example for such a gene is the programmed cell death 4 gene (Pdcd4), a novel cancer-associated gene, with putative tumor suppressor activity which was identified to be up or downregulated in many cancers (Jansen 2004). A detailed introduction about Pdcd4 is given in the section 2.2.

2.1.6 Cancer Therapeutics

Treating abnormalities of tumor suppressor genes is even more difficult, since the normal tumor suppressor gene has to be restored (Ames, 1995). Cancer gene therapy is one of the most promising areas of cancer therapeutics. Unlike the radiation and chemotherapy, the toxicity is only restricted to the tumor cells. As gene expression is cell-type specific, the transcription is targeted using a range of promoters which are tissue-specific, tumor-specific and inducible by exogenous agents. The major stumbling block lies in the mode of transfer of new DNA into the cancer cells (Hirst, 2002). In

addition to that problem, most cancers have several accumulated oncogene and tumor suppressor gene mutations, so replacing one gene may not curb the cancer cell growth or invasion. Though the cancer prevention and therapy is a daunting task, increasingly novel cancer-critical genes are identified and targets are explored for the treatment.

2.2 Pdcd4 – A Novel Putative Tumor Suppressor

2.2.1 The Cloning of Pdcd4

In 1995 Shibahara et al. cloned a mouse cDNA termed MA-3 that was upregulated during apoptosis in all cell lines tested and termed it as Programmed Cell Death 4 (Pdcd4). This study was followed by the identification of a homologous coding sequence called TIS for topoisomerase inhibitor suppressed gene by Onishi and Kizaki (1996). In the following years the cDNAs of the human (H731 and 197/15a), chicken (Pdcd4) and rat homologues (DUG) of Pdcd4 were identified (Matshuhasi et al., 1997; Azzoni et al., 1998; Schlichter, 2001a; Goke et al., 2002). In addition to the vertebrates, distantly related organisms such as the fruit fly *Drosophila melanogaster* (referred to the map element CG10990) or the marine sponge *Suberites domunculata* (Wagner et al., 1998) also possess the homologous counterparts of Pdcd4.

2.2.2 The Sequence Motifs of Pdcd4

The mouse gene spans about 21 Kb including 11 exons. The intron-exon junctions followed the GT-AG rule of eucaryotic genes. By primer extension experiments the transcription start site was located 192 bp upstream of the start codon. Analysis of the 5´-flanking region of the gene revealed two functionally active TATA sequences at position -21 and a CAAT-box at -81 (Onishi et al., 1998). Furthermore, putative binding sites for NFκB (from positions -488 to -470), NF1 (-326 to -314) and two C/EBPβ binding sites (-424 to -416 and -254 to -246) were found. However, the functionality of these sequences in transcription has yet to be tested. Concomitantly, the human Pdcd4 (Hpdcd4) gene was mapped to chromosome band 10q24 by in situ hybridization (Soejima et al., 1999)

2.2.3 The Structure of Pdcd4

Pdcd4 is a 55 KDa nuclear protein contains two conserved MA-3 domains, believed to be largely alpha-helical in the region of aa 164-275 and 329-440, respectively. Secondary structure of the C-terminal MA-3 domain was determined by NMR experiments (Waters et al., 2006). Two nuclear export signals (NES) at 182-192 and 241-251 were identified, one of which was shown to be very potent, 182-192 (Boehm et al., 2003). In addition, it was also found by the same investigators that the Pdcd4 protein has intrinsic RNA-binding activity and that the amino-terminal part of the protein is responsible for this activity. The domain organization of Pdcd4 is shown in figure 2. Two potential nuclear localization signals (NLS) have been predicted at the N- and C-terminus of the protein, but have not been proved experimentally. Furthermore,

the protein contains multiple phoshoprylation sites for protein kinases such as protein kinase C, proline-directed protein kinase and casein kinase II. It has been shown that Pdcd4 is phosphorylated by Akt kinase at the sites of Ser-67 and Ser-457, both *in vitro* and *in vivo* (Palamarchuk et al., 2005).

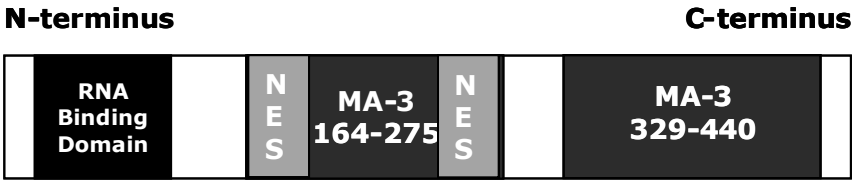

Figure 2: The domain organization of Pdcd4

Pdcd4 contains two MA-3 domains. There are two nuclear exporting signals present within the N-terminal MA-3 domain. A RNA binding domain is present in the N-terminal part of the protein.

2.2.4 The Subcellular Localization of Pdcd4

Immunofluorescence studies in human and quail fibroblast cell line using Pdcd4 and hemagglutinin (HA) antibodies against recombinant Pdcd4 and HA-tagged Pdcd4 fusion proteins, respectively, revealed a nuclear localization of Pdcd4 (Yoshinaga et al., 1999; Schlichter et al., 2001b). Further, it has been shown that although Pdcd4 protein is predominantly a nuclear protein under normal growth conditions, it is exported from nucleus by a leptomycin B-sensitive mechanism upon serum withdrawal (Bohm et al., 2003). Moreover, preliminary experiments using yeast two-hybrid system and separation of polysomes from cytosol in HeLa cells by sucrose density gradient centrifugation showed the localization of Pdcd4 to the ribosome complex (Kang 2002).

2.2.5 The Regulation and Expression of Pdcd4

Northern blot analysis of normal mouse tissues revealed higher Pdcd4 expression levels in the liver followed by testis, lung, brain, kidney and spleen (Onishi et al., 1998). Lower levels were found in skeletal muscle and heart. In most tissues the major transcript identified was about 2.3 kb. A similar expression pattern of Pdcd4 in mouse adult tissues was also found by Shibahara et al (1995) with strongest hybridization signals in thymus, followed by liver, intermediate signals in brain, kidney and spleen and least signals in lung and heart.

The expression of Pdcd4 is modulated by different cytokines. Downregulation was found in both human natural killer and T cells by IL-2 and IL-15, but upregulation by treatment with IL-12, whereas IL-4 and IL-7 had no effect (Azzoni et al., 1998). Programmed cell death plays an important role during embryogenesis. The ovulated

egg is destined to undergo cell death if not fertilized. Pdcd4 levels are abundant in oocytes and embryonic Pdcd4 expression seems to be induced at the 8-cell stage in mouse embryos (Jurisicova et al., 1998). V-myb was identified as an inducer of chicken Pdcd4 expression (Schlichter et al., 2001b). Moreover, cloning of the promoter region of the Pdcd4 gene revealed the existence of myb binding sites and Pdcd4 promoter/reporter gene constructs demonstrated the functional activity of these sites (Schlichter et al., 2001b). Additionally, targeted disruption of c-myb in the chicken DT40 B-cell line lowered the expression of the Pdcd4 gene (Appl and Klempnauer, 2002).

Pdcd4 was first identified as a gene upregulated during apoptosis (Shibahara et al., 1995). In this study, T-cell lines, a hematopoietic progenitor cell line or a B-cell line were stimulated with ionomycin, dexamethasone, deprived of IL-3 or IL-2 or stimulated by cross-linking of surface IgM, respectively. Recently, it has been shown that adenoviral transfer of the Fas ligand gene elevates expression of Pdcd4 and induces apoptosis in HEK 293 cells (Goke et al., 2002). However, other apoptotic stimuli like UV-irradiation, treatment with Ara-C or topoisomerase inhibitors failed to enhance or even suppressed Pdcd4 expression in other cell lines (Onishi et al., 1998; Onishi and Kizaki, 1996). This suggests that Pdcd4 expression might be different depending on the apoptotic stimulus used.

Phospholipase Cb3 (PLCB3) expression is frequently lost in sporadic tumors. Restoration of the PLCB3 levels in neuroendocrine cell lines suppresses cell growth and alters the phenotype indicating that PLCB3 might be relevant in tumorigenesis (Stalberg et al., 1999). By reverse transcription (RT) differential display it was shown that Pdcd4 is upregulated in PLCB3 transfected cells (Stalberg et al., 2001) stressing the impact of Pdcd4 as a tumor suppressor. The role of Pdcd4 in cell growth regulation is further emphasized by the fact that it is elevated at the mRNA and protein levels in cellular senescence (Kang et al., 2002). Additionally, for a human colon carcinoma cell line, it has been shown that after treatment with NS-398, a selective cyclo-oxygenase-2 (COX-2) inhibitor, mRNA levels of Pdcd4 were upregulated (Zhang and DuBois, 2001). COX-2 is a target of nonsteroidal anti-inflammatory drugs and inhibition of COX-2 may contribute to the anticancer effect of these drugs.

It has been shown that expression of Pdcd4 is low in human pancreatic cancer and is correlated with the differentiation levels of cancer (Ma et al., 2005). Pdcd4 is suppressed in squamous cell carcinoma, the most frequent malignant tumor of the oral cavity (Carinci et al., 2005). Moreover, nasal natural killer/T-cell lymphoma is an aggressive subtype of non-Hodgkin lymphoma that is closely associated with

Epstein-Barr virus and Pdcd4 was identified as a putative contributor of the disease progression (Zhang et al., 2006).

2.2.6 The Cellular Functions of Pdcd4

A system that was developed for the identification of proteins that drive tumor promotion is the mouse epidermal JB6 model of transformation response. The experiments using this model suggested a tumor suppressor function for Pdcd4 (Cmarik et al., 1999). It has been shown that the transactivation of transcription factors activator protein1 (AP-1) and NF-κB is essential for tetradecanoylphorbol acetate (TPA)- or TNFα-induced neoplastic transformation (Hsu and Twu, 2000). TPA-induced AP-1 dependent transactivation and basal AP-1 activity was inhibited in a concentration-dependent manner and similar results from another cell line confirmed this observation (Yang et al., 2003b). The inhibition involves phosphorylation of Pdcd4 at Ser-67 and Ser-457 by Akt kinase (Palamarchuk et al., 2005). Besides its effect on AP-1 there is evidence that Pdcd4 also acts via other signaling pathways, including TGFβ (zhang, 2006).

Sequence alignments revealed a significant amino acid homology of Pdcd4 with the proteins of eIF4G family (Goke et al., 2002). Additionally, Pdcd4 contains two conserved MA-3 domains which is also present in the eucaryotic translation initiation factors eIF4G I and eIF4G II. The MA-3 domain is thought to be involved in protein-protein interactions and enables eIF4G to interact with eIF4A (Ponting, 2000). The eIF4A is an ATP-dependent RNA helicase that unwinds the mRNA to allow the ribosome to migrate in the 3'direction to locate the initiation codon AUG. Moreover, it has been shown by coimmunoprecipitation experiments that Pdcd4 directly interacts with eIF4A suggesting that Pdcd4 has an impact on protein translation (Goke et al., 2002) which was confirmed by Yang et al. who identified eIF4A as a Pdcd4-interacting protein using a yeast two-hybrid system (2003a). Multicolor confocal immunofluorescence microscopy revealed a colocalization of eIF4A with Pdcd4 in the cytoplasm with a concentrated perinuclear distribution. Furthermore, Pdcd4 inhibited helicase activity in a concentration-dependent manner and acts as a specific dominant inhibitor of eIF4A (Yang et al., 2003a). This data were confirmed by *in vitro* and *in vivo* translation assays showing that Pdcd4 preferentially inhibits cap-dependent translation. Moreover, in *in vitro* binding assays Pdcd4 prevented binding of eIF4A to the C-terminal part of eIF4G. Interestingly, the mechanisms of action of Pdcd4 and the impact on protein translation seem to be even more complex since Kang et al. recently reported a direct interaction of Pdcd4 with eIF4G (2002). The inhibitory effect of Pdcd4 on translation initiation factors might explain its function as transformation inhibitor.

2.2.7 The Molecular Mechanisms of the Functions of Pdcd4

It has been shown that Pdcd4 suppresses the transactivation of AP-1 responsive promoters by c-Jun, suggesting that the transformation-suppressor activity of Pdcd4 might be partly due to the inhibition of c-Jun activity. Bitomsky et al. (2004) addressed the mechanisms of inhibition of c-Jun by Pdcd4. It was shown that Pdcd4 interferes with the phosphorylation of c-Jun by Jun N-terminal kinase (JNK). Moreover, it was suggested that Pdcd4 interacts with c-Jun and thereby blocks the phosphorylation of c-Jun. In addition to affecting c-Jun phosphorylation, Pdcd4 blocks the recruitment of the coactivator p300 by c-Jun.

Lankat-Buttgereit et al. (2004) showed that Pdcd4 suppresses carbonic anhydrase type II protein expression in HEK293 and Bon-1 carcinoid cells. As the tumor cells require a high bicarbonate flux for their growth, carbonic anhydrase suppression results in growth inhibition. Similar to Pdcd4, carbonic anhydrase inhibitor ethoxyzolamide reduces growth of several endocrine tumor cell lines. Thus, it was suggested that the translation inhibitor Pdcd4 represses endocrine tumor cell growth by suppression of carbonic anhydrase II.

Jansen et al. (2004) studied the relevance of Pdcd4 in a range of human cancers derived from multiple tissue sites. The hypothesis tested was that Pdcd4 levels would be prognostic or fundamental for antitumor activity of current or exploratory chemotherapeutic compounds. Pdcd4 expression patterns from the national cancer institute drug-screening panel of 60 human cancer cells (NCI60) were analyzed by western blotting. It revealed a frequent reduction of Pdcd4 protein levels in renal-, lung-, and glia-derived tumors. Pdcd4 was found to correlate with the antitumor activity of geldanamycin and tamoxifen. It was observed that the increased sensitivity of UO-31 cells to geldanamycin was accompanied by enhanced cell cycle arrest and apoptosis.

Eucaryotic cells regulate gene expression at multiple levels, such as transcription, splicing, stability and translation of mRNA. Transcriptional dysregulation is a well-studied contributor to cancer pathogenesis; increasing evidence implicates altered translational regulation as well (Jansen et al., 2005). Translation initiation is the predominant rate-limiting step of protein synthesis for most mRNAs. Exposure to skin tumor promoters, such as TPA enhances the formation of the translation initiation complex. Several tumors and tumor cell lines show elevated levels of components of the translation initiation complex, including eIF4A (Eberle et al., 1997), eIF4E (De Benedetti and Harris, 1999), and eIF4G (Bauer et al., 2001). Pdcd4 seems to be the

first example of a protein in mammalian cells that inhibits directly the helicase activity of eIF4A, a component of the translation initiation complex. Jansen et al. (2005) generated a transgenic mouse that overexpresses Pdcd4 in the epidermis to ascertain whether Pdcd4 suppresses tumor development *in vivo*. In response to the 7, 12-dimethylbenz(a) anthracene/TPA mouse skin carcinogenesis protocol, Pdcd4 overexpressing mice showed significant reductions in the papilloma formation, carcinoma incidence, and papilloma-to-carcinoma conversion frequency compared to wild-type (WT) mice.

The translational efficiency of an mRNA engineered to form a structured 5´untranslated region (UTR) was attenuated in primary keratinocytes when Pdcd4 was overexpressed. Pdcd4 inhibited by 46%, the TPA-induced AP-1-dependent transcription, an event involved in tumorigenesis. Cyclin dependent kinase and ornithine decarboxylase are candidates for Pdcd4-regulated translation as their mRNAs contain 5´structured UTRs. These results extend to an *in vivo* model to confirm the observations that Pdcd4 inhibits both translation initiation and AP-1 activation while decreasing benign tumor development and malignant progression.

Zhang et al. (2006) elucidated the function and regulatory mechanisms of expression of Pdcd4 in human hepatocellular carcinoma. It was reported that Pdcd4 protein is downregulated and it is a proapoptotic molecule which is involved in transforming growth factor-β1 (TGF-β1)-induced apoptosis in human hepatocarcinoma cells.

Furthermore, it was reported recently that Pdcd4 suppresses tumor progression in human colon carcinoma cells by downregulating MAP4K1 transcription, with consequent inhibition of c-Jun activation and AP-1 transcription (Yang et al., 2006). Pdcd4 blocks c-Jun activation by inhibiting the expression of mitogen-activated protein kinase kinase kinase kinase 1 (MAP4K1)/hematopoietic progenitor kinase 1, a kinase upstream of Jun N-terminal kinase (JNK). The cDNA microarray analysis of Pdcd4 overexpressing RKO human colon carcinoma cells revealed MAP4K1 as the sole target of Pdcd4 on the JNK activation pathway. Overexpression of either Pdcd4 or dominant negative MAP4K1 mutant in metastatic RKO cells inhibited not only c-Jun activation but invasion as well.

2.3 Objectives and Rationale of the Study

Pdcd4 is a novel gene originally identified as a gene upregulated during apoptosis (Shibahara et al., 1995), but later recognized as a tumor suppressor (Cmarik et al., 1999). The molecular functions of Pdcd4 such as the role of RNA binding and translational regulation have not been characterized in detail. The molecular mechanism by which Pdcd4 executes its function and the biological significance of its biochemical activities are yet to be unraveled. Apparently, the primary limitation for the further analysis of molecular functions of Pdcd4 is the lack of a well-characterized cell system, in which the Pdcd4 expression level can be modulated.

2.3.1 Pdcd4 Models

Gene-function studies require careful selection of representative models to ensure that the experimental findings do reflect the role of a gene in the organism. In molecular biology, based on the reverse genetic approach, generally two basic models are employed to study the function of a particular gene, viz., downregulation (knock-out or knock-down) and upregulation (overexpression) systems. In the present work, three cell systems were developed and characterized: A Pdcd4 knock-down system, a Pdcd4 knock-out system and a Pdcd4 overexpression system. The all three systems were employed to elucidate the molecular functions of the Pdcd4 gene. In particular, the primary aim was the identification of novel molecular targets for Pdcd4 by utilizing the three systems. Once identified, these novel targets of Pdcd4 could be used to further uncover the signaling pathways by which Pdcd4 functions as a tumor suppressor.

2.3.2 Pdcd4 Downregulation System

For studying the function of a gene, in particular, of a tumor suppressor gene, a downregulation cell system will be very useful as the gene of interest is completely or almost completely eliminated from the cell. This mimics the cancer cell in which the functional copies of tumor suppressor genes are inactivated during tumorigenesis.

Pdcd4 Knock-down System

The knock-down of Pdcd4 was attempted by RNA interference (RNAi) which is mediated through short double-stranded RNA molecules, known as small interfering RNA (siRNA). Formation of siRNA duplexes of 19-25 nt length followed by incorporation into the RNA-induced silencing complex (RISC) catalyzes cleavage of complementary mRNAs (Hammond, 2001). The knock-down system is preferred, due to two major advantages. First, silencing by siRNA is highly specific. Second, RNAi knock-down efficiencies range

from the entire extinguishing of the gene function to a graded loss-of function (Sui, 2002). It has been found after analyzing over 60 cancerous cell lines that inactivation of tumor suppressor genes occurs not only through gene mutation or deletion but alternatively also as a result of reduced gene expression (Jansen et al., 2004). For example, most of the non-small lung cancer cell lines and renal cancer cell lines showed less than mean Pdcd4 protein level (Jansen et al., 2004). As Pdcd4 showed altered gene expression in many cancers, knock-down system generated by RNAi mediated siRNA silencing is an apt tool for studying its function. The HeLa cell line was selected for developing the human Pdcd4 knock-down system. HeLa is an established cell line derived from cervical epithelial cells of adenocarcinoma origin. RNA and protein analysis of HeLa cells have shown that they express detectable amounts of Pdcd4 (Boehm, 2005).

Pdcd4 Knock-out System

Generating a Pdcd4 knock-out cell system was also of interest, as it could simulate tumors, in which expression of Pdcd4 is entirely eliminated. Complete loss of Pdcd4 protein was shown in several central nervous system tumors whereas their normal counterparts shown readily detectable Pdcd4 by immunohistochemical analysis (Jansen et al., 2004). The knock-out system was generated by homologous recombination, a procedure in which engineered targeting constructs are integrated into the genome and thereby disrupt the gene of interest.

Exchange of sequence information between two homologous DNA molecules, referred to as homologous recombination, makes a major contribution to the repair of DNA damage and thereby contributes to the preservation of genome integrity (Modesti and Kanar, 2001). This natural phenomenon can be exploited in gene targeting to disrupt a gene of interest in a predetermined way. In classical homologous gene targeting, a fragment homologous to the locus to be modified is transfected in the cell. If one can select for insertion in the genome (with a selectable marker placed between flanking homologous DNA sequences), the majority of the insertion events in most organisms will be found at random locations all over the genome. A few events will result from the integration at the homologous locus by homologous recombination; however, one needs to screen extensively for such rare events. This is not the case in a limited number of organisms and cell types where homologous integration is predominant. As the avian DT40 lymphoid cell line has extremely high rate of homologous recombination, the DT40 cell line was chosen for creating Pdcd4 knock-out cell system.

2.3.3 Pdcd4 Upregulation System

In addition to the downregulation system, cells overexpressing Pdcd4 were also generated. Although overexpression of a gene is an artificial condition, it might mimic the function of the gene in the normal cell. A549 is an epithelial human lung carcinoma cell line. A study has shown that Pdcd4 expression is widely lost in lung tumor cells. In addition, Pdcd4 might be a prognostic factor in lung cancer and may correlate with tumor progression (Chen et al., 2003). Therefore, the A549 cell line was chosen for the overexpression of Pdcd4 and thereby to revoke the normal functions of Pdcd4.

3 MATERIALS AND METHODS

3.1 Materials

3.1.1 Antibodies

Antibody	Catalog No.	Firm/Company
AKR1C2 Mouse Polyclonal IgG	A01	*Abnova*, Taipei, Taiwan
AKR1C3 Goat Polyclonal IgG	IMG-3773	*Imagenex*, CA, USA
ATF-2 (N-96) Rabbit Polyclonal IgG	Sc-6233	*Santa Cruz BiotechnologY,* CA, USA
p-ATF-2 (F-1) Mouse Monoclonal IgG	Sc-8398	*Santa Cruz Biotechnology,* CA, USA
C/EBPβ Rabbit Polyclonal Antiserum	-	Mink et al., 1996
c-Jun (D) Rabbit Polyclonal IgG	Sc-44	*Santa Cruz BiotechnologY,* CA, USA
p-c-Jun (KM-1) Mouse Monoclonal IgG	Sc-822	*Santa Cruz Biotechnology,* CA, USA
c-Myc Rabbit Polyclonal IgG	sc-764	*Santa Cruz Biotechnology,* CA, USA
CK-8/18 Mouse Monoclonal IgG	DLN-10749	*Dianova*, Hamburg, D
CK-17 Mouse Monoclonal IgG	C9179	*Sigma-Aldrich*, Missousri, USA
GluProRS Rabbit Polyclonal IgG	ab31531	*Abcam*, Hiddenhausen, D
HA.11 Mouse Monoclonal IgG		*Covance,* CA, USA
Human Pdcd4 Rabbit Polyclonal Antiserum	-	*Eurogentec*, Seraing, B
β-tubulin Mouse Monoclonal IgG	Sc-5274	*Santa Cruz Biotechnology,* CA, USA
Anti-Mouse HRP Conjugated IgG	P0260	*Dako-Diagnostika GmbH*, Hamburg, D
Anti-Rabbit HRP Conjugated IgG	P0217	*Dako-Diagnostika GmbH*, Hamburg, D
Anti-Goat HRP Conjugated IgG	A-5420	*Sigm-Biochemicals,* D

3.1.2 Cell Culture Products

Neubauer haemocytometer	*Merck AG*, Darmstadt, D
Chicken serum	*PAA Laboratories GmbH*, Linz, AU
Dulbecco's MEM-medium	*Biochrom KG*, Berlin, D
Fetal bovine serum	*Biochrom KG*, Berlin, D
Iscove's modified Dulbecco's medium	*Biochrom KG*, Berlin, D
L-Glutamine	*Biochrom KG*, Berlin, D
MEM-medium	*Biochrom KG*, Berlin, D

Non-essential amino acids	*Biochrom KG*, Berlin, D
PBS Buffer	*Biochrom KG*, Berlin, D
Penicillin / Streptomycin	*Biochrom KG*, Berlin, D
RPMI 1640 medium	*Biochrom KG*, Berlin, D
Tissue culture flasks	*Greiner Labortechnik*, Solingen, D
Tissue culture dishes	*Greiner Labortechnik*, Solingen, D
Trypsin/EDTA solution	*Biochrom KG*, Berlin, D

3.1.3 Chemicals and Reagents

The standard chemicals were purchased from *Acros Organics*, New Jersey, USA; *Amersham Bioscience*, Freiburg, D; *AppliChem*, Darmstadt, D; *Baker*, Deventer, NL; *Becton Dickinson*, Detroit, USA; *Biomol Feinchemikalien GmbH*, Hamburg, D; *Difco Laboratories*, Detroit, USA; *Merck KGaA*, Darmstadt, D; *Sigma-Aldrich Chemie GmbH* (including *Fluka*), München, D; *Gibco BRL Life Technologies*, Eggenstein; *ICN Biomedical*, Ohio, USA; *Invitrogen*, Groningen, NL; *Merck AG*, Darmstadt; *Roche*, Mannheim; *Fermentas*, St. Leon-Rot. Special chemicals were obtained from the following companies.

[α-^{32}P]-dCTP (10µCi/µl, ~3000Ci/mmol)	*Amersham Bioscience*, Freiburg, D
L-[^{35}S] *in vitro* Cell Labeling Mix	*Amersham Bioscience*, Freiburg, D
2 K Acrylamide (30%)-Mix 37.5:1	*AppliChem*, Darmstadt, D
Adenosine-5'-triphosphate (ATP)	*Amersham Bioscience*, Freiburg, D
Agar	*Sigma-Aldrich Chemie GmbH*, München, D
Agarose	*Gibco BRL Life Technologies*, Eggenstein
Ampicillin	*Sigma-Aldrich Chemie GmbH*, München, D
Ammonium per sulfate (APS)	*Merck KGaA*, Darmstadt, D
(β-D-arabinofuranosyl) cytosine	*Sigma-Aldrich Chemie GmbH*, München, D
B-Gal-Elisa-lysis-buffer	*Roche*, Mannheim, D
Blasticidin S	*Invitrogen*, Karlsruhe, D
Cationic polymer transfection reagent	*Eurogentec,* Belgium, DK
Coomassie Brilliant Blue R250	*Merck KGaA*, Darmstadt, D
Dithiothreitol	*Sigma-Aldrich Chemie GmbH*, Steinheim, D
D-Luciferin	*AppliChem*, Darmstadt, D
DNA-SmartLadder	*Eurogentec*, Lige, B
Doxycycline	*Sigma-Aldrich Chemie GmbH*, Steinheim, D
dNTP-Set	*Roche*, Mannheim, D
DryStrip pH 3-10, 13 cm	*Amersham Bioscience*, Freiburg, D
DryStrip pH 4-7, 13 cm	*Amersham Bioscience*, Freiburg, D

DryStrip pH 6-11, 13 cm	*Amersham Bioscience*, Freiburg, D
ECL western blotting detection reagent	*Amersham Bioscience*, Freiburg, D
EDTA	*Biomol Feinchemikalien GmbH*, Hamburg,D
Emerald enhancer	*Perkin Elmer*, Weiterstadt, D
Ethidium bromide	*Sigma-Aldrich Chemie GmbH*, Steinheim, D
Ethyl methane sulfonate	*Sigma-Aldrich Chemie GmbH*, Steinheim, D
Film developing solution	*Dunker*, Hattingen, D
Film fixation solution	*Dunker*, Hattingen, D
Galacton	*Perkin Elmer*, Weiterstadt, D
HEPES	*Sigma-Aldrich Chemie GmbH*, Steinheim, D
Immobiline drystrip cover fluid	*Amersham Bioscience,* Freiburg, D
IPG Buffer 3-10	*Amersham Bioscience*, Freiburg, D
IPG Buffer 4-7	*Amersham Bioscience*, Freiburg, D
IPG Buffer 6-11	*Amersham Bioscience*, Freiburg, D
IPTG	*Biomol*, Hamburg, D
L-Histidinol dichloride	*Sigma-Aldrich Chemie GmbH*, München, D
Lysozyme	*Sigma-Aldrich Chemie GmbH*, München, D
Mitomycin C	*Merck KGaA,* Darmstadt, D
NP-40	*Fluka Chemie AG*, Buchs, S
Phenol-Chloroform-Isoamylalcohol (25:24:1)	*Merck AG*, Darmstadt, D
Phorphol-12-myristate-13-acetate	*Calbiochem,* Darmstadt, D
Prestained molecular weight marker 7B	*Sigma-Aldrich Chemie GmbH*,Steinheim, D
Puromycin dichloride	*Merck KGaA,* Darmstadt, D
Rapid-gel-acrylamide 40%	*USB corporation*, OH, USA
Skim milk powder for microbiology	*Merck AG*, Darmstadt, D
Staurosporine	*Sigma-Aldrich Chemie GmbH*, München, D
TEMED	*Sigma-Aldrich Chemie GmbH*, Steinheim, D
Triton X-100	*Biorad*, Hercules, USA
Trypton	*Difco Laboratories*, Detroit, USA
X-Gal	*Biomol*, Hamburg, D
Yeast extract	*Difco Laboratories*, Detroit, USA
Zeocin	*Invitrogen*, Karlsruhe, D

3.1.4 Devices and Instruments

Agfa Curix60 (Film Developer)	*Agfa AG*, Leverkusen, D
Auto Lumat LB953	*EG & G Berthold*, Bad Wildbach, D
BASReader BAS-1800II	*Raytest*, Stauberstadt

Blotting device Trans-Blot CELL	*Biorad*, München
Centrifuges	
Avanti 300	*Beckmann*, München, D
Centrifuge 5810 R	*Eppendorf*, Hamburg, D
Centrifuge 5415 D	*Eppendorf*, Hamburg, D
Centrifuge 5417 R	*Eppendorf*, Hamburg, D
Centrifuge IL-21 (Rotor JA-14, 10.5)	*Beckmann*, München, D
TL-100 Ultracentrifuge	*Beckmann*, München, D
CO_2 Incubator	*WTB Binder*, Tuttlingen, D
Electroporator Easyjekt Plus	*Peqlab*, Erlangen
FACScan Flow Cytometer	*Becton Dickinson*, Heidelberg, D
Films	
BioMaX XAR Scientific Imaging Film	*Eastman Kodak Company*, NY, USA
RX Scientific Imaging Films	*W.Plus Röntgen GmbH*, Kamp-Lintfort, D
Film developer Agfa CuriX60	*Agfa AG*, Leverkusen
Gel dryer	*Biorad*, München
Heating Circulator MB-5	*Julabo Labortechnik GmbH*, Seelbach, D
Laminar flow hood	*Zapf Instruments*, Sarstedt, D
IPG-Electroporesis System	*Amersham Biosc.,,* Buckinghamshire, UK
IPG-strip holder (ceramic)	*Amersham Pharmacia Biotech,* Freiburg, D
LiCOR Gene ReadIR 4200	*MWG-Biotech*, Ebersberg
Mastercycler Gradient	*Eppendorf*, Hamburg, D
Nitrocellulose membrane (Protran)	*Schleicher & Schuell*, Dassel,D
Nylon membrane (Gene Screen Plus®)	*Perkin Elmer*, MA, USA
pH-Meter CG840	*Schott*, Hofheim, D
Phosphor-Imager BAS-1800 II	*FUJIFILM*, Düsseldorf
Power Pac 300	*Biorad*, München, D
Power Supply ECPS 3000/150	*Amersham Bioscience*, Freiburg, D
SDS-gel device (Hoefer SE 660)	*Amersham Bioscience*, Freiburg, D
UV-Spectrometers	
Gene Quant II	*Pharmacia*, Freiburg
UV-1602	*SHIMADZU*, Duisburg
VorteX L46	*Labinco BV*, NL
Whatman paper 3MM	*Schleicher & Schüll*, Dassel, D

3.1.5 Enzymes

Dnase I	*Roche*, Mannheim, D
Klenow-Polymerase	*Roche*, Mannheim, D

Proteinase K	*Roche*, Mannheim, D
Restriction Enzymes	*New England Biolabs*, Schwalbach, D
Rnase	*Roche*, Mannheim, D
Taq-DNA-Polymerase	*Gibco BRL Life Technologies*, Eggenstein, D
T4 DNA Ligase	*New England Biolabs*, Schwalbach, D

3.1.6 Genotype of *Escherichia coli* K12 strains

Top10F´: F' [lacI^{q}, Tn10(Tet^{R})] *mcrA* Δ(*mrr-hsdRMS-mcrBC*) *Φ80 lacZ*ΔM15 Δ*lacX74 deoR recA1 araD139* Δ (*ara,leu*)7697 *galU galK rpsL* (Str^{R}) *endA1 nupG*

3.1.7 Kits

Complete Mammalian Protein Extraction Kit	*Calbiochem,* Darmstadt, D
Dual Luciferase Reporter Assay System	*Promega GmbH,* Mannheim, D
DYEnamic Direct cycle sequencing Kit	*Amersham Bioscience*, Freiburg, D
Nucleobond Kit PC 500	*Macherey-Nagel*, Düren, D
NucleoSpin Mini Plasmid Quick Pure	*Macherey-Nagel*, Düren, D
Megaprime DNA-labeling-Kit	*Amersham Bioscience*, Freiburg, D
QIAGEN Plasmid Maxi Kit	*Qiagen*, Hilden, D
QIAprep Spin Miniprep Kit	*Qiagen*, Hilden, D
QIAquick Gel Extraction Kit	*Qiagen*, Hilden, D
Rapid-DNA-Ligation-Kit	*Roche*, Mannheim, D
TOPO TA Cloning Kit	*Invitrogen*, Karlsruhe, D

3.1.8 Plasmids and Constructs

The following vectors and constructs were used in the present research work.

Plasmid/Construct	**Description**
pCR®2.1-TOPO®	~3.9 Kb, Amp^{r}, Kan^{r}, P_{Lac}/LacZα, T/A-Cloning vector for cloning the PCR-products (Blue/White-Screening) (*Invitrogen*)
pBlueScript KS	~3 Kb, Amp^{r}, lacZ promoter, a cloning vector (*Stratagene*)
pbl-pdcd4-targetHisD	~9.7 Kb, histidinol resistance under the control of β-actin promoter, the targeting construct flanked by the genomic DNA sequences from the major part of the chicken Pdcd4 gene (Bitomsky, 2003*)*

pbl-pdcd4-targetPuro	~8.7 Kb, puromycin resistance under the control of β-actin promoter, the targeting construct flanked by the genomic DNA sequences from the major part of the chicken Pdcd4 gene (Bitomsky, 2003*)*
pcDNA3	~5.4 Kb, Amp^r, CMV-promoter, eucaryotic expression vector codes for β-galactosidase, (*Invitrogen*)
pcDNA3-CCR	~6.6 Kb, Amp^r, CMV-promoter, eucaryotic expression vector codes for the chicken C/EBPβ without upstream region (Mink et al., 1997)
pcDNA3-c-Jun	~6.6 Kb, Amp^r, CMV-promoter, eucaryotic expression vector codes for the human c-Jun (Schwarz et al., 2003)
pcDNA3-i11/6HA	~6.9 Kb, Amp^r, CMV-promoter, eucaryotic expression vector codes for the chicken Pdcd4-HA tagged (Schlichter et al., 2001b)
pcDNA4/TO/*myc*-His	5.1 Kb, Amp^r, CMV-promoter, eucaryotic tetracycline inducible expression vector (*Invitrogen*)
pcDNA4TomycHis-i11/6HA	6.6 Kb, Amp^r, Zeo^r, CMV-promoter, eucaryotic tetracycline inducible expression vector codes for the chicken Pdcd4-HA tagged (Schlichter et al., 2001b)
pcDNA4-Hpdcd4	6.6 Kb, Amp^r, Zeo^r, CMV-promoter, eucaryotic expression vector codes for the human Pdcd4
pcDNA6/TR	~6.7 Kb, Amp^r, CMV-promoter, eucaryotic expression vector codes for the tetracycline repressor protein (*Invitrogen*)
pCI-neo	~5.5 Kb, Amp^r, CMV-promoter, eucaryotic expression vector
pCI-neo WT β-Globin	~6.9 Kb, Amp^r, CMV-promoter, eucaryotic expression vector codes for the wild-type β-Globin (Neu-Yilik et al., 2001)
pCI-neo NS39 β-Globin	~6.9 Kb, Amp^r, CMV-promoter, eucaryotic expression vector codes for the β-Globin having a nonsense mutation at 39 (Neu-Yilik et al., 2001)
pcMVβ	7.2 Kb, Amp^r, CMV-promoter eucaryotic expression vector for β-galactosidase, (*Clontech,* GmbH, Hamburg)
pCMVluc	Amp^r, CMV-promoter, eucaryotic expression vector for firefly luciferase (600 bp *Nru/HindIII*-fragment from pcDNA3 is cloned into the *SmaI/HindIII* restriction sites of pGL3 basic vector). pGL3 basic is a eucaryotic expression vector for firefly luciferase under SV40 promoter
pCMV-RL	Amp^r, CMV-promoter, eucaryotic expression vector codes for firefly and renilla luciferase reporter genes. The CMV-

	promoter (654 bp) from pcDNA3 was cloned into phRnull (~3.3 Kb, *Promega*) vector (Ahlbory, 2005)
pGL3'	~5.3 Kb, Amp^r, SV40-promoter, eucaryotic expression vector codes for firefly luciferase (*Haines, UK*)
phc-jun(-1600/+740) –Luc	Amp^r, pXPI-eucaryotic expression vector codes for the human c-Jun promoter (-1600 to +740 bp) followed by luciferase gene
phpL	~5.4 Kb, Amp^r, SV40-promoter, eucaryotic expression vector codes for a RNA secondary structure followed by firefly luciferase gene (*Haines, UK*)
pRF	~6.5 Kb, Amp^r, CMV-promoter, eucaryotic expression vector codes for the renilla and firefly luciferases
pRApaf1F	~6.7 Kb, Amp^r, CMV-promoter, eucaryotic expression vector codes for the renilla and firefly luciferases, Apaf-1 IRES element of 233 bp is inserted in between the two luciferases (Coldwell et al., 2000*)*
pRc-MycF	~6.9 Kb, Amp^r, CMV-promoter, eucaryotic expression vector codes for the renilla and firefly luciferase, c-Myc IRES element of ~400 bp is inserted in between the luciferases (Stoneley et al., 1998*)*
pRMntF	~6.7 Kb, Amp^r, CMV-promoter, eucaryotic expression vector codes for renilla and firefly luciferases, Mnt IRES element of ~200 bp is inserted in between the two luciferases (Stoneley et al., 2001*)*
pRN-MycF	~6.9 Kb, Amp^r, CMV-promoter, eucaryotic expression vector codes for renilla and firefly luciferase, N-Myc IRES element of ~400 bp is inserted in between the two luciferases (Jopling and Willis, 2001*)*
pRSVc-Jun	5.4 kb, Amp^r, RSV-promoter, eucaryotic expression vector codes for the human c-Jun (~1.8 kb) (Angel et al., 1988)
pRXiapF	~8.1 Kb, Amp^r, CMV-promoter, eucaryotic expression vector codes for renilla and firefly luciferase, Xiap IRES element of ~1.6 bp is inserted in between the luciferases (Holcik and Korneluk, 2000*)*
pSG5-NFM#16.3	~5.4 Kb, Amp^r, SV40-promoter, eucaryotic expression vector codes for full length C/EBPβ
pTER+	~5.3 Kb, Amp^r, Zeo^r, H1 promoter (modified with tetracycline operator region), eucaryotic inducible expression vector.

	Derived from the pTER vector (4.5 Kb) inserted with 750 bp spacer region between the *BglII/HindIII* restrinction sites (Watering et al.,2003)
pUC18	~2.7 Kb, Amp^r , LacZ promoter, a cloning vector (*Invitrogen*)
pUC19	~2.7 Kb, Amp^r , LacZ promoter, a cloning vector (*Invitrogen*)

3.1.9 Primers

Primer	**5' ⟶ 3' sequence**	**Tm/°C**
BGH_rev (modified 5' IRD 800)	TAG AAG GCA CAG TCG AGG	56.0
human_pdcd4_cp_for	CTG GAT CCG CCA CCA TGG ATG TAG AAA ATG AGC AG	71.8
human_pdcd4_cp_rev	TCC TCG AGT TAG GCG TAG TCG GGC ACG TCG TAG GGG TAG TAG CTC TCT GGT TTA	>75
human_pdcd4_sense	ATG GAT GTA GAA AAT GAG CAG	54.0
human_pdcd4_antisen	TCA GTA GCT CTC TGG TTT AA	53.2
M13 Forward Primer	GTA AAA CGA CGG CCA GT	52.8
M13 Reverse Primer	GGA AAC AGC TAT GAC CAT G	54.5
siRNAhumpdcd4_603s	GAT CCC CGT GTT GGC AGT ATC CTT AGT TCA AGA GAC TAA GGA TAC TGC CAA CAC TTT TTA	>75
siRNAhumpdcd4_603as	AGC TTA AAA AGT GTT GGC AGT ATC CTT AGT CTC TTG AAC TAA GGA TAC TGC CAA CAC GGG	>75
siRNAhumpdcd4_1260s	GAT CCC CCA TTC ATA CTC TGT GCT GGT TCA AGA GAC CAG CAC AGA GTA TGA ATG TTT TTA	>75
siRNAhumpdcd4_1260as	AGC TTA AAA ACA TTC ATA CTC TGT GCT GGT CTC TTG AAC CAG CAC AGA GTA TGA ATG GGG	>75
T7 Primer (modified 5' IRD 800)	AAT ACG ACT CAC TAT AG	45.5
T3 Primer (modified 5' IRD 800)	ATT AAC CCT CAC TAA AG	45.5

3.1.10 Standard Buffers and Solutions

Buffer	**Quantity**	**Constituent**
Annealing Buffer pH 7.4	100 mM	Potassium acetate
	30 mM	HEPES
	2 mM	Magnesium acetate
DNA-Loading Buffer (5X)	20% (w/v)	Ficoll-400

(Agarose gel)	0.25% (w/v)	Orange G
DNA-Loading Buffer (5X)	96%	Formamide, deionized
(Sequencing gel)	20 mM	EDTA
	0.05% (w/v)	Bromophenol blue
	0.05% (w/v)	Xylencyanol FF
PBS-Buffer (10X) pH 7.4	137 mM	Sodium chloride
	2.7 mM	Potassium chloride
	4.3 mM	Disodium hydrogen phosphate
	1.4 mM	Potassium dihydrogen phosphate
RIPA Lysis Buffer	10 mM	Tris-HCl pH 7.8
	50 mM	Sodium chloride
	0.5% (w/v)	Sodiumdeoxycholate
	0.1% (w/v)	NP-40
	1 mM	SDS
Sequencing Gel Buffer	336 g	Urea
	80 ml	TBE long run buffer (10X)
	448 ml	Water
SSC-Buffer (20X)	3 M	Sodium chloride
pH 7.0	0.3 M	Sodium citrate-dihydrate
TAE (50X)	2 M	Tris base
pH 7.6	2 M	Sodium acetate
	0.05 M	EDTA
TBE-Buffer Long run (10X)	0.89 M	Tris base
pH ~ 8.3	0.89 M	Boric acid
	20 mM	EDTA
TE-Buffer (1X)	10 mM	Tris-HCl
	1 mM	EDTA
Plasmid DNA Isolation		
Resuspension Buffer	5 mM	Sucrose
	10 mM	EDTA
	25 mM	Tris-HCl pH 8.0
		RNase (add freshly)
Lysis Buffer	0.2 M	Sodium hydroxide
	1% (w/v)	Sodium dodecyl sufate (SDS)
Neutralization Buffer	3M	Potassium acetate
Genomic DNA Isolation		
Lysis Buffer	100 mM	Sodium chloride
	10 mM	Tris-HCl pH 8.0

	50 mM	EDTA
	0.5% (w/v)	SDS
	20 μg/ml	RNase A
	100 μg/ml	Proteinase K
PolyA RNA Isolation		
Lysis Buffer	500 mM	Sodium chloride
	10 mM	Tris-HCl pH 7.2
	10 mM	EDTA
Binding Buffer	0.5 M	Sodium chloride
	10 mM	Tris-HCl pH 7.2
	0.1 mM	EDTA
	0.2% (w/v)	SDS
Wash Buffer	100 mM	Sodium chloride
	10 mM	Tris-HCl pH 7.2
	0.1 mM	EDTA
	0.2% (w/v)	SDS
Elution Buffer	10 mM	Tris-HCl pH 7.2
	0.1 mM	EDTA
	0.2% (w/v)	SDS
Southern Blotting		
DNA-Loading Buffer (5X) I	50% (v/v)	Glycerol
(Southern Blotting)	0.25% (w/v)	Bromphenol blue
	0.25% (w/v)	Xylencyanol FF in 0.5X TBE
20X SSC	0.3 M	Sodium citrate pH 7.0
	3 M	Sodium chloride
Denaturation Buffer I	0.5 M	Sodium hydroxide
	1 M	Sodium chloride
Neutralization Buffer I	0.5 M	Tris-HCl
	1. 5 M	Sodium chloride
Denaturation Buffer II	0.4 M	Sodium hydroxide
Neutralization Buffer II	0.2 M	Tris-HCl in 1X SSC
Hybridization Solution	5X	SSC
	20 mM	Sodium phosphate buffer pH7.0
	5X	Denhardt's Solution
	1% (w/v)	SDS
	50% (v/v)	Formamide, deionised
	15 μg/ml	Denatured Salmon sperm DNA
		denatured by heat at 95°C, 10 min

Denhardt's Solution (50X)	1% (w/v)	Ficoll
	1% (w/v)	Polyvinyl pyrrolidone
	1% (w/v)	BSA
Washing Solution I	5X	SSC
	0.1% (w/v)	SDS
Washing Solution II	2X	SSC
	0.1% (w/v)	SDS
Stripping Solution	0.1X	SSC
	1% (w/v)	SDS
Northern Blotting		
RNA Loading Buffer	50% (v/v)	Formamide, deionized
	10% (v/v)	10X MOPS pH 7.0
	18% (v/v)	37% Formaldehyde
	0.2% (w/v)	Bromophenol blue
10X MOPS	0.2 M	MOPS pH 7.0
	0.1 M	Sodium acetate
	0.01 M	EDTA
20X SSPE	0.2 M	Sodium dihydrogen phosphate pH 7.4
	3 M	Sodium chloride
	0.02 M	EDTA
Hybridization Solution	5X	SSPE
	5X	Denhardt's Solution
	50% (v/v)	Formamide, deionised
	1% (w/v)	SDS
	10% (w/v)	Dextran sulfate sodium salt
	15 μg/ml	Denatured Salmon sperm DNA, denatured by heat at 95°C for 10 min
Transfection		
DNA-Precipitation Buffer	10 mM	Tris-HCl pH 7.8
	1 mM	EDTA
	300 mM	Sodium chloride
Glycerol-Shock Solution	15% (v/v)	Glycerol
	1X	HBS
β-Galactosidase Assay		
Reaction Buffer	0.1 M	Sodium dihydrogen phosphate pH 8.0
	1 mM	Magnesium chloride
	0.001% (v/v)	Galacton
Stop Buffer	0.2 M	Sodium hydroxide

	5% (v/v)	Emerald as enhancer
Luciferase Assay		
Reaction Buffer	25 mM	Glycyl-Glycine pH 7.8
	2.2 mM	ATP
	11.2 mM	Magnesium chloride
Injection Buffer	25 mM	Glycyl-Glycine pH 7.8
Isoelectric Focusing		
Rehydration Buffer	8M	Urea
	2% (w/v)	Triton-X-100
	Pinch	Bromophenol bule
	2.8 mg/ml	DTT
	0.5% (v/v)	IPG buffer
Equilibration Buffer	50 mM	Tris-HCL pH 8.8
	6 M	Urea
	30% (v/v)	Glycerol
	2% (w/v)	SDS
	10 mg/ml	DTT
	25 mg/ml	Iodoacetamide
	Pinch	Bromophenol blue
SDS-PAGE		
Laemmli Buffer (3X) [-DTT]	187 mM	Tris / HCl, pH 6.8
	6% (w/v)	SDS
	30% (w/v)	Glycerol
	0.01% (w/v)	Bromophenol blue
	5%	1 M DTT (added freshly)
SDS-PAGE Running Buffer	250 mM	Tris base
(10X)	1.92 M	Glycine
	0.1% (w/v)	SDS
CBB-staining solution	45% (v/v)	Ethanol
	10% (v/v)	Acetic acid
	0.25%	Coomassie Brillian Blue
CBB-destaining solution	45% (v/v)	Ethanol
	10% (v/v)	Acetic acid
Ponceau-S solution	1% (v/v)	Acetic acid
	0.5% (w/v)	Ponceau S
Western Immunoblotting		
Blotting Buffer (1X)	192 mM	Glycine
	25 mM	Tris base

	20% (v/v)	Methanol
Block Solution	5% (w/v)	Skimmed milk powder
	1X	PBS
Primary Antibody Solution	10% (v/v)	Primary antibody prepared in
	1X	PBS
Secondary Antibody Solution	0.1% (v/v)	HRP-conjugated secondary antibody prepared in
	1X	PBS
Wash Buffer	1X	PBS
	0.05% (v/v)	Tween

3.2 The Molecular Biology Techniques

3.2.1 Media and Agar plates

LB_0-medium	1% (w/v)	Sodium chloride
	1% (w/v)	Tryptone
	0.5% (w/v)	Yeast extract
For the plates	0.5% (w/v)	Agar
Antibiotics		
LB_{Amp}-Agar plates	+ 100 µg/ml	Ampicillin
LB_{Kan}-Agar plates	+ 50 µg/ml	Kanamycin
YT-medium	0.5% (w/v)	Sodium chloride
	0.8% (w/v)	Tryptone
	0.5% (w/v)	Yeast extract

3.2.2 Preparation of Competent *E.coli* cells

The term "competent cells" is used for the bacterial cells with enhanced ability to take up exogenous DNA and thus to be transformed. Competence can arise naturally in some bacteria (e. g. *Pneumococcus, Bacillus*); a similar state can be induced in *E. coli* by chilling the cells in presence of divalent cations, such as calcium chloride prepares the cell walls to become permeable to the plasmid DNA.

To produce competent *E.coli* cells 50 ml of LB-medium was inoculated with the bacterial strain of choice and incubated overnight at 37°C. The next day 100 ml LB-medium was inoculated with approximately 5 ml of the overnight culture to give a final optical density of OD_{650} = 0.1, and the bacterial suspension was grown at 37°C to OD_{650} = 0.7–1.0. 50 ml culture was centrifuged (5 min, 6500 rpm, 4°C), obtained pellet was resuspended in 20 ml of ice-cold 0.1 M magnesium chloride-solution and incubated on ice for 10 min. After a second centrifugation (5 min, 6500 rpm, 4°C) the cell pellet was resuspended in 20 ml ice-cold 0.1 M calcium chloride solution and kept on ice for further 25 min. Finally the suspension was centrifuged (5 min, 6500 rpm, 4°C), the pellet was resuspended in 2 ml ice-cold 0.1 M calcium chloride solution, and 550 µl of glycerol (87% (v/v)) was added. Aliquots of 100 µl were immediately freezed into the liquid nitrogen. Competent cells were stored at -70°C.

3.2.3 Transformation of Competent Bacteria and Blue/White Screening

The process of introducing naked DNA molecules into the competent bacterial cells is called bacterial transformation. The permeability of DNA into the competent cells is

achieved by subsequent, immediate heating and cooling at particular temperature for specific duration. During heat-shock the pores in the membrane of bacteria become wider and exogenous DNA can diffuse into the cells.

pCR®2.1-TOPO® vector has an expression cassette for the regulatory part of the *lac*-operon including the 5' part of the gene *lacZ*, which codes α-peptide-β-galactosidase. This peptide is able to complement *in vivo* the defective bacterial protein β-galactosidase, which lack amino acids 11-41 from the N-terminus of the protein (deletion *lacZ*ΔM15). As a result, transformation of the cells that have such a deletion (e. g. TOP 10F') by a vector carrying the beginning part of the *lacZ* change the phenotype of the bacteria form Lac^- to Lac^+. When a PCR product is inserted in the TOPO vector, the synthesis of the α-peptide is disrupted and bacteria have Lac^- phenotype. When the plates are added with the chromogenic substrate, X-Gal and the inductor, IPTG for the *lac*-operon, Lac^- colonies are colorless, while Lac^+ colonies have a blue color.

For transformation, one aliquot (100 µl) of competent cells was thawed on ice, 10 µl of ligation mix or 1 µg Plasmid DNA was added and the mixture was incubated in the ice for 5 min. To allow the DNA to permeate the cell membrane, the heat-shock procedure was applied for 2 min at 37°C. After incubation on ice for 5 min, 300 µl LB-medium was added and the cells were incubated at 37°C for 30 min. For the phenotypic selection of the antibiotic resistance, the cells were then plated onto LB-plates containing 100 µg/ml ampicillin and incubated at 37°C until single colonies were grown (~18hr). In case of blue/white screenings with pCR®2.1-TOPO® Cloning vector (*Invitrogen*), additionally 40 µg/ml, 0.01% (w/v) X-Gal and 1 mM IPTG had been spread on the LB-plates before seeding the bacteria.

3.2.4 Plasmid DNA Isolation

Plasmid DNA was isolated from the *E.coli* cultures grown overnight in the ampicillin containing LB-medium. The medium was inoculated with the bacteria and transformed with the desired plasmid DNA. The plasmid DNA could be isolated by different methods, depending on the further experimental step. For checking the colonies formed by routine cloning procedures, alkaline lysis method is used. In order to prepare plasmid DNA for sequencing, either the QIAprep Spinminiprep Kit or the Nucleospin kit was used. For the preparation of larger amount of plasmid DNA for transient transfection experiments of eucaryotic cells, the corresponding QIAGEN Plasmid Maxi Kit or the Nucleospin Maxi kit was used according to the kit instructions.

The method of plasmid DNA isolation by the kits is also based on the principle of alkaline lysis of bacterial cells. It irreversibly denatures and further precipitates the genomic DNA, proteins and the cell debris by using alkali and an anionic detergent. But only the plasmid DNA can be selectively renatured to its original structure by providing the neutralization pH. Then the plasmid DNA is absorbed to the silica column in the presence of high salt concentrations. After removal of molecular contaminants by washing at pH 7.0, plasmid DNA is eluted by a low salt buffer at pH 8.5. Further the DNA was precipitated and purified by isopropanol and ethanol treatment, respectively. For the minipreparation, up to 10 µg of plasmid DNA can be obtained from 1-2 ml of bacterial culture, while maxi preparations were performed with 200 ml of bacterial culture yielding up to 500 µg-1 mg of plasmid DNA.

For the minipreparation of plasmid DNA, overnight *E.coli* culture of 1.5 ml was pelleted by 1 min centrifugation at 13000 rpm. The pellet was suspended in 100 µl of resuspension buffer and kept at the RT for 5 min. Then 200 µl of lysis buffer was added, and the complete mixing was ensured by inverting the tubes. After the lysate has become clear, 150 µl of the neutralization buffer was added and mixed again by inversion. The mixture was centrifuged for 5 min at 13000 rpm, the supernatant was collected into a fresh 1.5 ml microfuge tube and the DNA was precipitated by adding equal volume of isopropanol. DNA pellet was formed by centrifugation for 20 min at 14000 rpm in a cold centrifuge and then washed with 500 µl of 80% ethanol. The pellet was suspended in 50 µl of TE buffer.

3.2.5 Quantification of DNA

UV spectrophotometer is used to measure the concentration of nucleic acids at the wavelength maximum of 260 nm. The pi electrons present in the aromatic ring system of the purine and pyrimidine bases absorb the UV light and make it suitable for the quantification of DNA/RNA. The absorption of 1 OD, using a 1 cm cuvette is equivalent to approximately 50 µg/ml dsDNA. The purity of the isolated nucleic acids is determined by measuring the optical density at 280 nm where aromatic amino acids of proteins show the highest absorbance. The ratio of OD_{260}/OD_{280} is about 1.8 for the pure DNA solutions. Lower values are a sign of protein contamination. The formula for the final concentration is: DNA concentration [µg/µl] = OD_{260} X dilution factor X 0.05

3.2.6 Modification of DNA by Enzymes

Restriction endonucleases are the enzymes, purified from the bacteria, which recognize and cut inside the double-stranded DNA at specific palindromic sites. After cutting, they produce DNA fragments with sticky ends having overhangs or blunt ends. Restriction

digests were performed at appropriate temperature and buffer conditions for each specific enzyme according to the information in the manufacturers' manual. For the cleavage of DNA the following reaction mixture was prepared and incubated for 60-90 min at required temperature in a water bath.

1 µg	DNA
1 µl	Enzyme 1 (10 U/µl)
0.5 µl	Enzyme 2 (20 U/µl)
2 µl	10X Buffer (1,2,3 or 4)
2 µl	10X BSA (optional)
Add to 20 µl	dd water

3.2.7 Agarose Gel Electrophoresis

Nucleic acids can be separated with respect to their size in an agarose matrix by gel electrophoresis. In order to obtain optimal separation of nucleic acid fragments, the concentration of agarose was varied according to the expected fragment sizes. The concentration of agarose in TAE buffer varied from 0.8% (w/v) for large fragments (>500 bp) and 2% (w/v) for smaller fragments. The electrophoresis was carried out for the separation of DNA fragments at 30-100V in 1X TAE buffer. Prior to electrophoresis DNA-loading buffer was added to the samples, and the DNA-SmartLadder (*Eurogentec*) was used as a reference for the size determination. For detection of the DNA fragments, gels were stained for 15-30 min in an ethidium bromide containing solution (0.5 µg/ml in 1X TAE buffer) and visualized under the UV-light at 256 nm excitation wavelength.

3.2.8 Extraction of DNA Fragments from Agarose gels

Extraction of the DNA fragments from the agarose gel was performed using the QIAquick Gel Extraction Kit according to the manufactures instructions. The DNA band was visualized under the UV-light and was cut out from the agarose gel. The piece was melted at 50°C in QG buffer, having appropriate high salt concentration and pH value ≤ 7.5 to allow the DNA to bind to the silica membrane. After washing, DNA was eluted from the membrane with elution buffer (pH > 7.5). The final volume for DNA fragment usually was 30 µl for PCR products and 50 µl for the digested vector.

3.2.9 Ligation

For the ligation of the restricted DNA fragments into the linearized vector, the Rapid DNA Ligation Kit was used according to the manual instruction. The buffers in the kit

allow the reaction to occur in 20 µl volume for 5 min at RT. The optimal molar ratio of vector/insert is 1/5 for best ligation.

3.2.10 Polymerase Chain Reaction (PCR)

PCR is a molecular biological technique, which allows to enzymatically amplify specific DNA fragments *in vitro.* Two synthetic oligonucleotide primers, which are complementary to two regions of the target DNA (one for each strand) to be amplified, are added to the target DNA, in the presence of excess of all 4 deoxynucleotides and heat-stable DNA polymerase (e. g. *Taq, Pfu* polymerases). In a series of temperature cycles, the target DNA is repeatedly denatured, annealed to the primers and a daughter strand extended from the primers. As the daughter strands themselves act as templates for subsequent cycles, DNA fragments matching both primers are amplified exponentially. The PCR allows insertion of desirable restriction sites into the end(s) of amplified fragments, which will be used in subsequent cloning of DNA into any required vector. Reaction components are mixed in 20 or 50 µl PCR microfuge tubes and placed into the PCR thermal cycler, where the required parameters for the reaction can be programmed. The following reaction mix was used:

5 µl	10 X PCR Buffer
2.5 µl	$MgCl_2$
0.5 µl	dNTP-Mix (20 mM)
1 µl	Template DNA (10 ng/µl)
2 µl	5’ primer (10 pMol/µl)
2 µl	3’ primer (10 pMol/µl)
1 µl	*Taq*-polymerase (1 U/µl)
36 µl	dd water

The following PCR program or small modified versions were used

Step	Time	Temperature	Cycle
1	5 min	95°C	1 X
2	1 min	95°C	
3	1 min	(Tm*-2)°C	30 X (steps 2-4)
4	1 min 30 sec	72°C	
5	10 min	72°C	1 X

Tm* is the lowest Tm of the two primers.

After the PCR reaction, 20 µl of the PCR products were loaded onto the 1.5% agarose gel for purification of the amplified fragments from the free nucleotides. The fragments

were cut and extracted from the gel. Then the fragments were ligated to the pCR®2.1-TOPO® vector for further sequencing analysis.

3.2.11 T/A-cloning of PCR products with TOPO TA System

The cloning vector pCR2.1-TOPO is supplied linearized with single 3´-thymidine (T) overhangs and topoisomerase I covalently bound to the vector. The *Taq* polymerase has a nontemplate-dependent terminal transferase activity that adds a single deoxyadenosine (A) to the 3´ ends of the PCR products. As the vector supplied in the kit has overhanging 3´ deoxythymidine (T) residues, it allows PCR inserts to ligate efficiently with the vector. The topoisomerase I from *Vaccinia* virus binds to the duplex DNA at specific sites and cleaves the phosphodiester backbone after 5′-CCCTT in one strand. The energy from the broken phosphodiester backbone is conserved by formation of a covalent bond between the 3′ phosphate of the cleaved strand and a tyrosyl residue (Tyr-274) of topoisomerase I. The phospho-tyrosyl bond between the DNA and enzyme can subsequently be attacked by the 5′ hydroxyl of the original cleaved strand, reversing the reaction and releasing topoisomerase. For the ligation, 0.5 µl of the pCR2.1-TOPO vector was mixed together with 4.5 µl of the gel purified PCR product and 1 µl of salt solution. The mixture was incubated for 5 min at RT and added to an aliquot of competent bacterial cells for transformation.

3.2.12 DNA Sequencing

The sequencing of the DNA is based on dideoxy method, where *in vitro* DNA synthesis is performed in the presence of chain-terminating dideoxyribonucleoside triphosphates (ddNTPs). If the primer is labeled with a fluorescent dye, it is possible to detect the DNA fragments generated by PCR automatically while they are running through a polyacrylamide gel. This strategy is followed by using *Thermo Sequenase fluorescent labeled primer cycle sequencing Kit* to create the fluorescently labeled PCR products and the automatic Sequencer Gen Read IR4200 to detect them by IR-laser (800 nm), while they are passing through the sequencing gel. The sequences obtained this way are analyzed using the supplied software. For the reaction, fluorescently labeled universal primers were used: T7 and T3 for pCR®2.1-TOPO® vector and M13 for pTER+ plasmids. The following mixtures were made for each "nucleotide":

0.5 µl	A, T, G or C labeling-mix
1 µg	Template to be sequenced
0.5 µl	Fluorescent labeled primer (1 pmol/µl)
5.5 µl	dd water

The PCR program

Step	Time	Temperture	Cycle
1	5 min	95°C	1 X
2	30 sec	95°C	
3	40 sec	(Tm*-2)°C	40 X (step 2-4)
4	1 min 30 sec	72°C	
5	10 min	72°C	1 X

When the PCR was finished, 4 µl of the loading dye was added to each sample, and 2 µl of each sample was loaded onto the sequencing gel (section 3.2.13).

3.2.13 Sequencing Gel

For the sequencing of the DNA fragments with universal fluorescent-labeled primers, the following sequencing gel mixture was used.

5.3% (v/v)	Rapid-Gel-Acrylamide 40%
10% (v/v)	10 X TBE (long run)
0.625% (v/v)	APS (10% (w/v))
0.13% (v/v)	TEMED

The gel was pre-run for ~15 min and then samples were loaded. The gel was run overnight at 1500 V.

3.2.14 Isolation of Genomic DNA from the Eucaryotic cells

For the isolation of genomic DNA, the cells are placed in a solution of proteinase K and SDS and incubated until most of the cellular protein is degraded. The digest is deproteinized by successive phenol-chloroform-isoamylalcohol extractions, recovered by ethanol precipitation, DNA pellet was dried and resuspended in buffer. Phenol efficiently denatures proteins and probably dissolves the denatured protein. Chloroform is another protein denaturant and isoamylalcohol is an antifoaming agent. The DNA is effectively precipitated by absolute ethanol at high salt concentration and 70% ethanol subsequently desalts the genomic DNA.

Genomic DNA was isolated from the DT40 WT and knock out clones. When the cells were confluent (~ $1x10^7$/ml), 2 flasks of suspension cells were spinned at 1500 rpm, 4°C for 5 min. The cell pellet was washed with ice cold PBS twice. The cell pellet was resuspended in 1 ml of genomic DNA lysis buffer, and Proteinase K and RNAse were added to a final concentration of 100 µg/ml and 20 µg/ml, respectively. The cells were lysed and incubated in a water bath at 50°C for 6 hr to overnight. The lysate was transferred to a 2 ml microfuge tube and extracted with equal volume of

phenol-chloroform-isoamylalcohol (25:24:1) mixture followed by centrifugation (3000-5000 rpm, 10-15 min, 4°C). The upper phase was recovered and repeatedly extracted with the solvent mixture. Half volume of 5M lithium chloride and 1 volume of absolute ethanol were added to the upper phase and vigorous shaking followed by centrifugation (14000 rpm, 15 min, 4°C) precipitated the genomic DNA. Finally the DNA pellet was washed, dried and dissolved in 200 µl of TE buffer by placing in a water bath upto 67°C. The DNA concentration was measured.

3.2.15 Isolation of PolyA RNA from the Eucaryotic cells

For handling RNA, all solutions and devices as well as pipette tips and reaction tubes were sterilized by routine sterilization techniques. Gloves were worn throughout the procedure, glassware was treated at 200°C for at least 4 hr and solutions were treated additionally with 0.1% (v/v) diethylpyrocarbonate (DEPC) to inactivate RNAses.

The nascent mRNA in eukaryotic systems is modified by adding adenine (~250, Poly AMP nt) at the 3' end. The PolyA enhances both the lifetime and translatability of mRNA. These polyA tails are exploited in their extraction and purification. In chromatography, oligo dT are attached to the cellulose matrix. The Oligo dT are short segments of deoxyribose thymidine nt, which could anneal to complementary sequences, polyA. When the cell extract is run through the column the mRNA with polyA tail get attached to the oligo dT bound to cellulose matrix of the column and are eluted by either slightly changing the pH or ionic strength.

For one sample 3-5 petri dishes (1.0-1.5x10^7 cells) of untransfected or transfected cells were harvested in ice cold PBS and washed once with 5 ml PBS. The cells were suspended in 3 ml of cold lysis buffer and proteinase K was added to a final concentration of 200 µg/ml. After a min, SDS was added to a final concentration of 10% (w/v), followed by shearing of the DNA by passing the cell suspension first through a 50 mm, later through a 25 mm needle. The proteinase K concentration was raised to 300 µl/ml and cells were incubated at 37°C for 2-3 hr. In between the oligo dT cellulose was washed for 3 times with 0.1 M sodium hydroxide (centrifugation: 3 min, 2000 rpm, 4°C) and several times with water until the pH of the solution is neutral. After washing for three times with binding buffer oligo dT cellulose in binding buffer (~1-2 ml packed volume dT cellulose) was applied to the cell extracts. Solutions were stirred overnight at RT. After pelleting of the cellulose (3 min, 2000 rpm, 4°C) it was resuspended twice in 10 ml binding buffer and finally resuspended in 5 ml binding buffer and loaded onto the column. The columns were also treated with 0.1 M sodium hydroxide and washed with water before loading. Loaded columns were washed three

times with 5 ml wash buffer and finally polyA RNA was eluted with 3 ml elution buffer. The concentration was determined by measuring the OD_{260} and for storage at -20°C, RNA was precipitated by adding 0.3 M sodium acetate and 3 volumes of absolute ethanol.

3.2.16 Genomic DNA-Agarose gel Electrophoresis and Southern Blotting

In Southern blotting, the DNA fragments are transferred from an agarose gel to a nylon or nitrocellulose membrane by capillary action, preserving the spatial arrangement. The DNA molecules are immobilized on the membrane, either by heating or by ultraviolet irradiation and can be detected by hybridization with a radioactive DNA probe.

Southern blotting was used to analyze the DT40 knock-out clones generated by homologous recombination. 10 µg of prepared genomic DNA from the WT and the clones were digested by using 10 U of *ApaI* enzyme in a 50 µl digest for overnight at RT. The next day 10 µl loading buffer was added to the digest. Then 50 µl of each DNA sample were loaded to a thick 0.9% agarose gel and the gel was run for 3-4 hr at 120 V. The gel was denatured by incubating with denaturation buffer for 30 min followed by incubation with the neutralization buffer for 30 min by placing on a shaker at RT. DNA was then blotted onto a nylon membrane, where the mobile phase was 10X SSC buffer.

Here, the upward capillary transfer method was used to transfer the DNA from the gel to the nylon membrane. The transfer pyramid set up stacks the following materials in the given order. A clean glass tank containing 10X SSC was overlaid by a clean glass plate. Over the glass plate, the 3MM whatman filter paper wick is placed and both ends of the whatman filter paper were submerged into the tank buffer. The gel was placed over the whatman filter paper followed by the nylon membrane over the gel at once. The whatman filter papers were cut to the same size of the membrane and covered the membrane. Then, filter paper towels were cut and stack over the whatman filter paper upto 4-5 cm height. Above this set up, a glass plate and a weight was placed. This pyramid structure was left overnight. The next day membrane was washed with 2X SSC to remove the agarose particles, again treated with denaturation and neutralization buffer each for 1 min and irradiated for 100 sec with UV-light (254 nm) for immobilizing the DNA non-covalently on the nylon membrane.

3.2.17 RNA-Agarose gel Electrophoresis and Northern Blotting

RNA samples were separated on a 1% denaturing agarose gel. For 10 ml gel solution 1% (w/v) agarose was dissolved in 1 ml 10X MOPS and 7.2 ml DEPC treated water using a microwave oven. For small gels (8 samples) 35 ml were needed and for bigger

gels (upto 20 samples) 180 ml of gel solution were prepared. After cooling down to 60°C, 18% (v/v) formaldehyde was added to the gel solution and the solution was poured into the gel running device. From the RNA preparations a volume containing around 2 µg of RNA was taken for each sample, RNA was precipitated (30 min, 14000 rpm, 4°C) and air died. The pellet was resuspended in 20 µl RNA loading buffer and heated for 10 min at 65°C. The composition of the loading buffer is given below. Gel electrophoresis was performed in 1X MOPS running buffer at 100-120 V for 3 hr. It is an optional step that the gel is stained in ethidium bromide for 15 min and visualized under UV-light (320 nm). The northern blotting was done as shown in the section 3.2.16 by upward capillary transfer method.

3.2.18 Radioactive Labeling of DNA with α^{32}P-dCTP and with ^{3}H-dUTP

Radioactive labeling of DNA for Southern and northern blotting (section 3.2.16 and 3.2.17) experiments was performed with α^{32}P-dCTP, using the Klenow fragment of the DNA polymerase I. Radioactive labeling of DNA probes was performed using the 'Megaprime DNA labeling system'. This system uses random sequence nanomer as primers for DNA synthesis on denatured template DNA at numerous sites along its length. The primer-template complex is a substrate for the Klenow fragment of DNA polymerase I. By substituting a radiolabeled nucleotide for a non-radioactive equivalent in the reaction mixture, makes the newly synthesized DNA, radioactive. The absence of the 5'-3' exonuclease activity associated with the DNA polymerase I ensures that labeled nucleotides incorporated by the polymerase are not subsequently removed as monophosphates.

For this procedure 25-35 ng of DNA were taken, denaturated for 5 min at 95°C with 5 µl of primer solution. Then 10 µl of labeling buffer, 2 µl of Klenow enzyme (1 U/µl) and 5 µl of α^{32}P-dCTP (10 mCi/µl, ~3000Ci/mmol) were added and incubated for 30 min at 37°C. Purification from the non-incorporated radioactive nucleotides was performed with centrifugation for 3 min at 3000 rpm through MicroSpin^{TM}G-50 Columns. After this procedure the pure radiolabeled DNA probe denatured and directly added to the Southern hybridization solution.

3.2.19 Hybridization and Washing

The hybridization experiment can be divided into three steps. First, the membrane is incubated in a prehybridization solution containing reagents that block nonspecific DNA binding sites on its surface, thereby reducing the background hybridization. Denhardt's solution and sperm DNA are the blocking agents. In the second step, the prehybridization solution is replaced by fresh buffer containing the labeled probe and

an overnight incubation is carried out to allow the probe to bind to the target sequences in the immobilized DNA. In the final stage of the experiment, the membrane is washed with a series of solutions that gradually remove the non-specifically bound probes. The membrane was placed in a hybridization flask and prehybridized with 10 ml of the hybridization mixture containing denaturated Salmon-sperm for 2-3 hr in hybridization oven at 42°C. Afterwards the prehybridization solution was changed and 10 ml of fresh hybridization solution containing the denaturated-labeled probe was added for hybridization.

Washing, Exposure and Stripping

After hybridization the membrane was washed first with washing solution I for 20 min and then with washing solution II 2-3 times for 20 min each with shaking at 55°C. Finally the membrane was wrapped with polyethylene and exposed to the phosphorimager screen. The screen was developed by phosphorimager. For the hybridization of a northern blot with different probes previously hybridized probes were removed by heating the membrane in stripping solution for 20 min at 100°C.

3.2.20 Cell Cycle Analysis by FACS Method

Flow cytometry is a technique for counting, examining and sorting microscopic particles suspended in a stream of fluid. The measurement of the DNA content of cells was one of the first major applications of flow cytometry. The DNA content of the cell can provide a great deal of information about the cell cycle, and consequently the effect of the added stimuli on the cell cycle. e.g. downregulated genes or UV treatment. Fluorescence-activated cell sorting (FACS) is a type of flow cytometry, a method for sorting a suspension of biologic cells into two or more containers, one cell at a time, based on the specific light scattering and fluorescence characteristics of each cell. The most commonly used dye for DNA content/cell cycle analysis is propidium iodide (PI). It can be used to stain whole cells or isolated nuclei. The PI intercalates into the major groove of double-stranded DNA and produces a highly fluorescent adduct that can be excited at 488 nm with a broad emission centered around 600 nm. Since PI can also bind to double-stranded RNA, it is necessary to treat the cells with RNAse for optimal DNA resolution.

In the present work, the adherent or suspension cells were harvested and washed with PBS for twice. The cells were fixed with 70% methanol at 4°C for few hr to overnight. After fixation, the cells were washed with PBS and eluted in 425 µl PBS and 50 µl RNAse followed by incubation for 20 min at 37°C. Finally, 25 µl of PI was added to the cell suspension and fluorescently labeled cells were measured by FACS.

3.3 The Cell Culture Techniques

3.3.1 Cell lines and Medium

Name	Nature of the Cell line	Medium
A549	Human, small cell lung carcinoma, adherent cell line derived from epithelial cells	MEM Medium 10% (v/v) Fetal bovine serum (FBS) 1% (v/v) L-Glutamine 1% (v/v) Penicillin/Streptomycin (P/S)
DT40	Chicken, borsa lymphoma suspension cell line derived from lymphoblast cells	ISCOVE'S Medium 8% (v/v) FBS 2% (v/v) Chicken serum 1% (v/v) L-Glutamine 1% (v/v) P/S 0.001% (v/v) β-Mercaptoethanol
HeLa	Human, cervical carcinoma, adherent cell line derived from epithelial cells	DMEM/RPMI Medium 10% (v/v) FBS 1% (v/v) L-Glutamine 1% (v/v) P/S
HTB-133	Human, breast ductal carcinoma, adherent cell line derived from epithelial cells	DMEM/RPMI Medium 10% (v/v) FBS 1% (v/v) L-Glutamine 1% (v/v) P/S
QT6	Japanese Quail, fibrosarcoma, adherent cell line derived from fibroblasts	DMEM Medium 10% (v/v) FBS 1% (v/v) L-Glutamine 1% (v/v) P/S

3.3.2 Passage and Cultivation of cells

Cells were cultured in 10 cm sterile petri dishes or T75 culture flasks with the appropriate medium (section 3.3.1) and grown in a CO_2-incubator, at 37°C in a water saturated atmosphere with 5% (v/v) CO_2. Confluent cells were passaged and plated at 1:5 to 1:40 dilutions in new culture flasks. For passaging, adherent cells were washed with 1X PBS after removal of the medium and treated with 0.5-1 ml trypsin/EDTA (0.2%-0.5% (w/v)) solution at 37°C for 2 min. They were plated after resuspension in fresh culture medium. Suspension cells were passaged by taking the appropriate volume aliquots according to the desired dilutions from the dish with confluent cells and transferring them to fresh medium in the new dishes.

3.3.3 Cell Counting

The number of cells for the transfection experiments was determined using a Neubauer haemocytometer, and the cell suspension was diluted with growth medium in order to obtain the desired concentration. 10 µl of the cell suspension was loaded onto the haemocytometer and counted under the microscope.

3.3.4 Transfection and Harvesting of Adherent and Suspension Cell lines

During transfection, foreign DNA is introduced into the eucaryotic cells. A part of it enters the nucleus during the cell division and is transcribed. In the transient transfection, most of the DNA is not integrated in the chromosomes of the cell and therefore will be degraded after some time. The transfected DNA is integrated into the genome in the stable transfection method.

Transfection and Harvesting of Adherent cells

In this work, A549, HeLa, HTB-133 and QT6 cells were transfected using the calcium co-precipitation method, wherein co-precipitation of calcium phosphate and DNA cause their adsorption on the cell surface, from where it can be taken up by the cells via phagocytosis. To increase the transfection efficiency a glycerol-shock is applied 3-4 hr after transfection, which facilitates the uptake of the foreign DNA.

One day prior to the transfection, $1.5x10^5$/ml cells were seeded on 10 cm petri dishes described in 3.3.2. The plasmid DNA to be transfected was precipitated at -20°C overnight by adding 144 µl of DNA precipitation buffer and 600 µl of absolute ethanol. Immediately before the transfection DNA was pelleted (13000 rpm, 20 min, 4°C), and supernatant was removed. The pellet was dried in the laminar-flow hood and resuspended in 438 µl of sterile water and 62 µl of 2 M sterile calcium chloride-solution. This mixture was added to 500 µl of sterile 2X HBS buffer with vortexing. This solution was then pipetted drop wise onto the cells in the petri dish and incubated for 3-4 hr in the CO_2-incubator. To apply the glycerol shock, the culture medium was removed, cells were treated with 2 ml of shock solution for 2 min, washed twice with PBS and fresh culture medium was added. The cells were harvested after 24 or 48 hr of the transfection. The culture medium was removed and cells were washed twice with ~5 ml of PBS at RT, scraped in 1 ml of PBS and transferred to a microfuge tube. Cells were then pelleted (1500 rpm, 5 min, at 4°C) and used either for reporter gene assays or boiled with Laemmli buffer for SDS-PAGE (section 3.4).

Transfection and Harvesting of DT40 cells

To transfect the suspension cells, an electrophysical method was used by employing a short electric pulse to increase permeability of the cell membrane. DNA can penetrate into the cells through the pores generated by such electric impulse. Membranes restore their properties after the termination of the applied electrical pulse. The DT40 cells were counted, pelleted (750 rpm, 10 min, RT), washed once with PBS, and suspended in PBS at a concentration of $1.5x10^7$ cells/ml. 300 µl of the cell suspension containing $1.5x10^7$ cells/ml were taken in an electroporation cuvette (0.4 cm) and then the plasmid DNA was added. The cuvette was placed on ice for 10 min prior to the electroporation. The following electroporation programs were used in the electroporation device. After the electroporation, the cells were incubated on ice for 5 min before culturing in the dishes.

Transient tranfection	330 V	
	900 µF	
	86 ms	
	99 ohms	
Stable transfection (2 consecutive pulses)	Pulse I	Pulse II
	1200 V	160 V
	25 µF	1500 µF
	2.47 ms	148 ms
	99 ohms	99 ohms

For transient transfection, the electroporate was suspended in 10 ml of the culture medium in 10 cm petri dishes and incubated for 24 hr and harvested by centrifugation (1500 rpm, 5 min, at 4°C) in the next day. The pellet was transferred to a microfuge tube, washed twice with PBS, and lysed in respective lysis buffer either for reporter gene assay or SDS-PAGE analysis. For stable transfection, the electroporate was suspended in 10 ml medium, distributed as 100 µl/well into a 96 well plates. The following day the required amount of antibiotics were diluted in 10 ml medium and distributed as 100 µl per well. In 2-3 weeks, the stable clones were developed, the cells from single well/single clone were transferred into the 24/6 wells plates and further grown for analysis.

3.4 The Protein Biochemical Techniques

3.4.1 Reporter-gene Assays

A reporter-gene encodes an easily assayable product that is coupled to the regulatory sequences and a promoter of interest. Upon transfection into suitable cells reporter-gene can then be used to determine the functional efficiency of the promoter or the factors that affect the promoter or the regulatory sequence. In this work renilla and firefly luciferase dual reporter gene constructs were generated by inserting DNA fragments of the untranslated region from different genes associated with apoptosis and cancer. The activity of the reporter-gene is determined by the emission of light. The second reporter vector used in most experiments as a reference for the transfection efficiency is the pCMVβ expression vector. It contains the *lacZ* gene coding β-galactosidase expressed under the SV40 early promoter and enhancer. Cell pellets obtained after harvesting (3.3.4) were lysed in 100 µl of β-gal lysis buffer, incubated on ice for 15 min and centrifuged (15 min, 14000 rpm, 4°C). Then, the supernatant was used in luciferase or β-galactosidase assays.

β-Galactosidase assay

Glycoside bonds of lactose and its derivatives can be cleaved by β-galactosidase. The commercially supplied substrate galacton is a 1,2-dioxetane-based derivative, which emits visible light upon enzyme-catalyzed decomposition. For measuring β-galactosidase activity, 8 µl of cell extract was pipetted into the sample tubes. These tubes were placed into the luminometer and buffers were automatically added. First 100 µl of reaction buffer was added. After 30 min of incubation, 300 µl of stop buffer was injected into the tubes.

Luciferase assay

Firefly luciferase protein catalyzes ATP- and Mg^{2+}-dependent oxidation of the firefly specific substrate, D-luciferin, to oxy-luciferin that causes the generation of light, which can then be detected and quantified by luminometer. To measure the luciferase concentration 20 µl of the cell extracts were pipetted into the sample tubes, which were placed into the luminometer, where the reaction and injection buffers were automatically added. At first 300 µl of the reaction buffer was injected into the tubes followed by 100 µl of the injection buffer.

3.4.2 2-Dimensional-Sodium Dodecyl Sulfate-Polyacrylamide Gel Electrophoresis

The 2-dimensional-sodium dodecyl sulfate-polyacrylamide gel electrophoresis (2D-SDS-PAGE) is a widely used method for the analysis of complex protein mixtures extracted from cells, tissues or other biological samples. This technique sorts protein according to two independent properties in two discrete steps: the first-dimension (1D) step, isoelectric Focusing (IEF), separates proteins according to their isoelectric points (pI); the second dimension step, SDS-polyacrylamide gel electrophoresis (SDS-PAGE), separates proteins according to their molecular weights (MW).

Sample Preparation

For the complete analysis of all the cellular proteins, the cells must be effectively disrupted. The liberated proteases upon cell disruption have to be inactivated or inhibited. Precipitation of the non-protein impurities is important as they can interfere with the resolution of the 2D results. Sample proteins must be completely disaggregated and fully solubilized. It is achieved by denaturants including urea and a zwitterionic detergent. The protein modifications during the sample preparation can be avoided by storing the samples always on the ice. In particular after urea treatment, the samples are maintained below 30°C. In the present work, the total protein extract was prepared by using the *complete mammalian proteextract kit (C-PEK)*. It includes a hypotonic buffer for cell resuspension and lysis and a denaturing extraction reagent for the solubilization of proteins. The nucleic acid impurities are degraded and a non-viscous protein solution is obtained by DNAse treatment. Protease inhibitors prevent proteolysis.

Isoelectric Focusing (IEF)

IEF is an electrophoretic method that separates proteins according to their isoelectric points (pI). Proteins are amphoteric molecules; they carry either positive or negative or zero net charge, depending on the pH of their surroundings. The net charge of a protein is the sum of all the negative and positive charges of its amino acid side chains and amino- and carboxyl-termini. The isoelectric point is the specific pH at which the net charge of the protein is zero. Proteins are positively charged at pH values below their pI and negatively charged at pH values above their pI. In a pH gradient, under the influence of an electric field, a protein will move to the position in the gradient where its net charge is zero. A protein with a positive net charge will migrate toward the cathode, becoming progressively less positively charged as it moves through the pH gradient until it reaches its pI. A protein with a negative charge will migrate toward the anode, becoming less negatively charged until it also reaches zero net charge. If a

protein should diffuse away from its pI, it immediately gains charge and migrates back. This is the focusing effect of IEF, which concentrates proteins at their pIs and allows proteins to be separated on the basis of very small charge differences. Immobilized pH gradients (IPG) is created by covalently incorporating a gradient of acidic and basic buffering groups into a polyacrylamide gel at the time it is cast.

IPG Strip Equilibration

The equilibration step saturates the IPG strip with the SDS buffer system required for the second dimension separation. The equilibration buffer contains many reagents to maintain the pH of the IPG strip. Urea is added together with glycerol, reduces the effects of electroendoosmosis by increasing the viscosity of the buffer. Glycerol together with urea improves transfer of protein from the first to the second dimension. DTT preserves the fully reduced state of denatured unalkylated proteins. SDS denatures proteins and forms negatively charged protein-SDS complexes.

Second Dimension SDS-PAGE

SDS-PAGE alone is used to detect/quantitate and check the purity of the proteins expressed in prokaryotic and eucaryotic systems by either staining with Coomassie brilliant blue or by immunoblotting. SDS-PAGE is a method that allows separation of the proteins according to their molecular weight but not by charges. Besides, first dimensional IEF followed by the SDS-PAGE separates the isoelectrically focused proteins based on their molecular weight in the second dimension.

Proteins usually possess positive or negative charge depending on their amino acid composition and have different native three dimensional structures. To make different proteins similar in shape and charge, they are subjected to denaturation in Laemmli sample buffer at high temperature (95°C) for 10 min. This buffer contains a powerful negatively charged detergent, sodium dodecyl sulfate (SDS). SDS binds to the hydrophobic regions of the protein molecules (1.4 g SDS/g protein) and disrupting all non-covalent bonds, thereby causing them to unfold into extended polypeptide chains. The individual proteins are released from their associations with other proteins and rendered freely soluble in detergent solution. The β-mercaptoethanol is a reducing agent which reduces the disulphide bonds and makes the multiple unit proteins into single units. In addition, each protein in the mixture binds a large number of detergent molecules which mask their intrinsic charge and causes it to migrate towards the positive electrode when a voltage is applied. Tetramethylethylene diamine (TEMED) initiates the free radical polymerization and ammonium persulfate (APS) enhances it. During the discontinuous gel electrophoresis, proteins are first focused by running through a short stacking gel prior to entering the resolving gel.

Separating gel (12.5%)	6.25 ml	lower Tris (1.5 M Tris-HCl, pH 8.8; 0.4% (w/v) SDS)
	8.1 ml	dd water
	10.4 ml	Acrylamid/Bisacrylamide (30%) 37.5:1 mix
	250 µl	APS
	10 µl	TEMED
Stacking gel (4.3%)		upper Tris (1 M Tris-HCl, pH 6.8; 0.4% (w/v) SDS)
	3 ml	dd water
	717 µl	Acrylamide/Bisacrylamide (30%) 37.5:1 mix
	50 µl	APS
	5 µl	TEMED

2D-SDS-PAGE Protocol

$1x10^5$ cells/ml were seeded in 10 cm petri dishes, the cells were harvested the next day and washed with PBS and wash buffer each twice (1000 rpm, 5 min, 4˚C). The total protein extract was prepared as directed in the *C-PEK*. The sample was prepared as mentioned below and loaded in the IPG strip holder. The IPG strip was carefully placed over the sample without capturing air bubbles. The strip holder was placed in the IPGphor electrophoresis system and IEF program was run for overnight.

Sample Preparation	250 µl	Total protein extract
	1000 µl	Rehydration buffer
	2 µl	DTT
	IPG Buffer	1.5 µl
IEF Program		
Rehydration	Passive 1-4 hr	
	Active 12 hr	30V
IEF	1 hr	500V
	1 hr	1000V
	30 min	5000V
	30 min	8000V
	2 hr	8000V

On the next day, the strip was removed from the chamber and equilibrated with 5 ml of equilibration buffer added with 333.3 µl of 1M DTT by shaking for 10 min at RT followed by 676 µl of iodoacetamide was added and placed on a shaker for another 10 min at RT. A 10% SDS-PAGE was prepared and the equilibrated IPG strip was placed horizontally over the SDS-PAGE. Over the IPG strip the melted 0.5% low melting point agarose was pipetted and allowed to cool for 45 min. Then, the SDS-PAGE was pre-run

for 20 min at 10 mA and later at 35 mA for 4 hr. The gels were stained or transferred to a membrane for different purposes.

3.4.3 Coomassie Brilliant Blue Staining

Coomassie Brilliant Blue (CBB) dye can bind nonspecifically to the proteins, and is used for the detection of proteins and estimation of protein concentration on the gels. Staining with the dye allows detecting the sufficient amount of the protein (>0.3 µg). The fractionated proteins in the SDS-PAGE were precipitated using a fixing solution containing methanol/acetic acid. The location of the precipitated proteins was then detected using CBB (which turns the entire gel blue). After destaining, the blue protein bands appeared against a clear background. For staining, the gels were kept for 30 min in CBB-staining solution with shaking and then destained with CBB-destaining solution until an appropriate signal/background ratio was reached.

3.4.4 Western Blotting and Immunodetection

In western blotting, proteins are transferred from an acrylamide gel to a nitrocellulose membrane by an electric field, preserving their spatial arrangement. When the molecules are immobilized on the membrane they can then be detected with high sensitivity by labeling with specific antibodies.

Blotting was performed at 80 V for 1 hr in blotting buffer, and then non-specific, reversible Ponceau-S staining of the proteins was performed to confirm the transfer of proteins. Unoccupied binding sites on the membrane were blocked by incubation for 1 hr at RT in the block solution. The membrane was then kept for 1 hr at RT in the solution with the protein specific primary antibody (dilution 1:1000). To remove the nonspecifically bound primary antibody, the membrane was washed thrice with the wash buffer each for 6-10 min followed by incubation for 45 min at RT with the corresponding horseradish peroxidase (HRP)-conjugated secondary antibody (dilution 1:1000). Afterwards, the membrane was washed thrice with the wash buffer each for 6-10 min, and the proteins were detected using the ECL chemiluminescence detection system. For that purpose, the membrane was incubated for 1 min in a 1:1 mixture of the ECL solution A and B. Then the solution was removed, and X-ray film was exposed to the membrane. The exposition time had to be adjusted to the signal intensity for every protein.

3.4.5 ^{35}S-Methionine Labeling

Protein biosynthesis in mammalian cells relies on the continuous uptake of essential amino acids from the environment. Acute amino acid restriction leads to block in the

protein synthesis and when radioactive amino acids are provided, they are incorporated into the newly synthesized proteins. Because of its high specific activity and ease of detection, ^{35}S-methionine is the amino acid of choice for the biosynthetic labeling of proteins. 1x10^5 cells/ml was seeded in the dishes and the next day the serum containing medium was removed and medium without methionine was added to starve the cells for 30 min. Then the cells were provided with medium containing ^{35}S-methionine for labeling the cells. After labeling for different times, the cells were harvested and washed three times with 1X PBS. Then the cell pellet was either lysed in 1X Laemmli buffer for SDS-PAGE or 10 µl of the cell pellet was loaded on a whatman filter paper as spots. The SDS-PAGE was followed by fixing, washing and drying the gel. The composition of the fixing solution is given below. The cell pellet loaded on the whatman paper were fixed and washed by trichloro acetic acid. Then the filter paper is air-dried, followed by exposed to the phosphor imager screen for detection and quantification.

Fixing Solution	25% (v/v)	Methanol
	10% (v/v)	Acetic acid
		Fixing followed by shaking with
	0.5 M	Sodium salicylate

3.4.6 Immunoprecipitation

The Pdcd4 knock-down stable clones were analyzed for the siRNA mediated silencing of Pdcd4 by immunoprecipitation experiment. The basic principle is that the endogenous proteins can be isolated from a protein extract as a complex via an antibody specific to the protein. After coupling of the constant region of the antibody onto a matrix (e.g. protein A or protein G sepharose) non-interacting proteins can be washed away and all interacting proteins can be analyzed by SDS-PAGE and western blotting or used for further experiments. The ^{35}S-methionine labeled cells were harvested, lysed by the stringent RIPA lysis buffer and 3µl of Pdcd4 specific antibody was applied to 1 ml of cellular extract followed by incubation on a rotating device for 1 hr at 4°C. Depending on the antibody used, protein A (for rabbit antibodies) was washed three times with the corresponding lysis buffer and about 15 µl of bed volume was applied to each sample, with and without block peptide. After incubation under rotation for 1 hr at 4°C, the samples were washed thrice with ice cold lysis buffer and then boiled for 10 min at 95°C in 100 µl of 1X Laemmli buffer. The immunoprecipitate was analyzed by SDS-PAGE. The gels were fixed by shaking with fixing solution followed by sodium salicylate and finally dried. Then, the dried gel was exposed to the phosphorimager screen.

4 RESULTS

4.1 Downregulation of Pdcd4 – A Knock-Down System

4.1.1 Targeted Silencing of the Human Pdcd4 gene

Pdcd4 is a highly conserved gene among the vertebrates as well as in distantly related organisms such as the fruit fly *Drosophila melanogaster* (referred to as CG10990) or the marine sponge *Suberites domunculata* (Wagner et al., 1998). Although growing experimental evidence identifies Pdcd4 as a tumor suppressor gene, the molecular mechanism behind the tumor suppressor function is yet to be understood. Eventually, developing a well-characterized cell system is inevitable to elucidate the molecular functions of Pdcd4.

In general, a knock-down cell system is preferred for studying the function of a gene, as the activity of the gene is completely or almost completely eliminated which facilitates the search for the phenotypic changes in a cell. RNA interference (RNAi) was chosen to silence the Pdcd4 gene as it is a novel technique that has recently emerged as a reverse genetic approach to study new genes when the sequence is available. RNAi, an evolutionarily conserved phenomenon, represents a unique form of posttranscriptional silencing (PTGS). RNAi was first identified in plants and fungi, which is mediated by generating siRNA of 19-25 nt with characteristic 3’ dinucleotide overhangs (Jorgenesen, 1990). The siRNA is incorporated into the RNA-induced silencing complex (RISC), whereupon a RISC-associated, ATP-dependent helicase activity unwinds the duplex, thus enabling the two strands of siRNA to target mRNA recognition. The degree of complementarity between the siRNA and target mRNA determines the silencing via site-specific cleavage of the message in the region of the mRNA-siRNA duplex. The cleaved mRNA products are released and degraded and thereby silenced (Hammond et al., 2001). The mechanism of generation and activation of siRNAs inside the cell is explained in the figure 3 (Elbashir et al., 2001b; Bernstein et al., 2001; Ishizuka et al., 2002).

siRNA Expression Construct

In order to produce a human Pdcd4 (Hpdcd4) knock-down system, HeLa cells were chosen as they were found to express Pdcd4 and are easy to transfect (Boehm, 2005). For this purpose, two different siRNA duplexes targeting at two different regions of Hpdcd4 gene (Hpdcd4) were designed with the help of siRNA design software from OligoEngine. It designs the siRNA according to the following criteria (Brummelkamp et al., 2002): first AA dimer 75 bases downstream from the start codon should be located

and the next 19 nucleotides (nt) are extracted as a target sequence. The target sequence should have a GC content of 30-50%, should be flanked in the mRNA with TT at the 3' end and must not contain a stretch of four or more A's or T's to avoid premature termination of the transcript. Finally a Blast search was performed against NCBI Unigene/EST library to ensure that only one gene is targeted.

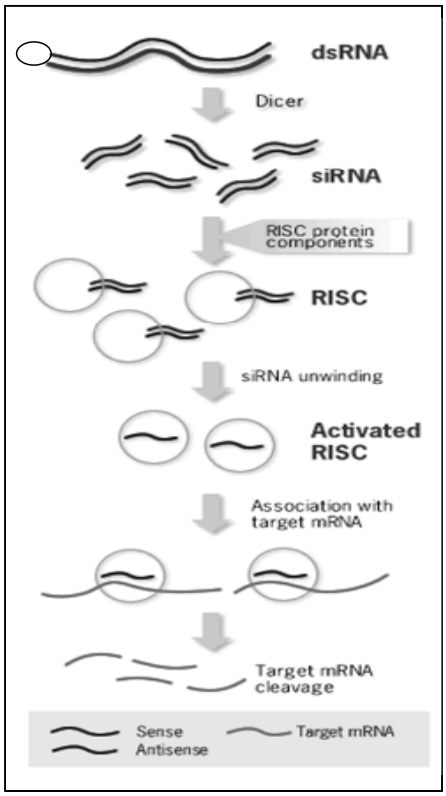

Figure 3: RNA interference mediated by sequence specific siRNA silencing

The transfected pTER+ vector expresses siRNA with a stem loop structure, which are recognized by Dicer. Subsequently the dsRNA is cleaved resulting in 21 nt RNA duplexes, called the siRNAs. These siRNAs incorporated into the RISC where they are unwound by an ATP-dependent process, transforming the complex into an active state. Activated RISC uses one strand of the RNA as bait to bind homologous RNA molecules, then the target mRNA is cleaved and degraded.

The engineered two siRNAs following the positions 603 and 1260 of Hpdcd4 mRNA were recommended for silencing of Hpdcd4. Within the 60-mer siRNA oligos, the 20 nt target appears in both sense and antisense orientation, separated by a 9 nt spacer sequence. The resulting transcript is predicted to fold back on itself to form a stem-loop structure, which is later cleaved to produce a functional siRNA inside the cell. The siRNA oligos were annealed and cloned into the pTER+ vector (Fig.4). A single nucleotide mismatch in the siRNA sequence abrogates the ability to suppress gene expression (Brummelkamp et al., 2002). Therefore, the positive clones were sequenced and the clones with the correct siRNA sequence were chosen for further knock-down experiment.

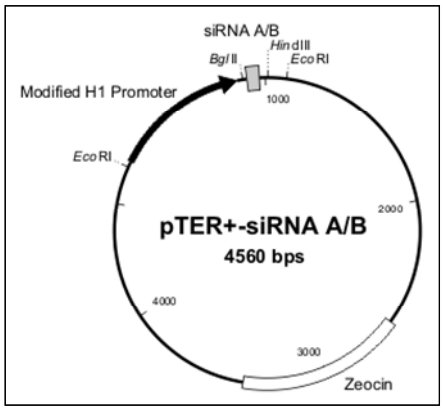

Figure 4: The siRNA expression construct

The siRNA oligos were annealed and cloned between the *BglII/HindIII* restriction sites of the pTER+ vector. The clones were selected using zeocin antibiotic. The positive clones were sequenced by using BGH reverse primer. The siRNA expression is controlled from the H1 promoter of the RNA Polymerase III gene. The H1 promoter is modified by inserting the tetracycline operator (TO), thereby enabling the binding of tetracycline repressor to this region and the regulation of siRNA expression by the addition of doxycycline.

Transient Transfection

For checking the integrity and functionality of the siRNA constructs, they were transiently transfected into QT6 cells. A eucaryotic expression vector overexpressing Hpdcd4 under the control of CMV-promoter was cotransfected with the siRNAs to see the siRNA effect. The 3' end of the Hpdcd4 was tagged with hemagglutinin (HA) epitope and could be detected by mouse monoclonal anti-HA antibody. Figure 5 shows that both siRNAs downregulate the externally transfected Hpdcd4 and that the effect was increasing with increasing concentration of siRNA.

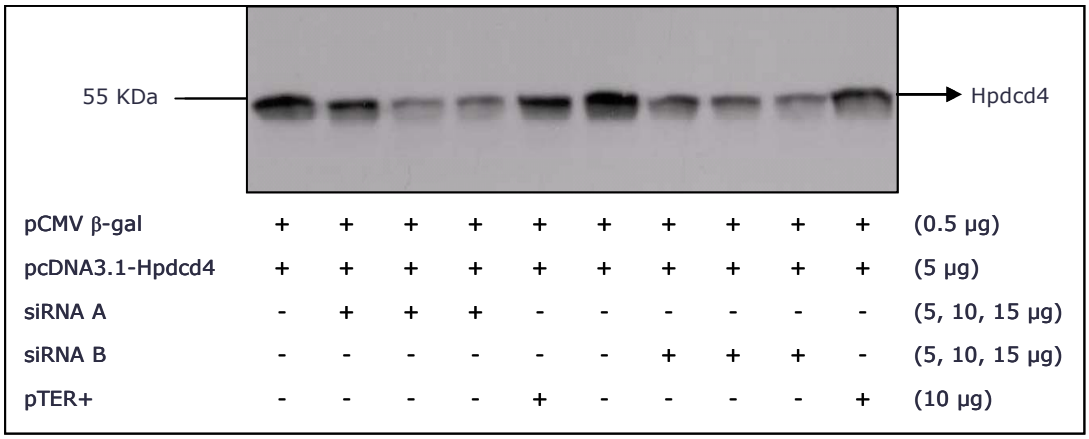

Figure 5: Downregulation of Hpdcd4 by siRNAs

QT6 cells were transiently co-transfected with increasing concentrations (5, 10 & 15 µg) of pTER+-siRNA A & B and the Hpdcd4 overexpression construct (pcDNA3-Hpdcd4-HA 5 µg). To measure the efficiency of transfection, the cells were additionally transfected with pCMV β-gal (0.5 µg). 24 hrs after transfection, the cells were harvested, lysed, and part of the cells was used for measuring the β-galactosidase activity. Samples were electrophoresed on a 10% SDS-PAGE followed by western blotting. The blot was incubated with mouse monoclonal anti-HA antibody as primary antibody (Ab) and Horse Radish Peroxidase (HRP) conjugated polyclonal rabbit anti-mouse antibody as secondary antibody. Hpdcd4 bands are highlighted by an arrow at 55 KDa.

Stable Transfection

After confirming the proper functioning of the siRNA constructs, both the siRNA constructs were together stably transfected into HeLa wild-type (WT) cells and selected by their resistance to zeocin. The clones were analyzed for the downregulation of Hpdcd4 by immunoprecipitation (Fig.6) and western blotting (Fig.20). Among the identified clones downregulating Hpdcd4, K11 and K12 were further used for the functional analysis of Hpdcd4.

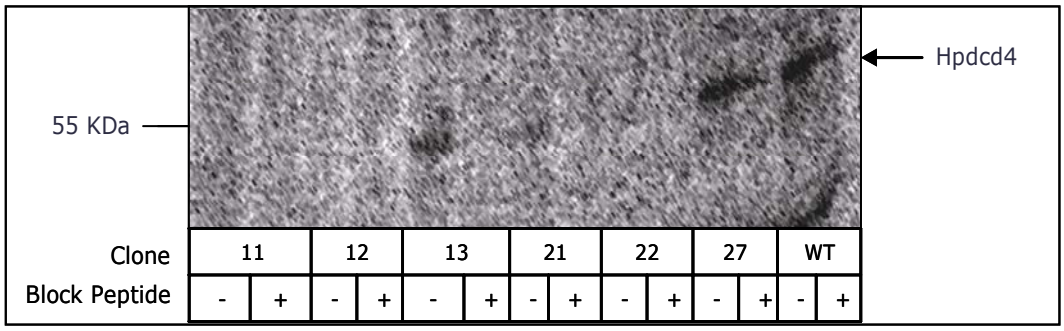

Figure 6: Analysis of HeLa stable clones by immunoprecipitation

Six HeLa stable clones (11, 12, 13, 21, 22 and 27) were analyzed by immunoprecipitation. The cells were starved without methionine, and then labeled for 1 hr using ^{35}S-methionine. Then harvested, lysed, incubated with rabbit polyclonal antiserum raised against mouse-pdcd4 and treated with and without recombinant Pdcd4 to control the specificity of the immunoprecipitation. HeLa WT cells were used as a negative control. Hpdcd4 bands are indicated by an arrow at 55 KDa. The clones 11, 12 and 22 were identified as positive clones.

4.1.2 The effect of Hpdcd4 on Cap-Dependent Translation

It has been previously shown that Pdcd4 overexpression inhibits translation of a luciferase transcript containing a structured 5' untranslated region (UTR) in primary keratinocytes (Jansen et al., 2004). The secondary structured region in the mRNA hinders the cap-dependent ribosomal scanning mechanism during the translation. Thus, in order to check the effect of Hpdcd4 on translation of 5' structured mRNAs, luciferase constructs containing or lacking 5' secondary structures (Fig.7) were transiently transfected into the HeLa WT and K12 cells.

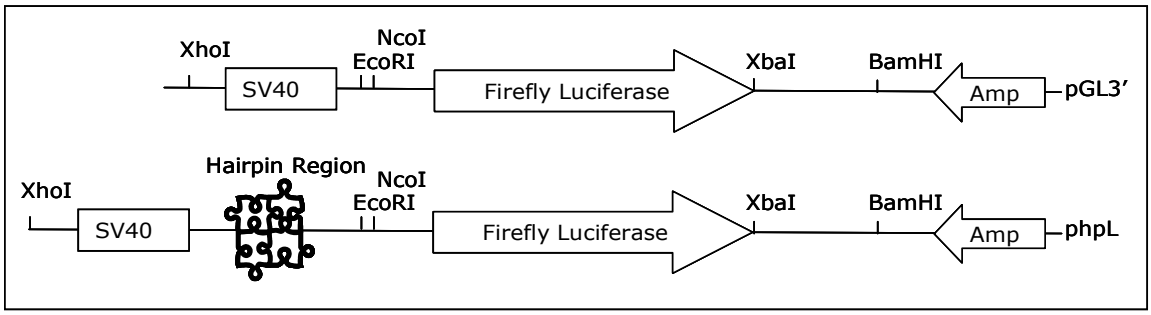

Figure 7: Schematic diagram of reporter gene constructs

The pGL3' vector expresses firefly luciferase immediately after the SV40 promoter. The phpL vector codes for a RNA secondary structure and then expresses firefly luciferase.

The pGL3' vector expresses firefly luciferase immediately after the promoter but the phpL expresses the luciferase after reading a RNA secondary structure which is believed to be hindering the normal cap-dependent translation. The experiment showed that there was no difference in the cap-dependent translation between WT and K12 cells when pGL3' was transfected (Fig.8a). The introduction of secondary structure reduced the cap-dependent translation in both WT and K12 cells but the fold of reduction was less in the K12 cells compared to the WT cells (Fig.8b). However, this experiment showed that the translation of secondary structured-mRNA was higher in the absence than in the presence of Hpdcd4 (Fig.8a). It suggests that the Hpdcd4 inhibits the translation of mRNAs with RNA secondary structure.

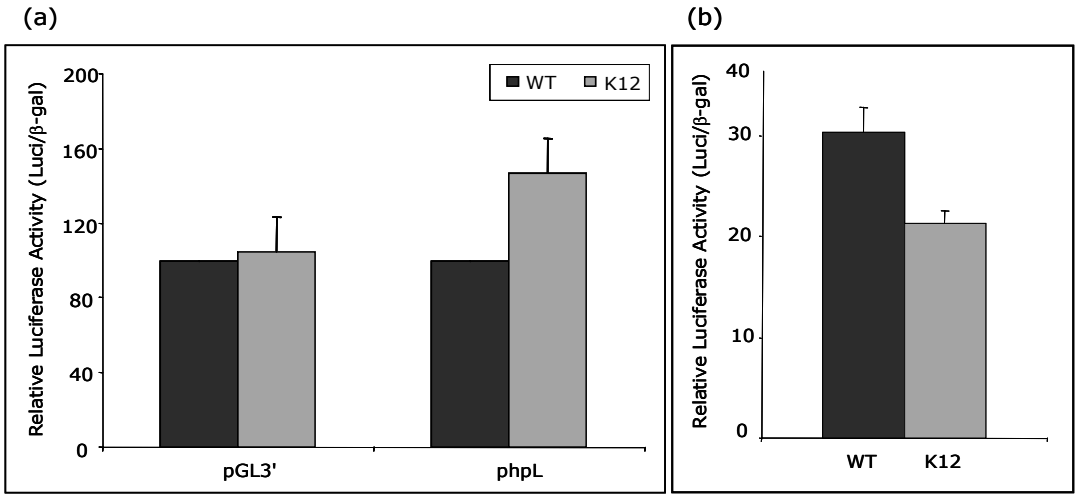

Figure 8: Effect of Hpdcd4 on RNA secondary structure

10 µg each of pGL3' and phpL were transiently transfected into the HeLa WT and K12 cells. To measure the efficiency of transfection, the cells were additionally transfected with pCMV β-gal (0.5 µg). 24 hrs after transfection the cells were harvested, lysed and assayed for β-galactosidase and luciferase activity. The luciferase activity was normalized to β-galactosidase activity. Average normalized values from triplicate experiments are shown in the figure.

4.1.3 The effect of Hpdcd4 on IRES-Dependent Translation

Cellular Internal Ribosome Entry Site (IRES) elements were preferentially found in the mRNAs of genes involved in the control of cellular proliferation, survival and death (Hellen and Sarnow, 2001). For example PDGF, VEGF, IGFII, c-Myc, c-Jun, PITSLRE, XIAP, DAP5, Apaf-1, Mnt and bag-1 mRNAs contain the IRES elements (Tara et al., 2003). In order to study the effect of Hpdcd4 on IRES elements, IRES elements of genes related to apoptosis and cancer were chosen (Apaf-1, c-Myc, Mnt, and N-Myc) and the respective dual reporter gene constructs were obtained.

Though the firefly luciferase gene is widely used as a reporter gene for studying the promoter function and gene expression, normally a second reporter gene (e.g., beta-galactosidase) is used as an internal experimental standard to normalize for the differences in transfection efficiencies and other experimental variations. Dual reporter refers to the simultaneous expression and measurement of two individual reporter enzymes within a single system and it is commonly used to improve the experimental accuracy. Here, we used a dual luciferase system having two non-overlapping open reading frames (ORFs) for firefly (*Photinus pyralis*) and renilla (*Renilla reniformis*) luciferases. The renilla luciferase is expressed under the control of the SV40 promoter and enhancer region and the IRES element can be cloned upstream of the firefly luciferase gene (Fig.9). The firefly luciferase is expressed as a result of IRES-dependent translation. The bicistronic constructs with specific IRES elements were transiently transfected into the HeLa WT and K12 cells and both luciferase activities were measured sequentially from a single sample using dual luciferase assay kit (Fig.10).

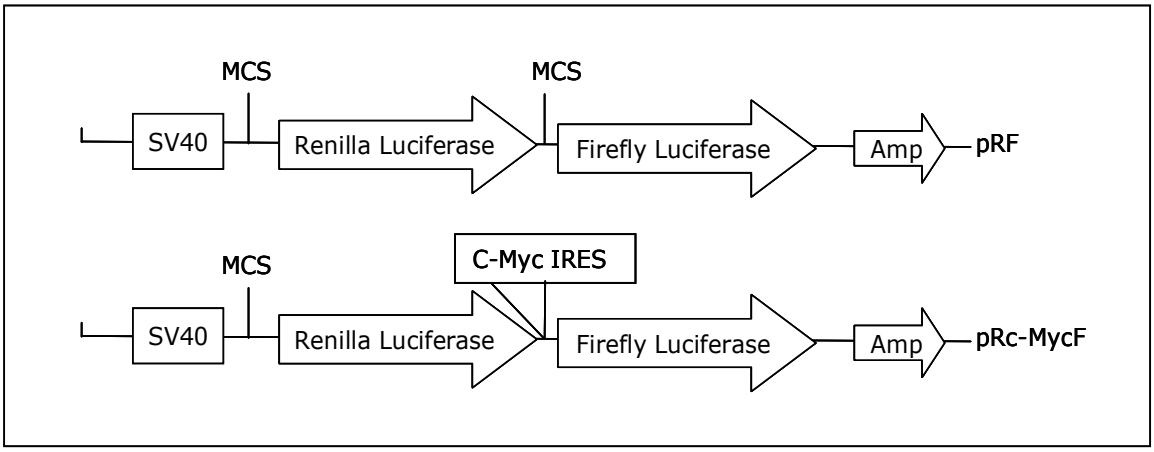

Figure 9: Schematic diagram of dual luciferase constructs

pRF is originally derived from pGL3 vector modified by inserting the renilla and firefly luciferases. The renilla luciferase is expressed from the SV40 promoter/enhancer region and the firefly luciferase is expressed from the IRES element. Various IRES elements could be cloned in between the two luciferases to assess their functional efficiency. (e.g.) pRc-MycF is cloned with c-Myc IRES using the multiple cloning sites in between the renilla and firefly luciferases.

All different IRES elements show more firefly luciferase activity in the K12 cells compared to the WT cells. This demonstrates that the absence of Hpdcd4 increases the IRES element-dependent translation. Thus, this experiment shows that Hpdcd4 may have a direct or indirect inhibitory control over the IRES elements during normal physiological conditions.

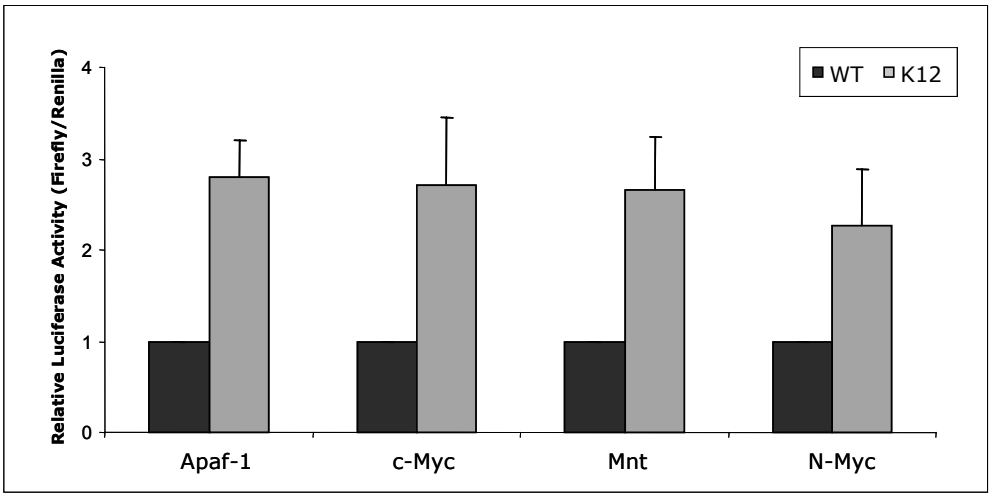

Figure 10: Effect of Hpdcd4 on IRES elements

Each 3 µg of pRApaf-1F, pRc-MycF, pRMntF and pRN-MycF dual luciferase constructs were transiently transfected into the HeLa WT and K12 cells. After 24 hrs cells were harvested, lysed and protein extract was prepared using promega dual luciferase kit. The firefly and renilla luciferase activities were measured sequentially in automated luminometer. Renilla luciferase activity was used for normalizing the firefly luciferase activity. The average normalized values from three independent experiments are shown in the figure.

The effect of Hpdcd4 on c-myc IRES

The proto oncogene c-myc is required for both cell proliferation and programmed cell death and deregulated c-myc expression is associated with a wide range of cancers (Henriksson and Luscher, 1996; Prendergast, 1999). The predominant mRNA of c-myc contains an IRES (~400 nt) in the 5´UTR region (Nanbru et al., 1997; Stoneley et al., 1998). Thus, the initiation of translation of c-myc can occur by either a cap-dependent scanning mechanism or by internal ribosome entry. It has been shown that the IRES element was required to maintain the c-Myc protein synthesis under conditions when the cap-dependent translation initiation is compromised; for example during apoptosis (Stoneley et al., 2000a). Since Pdcd4 was shown to be involved in apoptosis and tumor suppression, the effect of knock-down of Pdcd4 on the c-Myc IRES was selected. The effect of Hpdcd4 on c-myc IRES was reproducible and the IRES activity was increased 2.5 times more in the K12 cells compared to the WT cells as shown in figure 10.

The effect of Hpdcd4 on c-myc IRES during Stress Conditions

Previous studies have shown that c-myc IRES was active and c-Myc protein expression was maintained although a large reduction in total protein synthesis was observed during genotoxic stress (Subkhankulova et al., 2001). Therefore, in the next experiment the effect of Hpdcd4 on the c-myc IRES was assessed when stress was induced by UV treatment (Fig.11). The UV-irradiation is a nonreceptor-mediated induction of apoptosis (Spriggs et al., 2005; Latonen and Laiho, 2005).

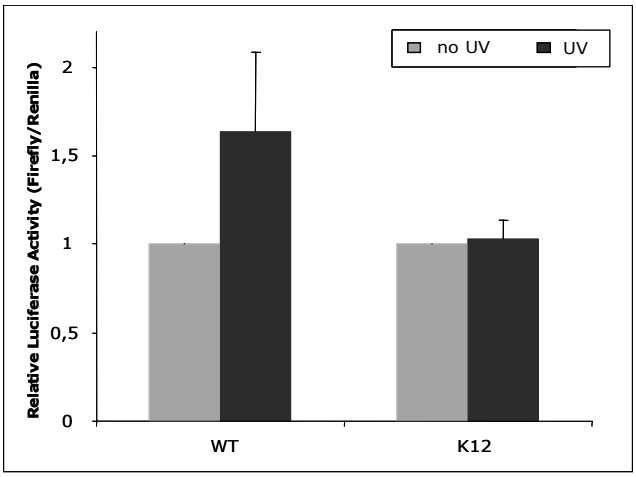

Figure 11: Effect of Hpdcd4 on c-*myc* IRES during UV-induction

Five µg of pRc-MycF was transiently transfected into the HeLa WT and K12 cells. 24 hrs later the transfection, cells were split and treated with UV 100 J/m^2 (10 sec) or left untreated. 6 hrs later, cells were harvested, lysed and assayed for both, firefly and renilla luciferase activity using the promega dual luciferase assay kit. The figure shows the average normalized values from triplicate experiments.

In the WT cells, the c-myc IRES activity is increased when the stress is induced compared to the untreated WT cells, however, the K12 cells did not show any difference in the IRES activity due to the UV treatment. Moreover, there was no significant difference in the IRES dependent translation between the UV treated WT and K12 cells.

AraC, EMS, MMC, SSP, and TPA are known to induce genotoxic stress and thereby apoptosis (Subkhankulova et al., 2001). Cytosine arabinoside (AraC) is an analog of cytidine used as antineoplastic agent by selectively inhibiting DNA synthesis (DBR, 1986). Ethylmethane sulfonate (EMS) is an alkylating agent which produces reactive electrophiles, which in turn causes single strand breaks in the DNA and induces cells to undergo apoptosis (Alderson, 1965). Mitomycin C (MMC) inhibits DNA synthesis. It reacts covalently with DNA, forming cross links between the complementary strands of DNA thereby preventing the separation of DNA strands. Thus, it inhibits DNA replication (Ueda and Komano, 1984). Staurosporine (SSP) is an alkaloid, a potent inhibitor of cap-dependent translation, and acts via inhibition of the phospholipid/Ca^{2+}-dependent protein kinase (Tamaoki et al., 1986). Tetradecanoylphorbol acetate (TPA) is the most commonly used potent tumor promoter via activation of protein kinase C (Powell, 2003). In the present work, HeLa WT and K12 cells were treated with specific concentrations of these different chemicals to check the effect of Hpdcd4 on the c-myc IRES while the cells were undergoing stress (Fig.12). There was no significant difference in the IRES-dependent translation in the K12 cells compared to the WT cells.

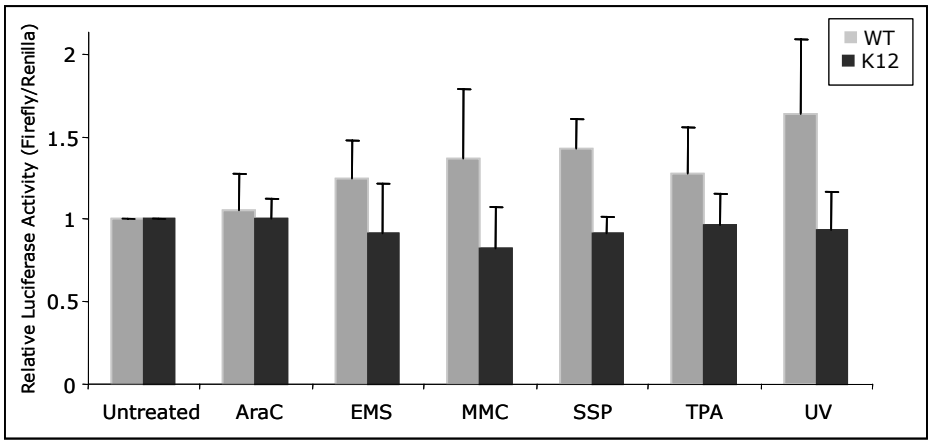

Figure 12: Effect of Hpdcd4 on c-*myc* IRES during stress conditions

2 µg of pRc-MycF was transiently transfected into the HeLa WT and K12 cells. After 24 hrs, cells were split and parallel culture were treated with 10 µM AraC, 50 mM EMS, 50 µM MMC, 500 µM SSP, and 10 nM TPA and harvested after 6 hrs. One culture was treated with UV 100 J/m^2 (10 sec). The cells were harvested 24 hrs later, lysed and assayed for firefly and renilla luciferase activity. The average normalized values of triplicate experiments are shown in the figure.

4.1.4 The search for Novel Molecular Targets of Hpdcd4 – Transcription Factors

Initially, a few transcription factors were identified as potential molecular targets of Hpdcd4. These factors are: ATF-2, c-Jun, c-Myc and C/EBPβ. The following table 2 briefly describes their molecular functions.

Table 2: The transcription factors as molecular targets of Hpdcd4

Targets	Mol.Wt (KDa)	Molecular Functions
ATF-2	70	Forms homo or hetero dimers with c-Jun to initiate CRE dependent transcription
C/EBPβ	50	C/EBP family of transcription factor, control cell proliferation, differentiation and metabolism
c-Jun	44	Major component of the leucine-zipper-dependent, heterodimeric AP-1 transcription factor
c-Myc	67	Function in cell proliferation, differentiation and neoplastic diseases

The effect of Pdcd4 on Phosphorylation of Transcription Factors

One way to alter protein activity in response to extra- or intracellular signals is the modification of certain amino acid residues. The most prevalent covalent modification of proteins is the phosphorylation of certain amino acid residues. Approximately 30% of all cellular proteins contain covalently bound phosphate (Cohen et al., 2000). In general, the terminal (γ-) phosphoryl group of an ATP molecule is transferred to a

hydroxyl group of a serine, threonine or tyrosine residue of the protein and protein kinases catalyze the phosphorylation. Upon phosphorylation the chemical properties of the protein are influenced primarily by the introduction of two additional negative charges of the phosphoryl group and the ability to form three supplementary directed hydrogen-bonds (Hunter and Karin, 1992). Conformational changes of the protein might occur and result in different protein-protein interactions.

The phosphorylation status of a few proteins was also of interest when studying the molecular targets of Hpdcd4. When the cells were treated with UV, the cells undergo nonreceptor-mediated apoptosis due to stress (Spriggs et al., 2005; Wang et al., 2006). In that process, many critical proteins involved in the cell survival and cell death get activated or deactivated by phosphorylation. To check the effect of Hpdcd4 on the phosphorylation status of the targets identified by 1D-SDS-PAGE, cells were UV induced and analyzed by immunoblotting.

Activating transcription factor 2 (ATF-2) is a member of the ATF/cyclic AMP-responsive element binding protein family of transcription factors, found to possess growth factor-independent proliferation and transformation capacity (Papassava et al., 2004). It has been shown that UV and MMS stimulate ATF-2-dependent transactivation, which requires the presence of threonines 69 and 71 located in the transactivation domain. These sites were the targets of p54 and p46 stress-activated protein kinases (SAPKs), which phosphorylate ATF-2 (Van Dam et al., 1995). JNK1 is also a member of SAPK family, which is activated by many forms of stress including UV-irradiation, resulting in the phosphorylation of c-Jun, ATF-2, Elk-1 and p53 (Ramaswamy et al., 1998). Furthermore, another study has confirmed the phosphorylation of ATF-2 and c-Jun by JNK and p38 when induced by UV (Fisher et al., 1998).

Therefore, UV-irradiation was chosen to study the phosphorylation profile of ATF-2, c-Jun and c-Myc transcription factors in the presence and absence of Hpdcd4. In the UV untreated cells, ATF-2 expression is barely observed. ATF-2 was expressed in detectable amounts only after the UV treatment. WT cells showed higher expression compared to the K12 cells (Fig.13). The phosphorylation of ATF-2 was very well seen after UV-induction by both ATF-2 and P-ATF-2 immunoblotting. The degree of phosphorylation of ATF-2 was lower in K11 and K12 cells compared to the WT cells (Fig.13).

The Jun proto-oncogene codes for the major 44 KDa form of the transcription factor AP-1 and it appears to occupy a central role in cellular signal transduction and regulation of proliferation (Angel et al., 1988). The c-Jun was slightly overexpressed in

knock-down cells compared to the WT cells (Fig.14). After the UV-induction, the expression level of c-Jun was higher compared to the untreated cells, but this increase was found to be similar in both WT and K12 cells (Fig.14). Phosphorylated c-Jun was seen as two major bands at ~40 KDa and less than 40 KDa connected by puffy signal; its expression was similar in all the three (WT, K11 and K12) untreated cells and was found to increase after UV treatment in all the cells (Fig.13). The lower band is more intense in untreated cells and the upper band is more intense in the UV treated cells. Although there is no difference in the phosphorylated c-Jun of the WT and the knock-down clones (K11, K12) (Fig.13), in comparison to the unphosphorylated c-Jun as input control (Fig.14), the phosphorylation of c-Jun was considered to be lower in the K12 cells compared to the WT cells.

Deregulation of Myc expression is a common feature in cancer and leads to tumor formation in experimental model systems (Hooker and Hurlin et al., 2006). The potent oncoprotein plays a pivotal role as a regulator of tumorigenesis in numerous human cancers of diverse origin (Ponzielli et al., 2005) and this prompted us to check c-Myc expression. The c-Myc showed decreased levels of expression in the K11 and the K12 cells compared to the WT cells under normal conditions. When UV induced, the expression of c-Myc has gone down in the WT as well as in the K12 cells (Fig.14).

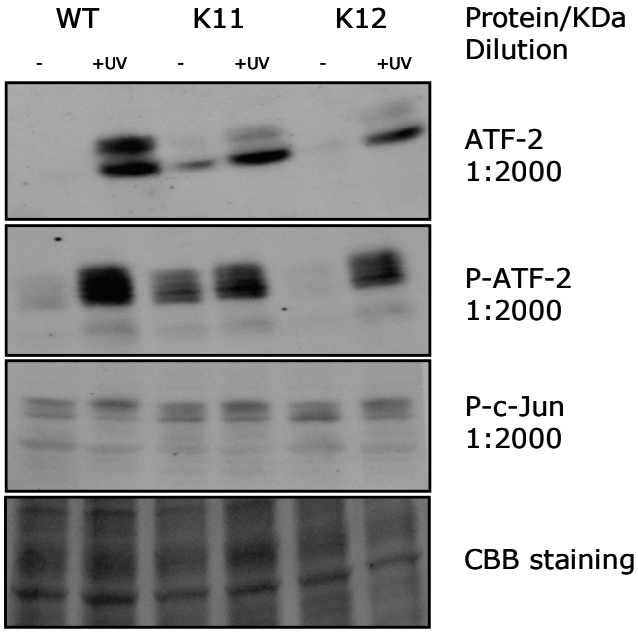

Figure 13: The effect of Hpdcd4 on phosphorylation of the transcription factors

HeLa WT, K11 and K12 cells were treated with UV 100 J/m^2 (10 sec), incubated for 6 hrs, harvested, lysed in SDS-Laemmli buffer, samples were electrophoresed on 10% SDS PAGE followed by western blotting using specific mouse or rabbit mono/polyclonal antiserum as 1°Ab at specified dilution. Respective HRP conjugated 2° Ab was used. Loading of the cell lysates was normalized using the most abundant protein in the CBB staining.

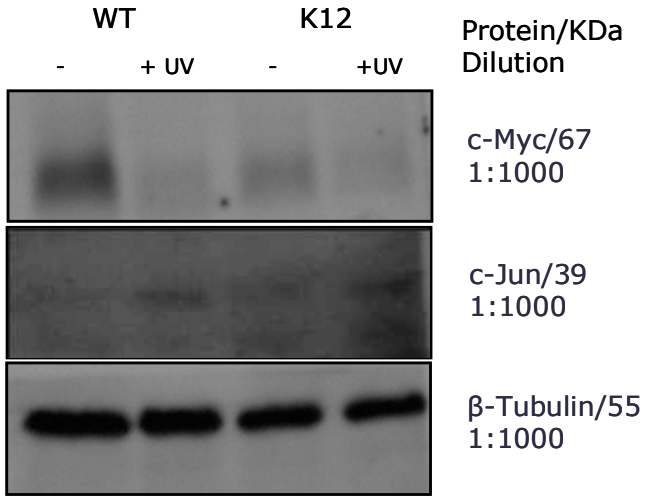

Figure 14: The effect of Hpdcd4 on transcription factors during UV-induction

HeLa WT and K12 cells were treated with UV 100 J/m^2 (10 sec), incubated for 6 hrs and harvested. Then cells were lysed in SDS-Laemmli buffer, were electrophoresed on 10% SDS-PAGE followed by western blotting. The blot was probed with specific mouse or rabbit mono/polyclonal antibody as 1° Ab at specified dilution. Respective HRP conjugated 2° Ab was used. β-Tubulin was used as a loading control.

4.1.5 The effect of Hpdcd4 on Transcription Factor C/EBPβ

The transcription factor C/EBPβ belongs to CCAAT/enhancer-binding protein (C/EBP) family of transcription factors. This family consists of six transcriptions factors and C/EBPβ gene controls differentiation and proliferation in a variety of tissues. The C/EBPβ gene is intronless, but various isoforms are produced by alternative use of translation initiation codons from the same mRNA molecule through a leaky ribosomal scanning mechanism (Kozak, 1989). In addition, amino-terminal truncated isoforms are produced by limited proteolytic cleavage (Baer et al., 1998). C/EBPβ mRNA can produce the three isoforms (Fig.15) LAP*, LAP and LIP with the LAP and LIP forms being the major polypeptides produced in the cells (Descombes and Schibler, 1991).

These isoforms retain different parts of the amino terminus and therefore display different functions in gene regulation and proliferation control. An evolutionarily conserved upstream open reading frame in C/EBPβ mRNA is a prerequisite for regulated initiation from the different translation initiation sites and integrates translation factor activity. Deregulated translational control leads to aberrant C/EBPβ isoform expression which determines the cell fate. For example the LIP isoform consists only of the negative regulatory domain and is therefore capable of acting as a dominant negative inhibitor of C/EBPβ function by forming non-functional heterodimers (Ossipow et al., 1993). Expression of such truncated isoforms disrupts terminal differentiation and induces a transformed phenotype (Calkhoven and Ab, 1996).

In the present experiment the question addressed was whether Hpdcd4 influences the ratio of C/EBPβ isoform expression and thus the transformation of cells by affecting their cell growth. Figure 16 shows the schematic diagram for various C/EBPβ constructs used for the transfection.

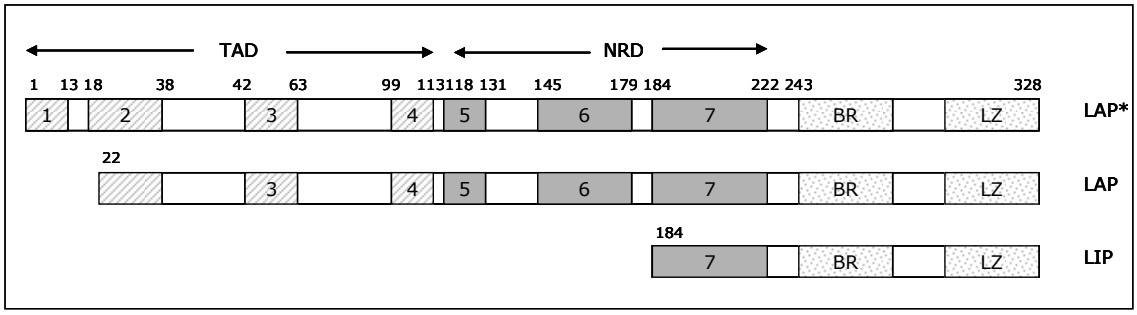

Figure 15: The schematic diagram of C/EBPβ isoforms (Descombes et al., 1991 and Leutz et al., 1994)

Three different C/EBPβ isoforms can be produced by a leaky ribosomal scanning mechanism from the same mRNA. The numbers inside the scheme represent conserved regions; the numbers on top are amino acid residues; other abbreviations are: TAD: transactivation domain; NRD: negative regulatory domain; BR: basic region; LZ: leucine zipper; LAP: liver enriched protein; LIP: liver inhibitory protein

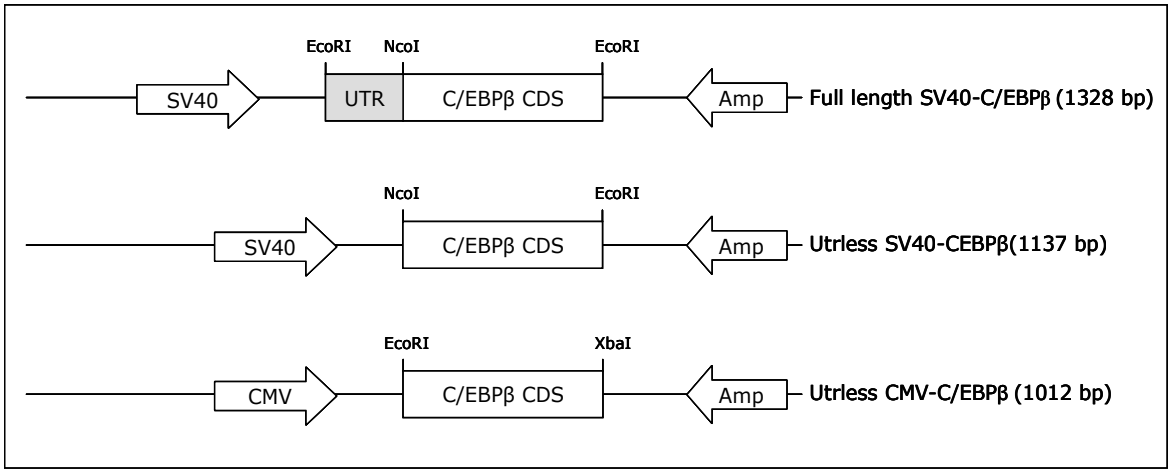

Figure 16: The C/EBPβ constructs used for transfection

pSG5/NF-M#16.3 is the full length SV40-C/EBPβ of 1328 bp length. C/EBPβ is expressed under the control of SV40 promoter in this vector. Utrless-pSG5-C/EBPβ (~1.1 Kb) is deprived of the upstream region, expressed from SV40 promoter and termed as Utrless SV40-C/EBPβ. pcDNA3-CCR is C/EBPβ without the upstream region; length 1012 bp expressed from pCMV-promoter, termed as Utrless pCMV-C/EBPβ. Abbreviations: UTR:Untranslated Region; CDS: Coding Sequence.

The effect of Hpdcd4 on C/EBPβ was analyzed by transiently transfecting the full length C/EBPβ (Full length SV40-C/EBPβ) into HeLa WT and K12 cells (Fig.17). The full length and truncated version of the C/EBPβ are corresponding to the molecular weight of 46 KDa and 40 KDa, respectively. There were two bands observed both in the WT and K12 cells which correspond to the transfected C/EBPβ. In addition, a middle band between these two bands was also seen in the transfected as well as untransfected cells. This

band might correspond to endogenous C/EBPβ or to non-specific protein. In both cells, the full length isoform was less intense than the truncated isoform. The expression of both the isoforms was found to be increased in the K12 cells compared to the WT cells.

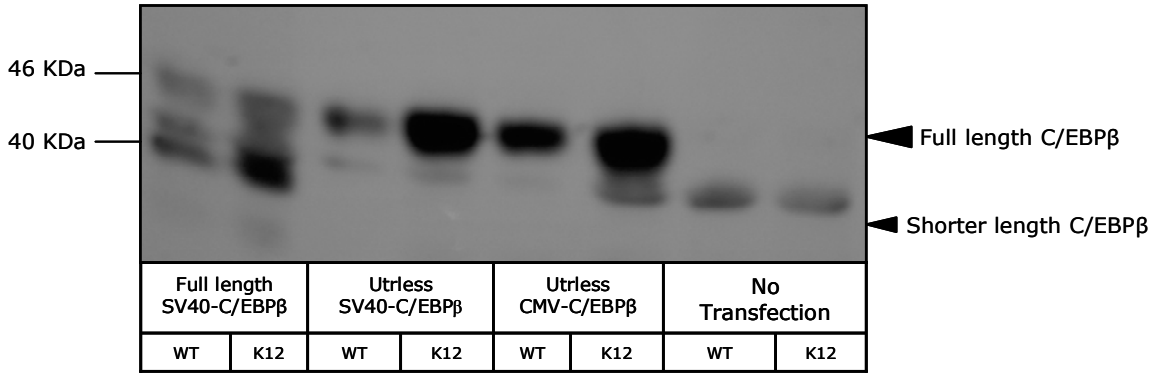

Figure 17: The effect of Hpdcd4 on C/EBPβ

HeLa WT and K12 cells were transiently transfected with each 10 µg of full length SV40-C/EBPβ (pSG5-NFM#16.3) and Utrless SV40-C/EBPβ (Utrless-pSG5-C/EBPβ) and 3 µg of Utrless CMV-C/EBPβ (pcDNA3-CCR). In addition, pCMV-β-gal (0.5 µg) was transfected. 24 hrs later the cells were harvested and lysed in SDS-Laemmli buffer. The transfection efficiency was calculated by measuring β-galactosidase activity and the loading of cell lysates was normalized. Samples were run on 10% SDS-PAGE followed by western blotting. The blot was probed with rabbit polyclonal antiserum as 1° Ab at 1:1000 dilution then anti-rabbit HRP conjugated 2° Ab was used. The different isoforms of C/EBPβ are indicated by arrows.

However, to study the effect in detail, and to assess whether Hpdcd4 operates at the promoter level of C/EBPβ or at a different level, C/EBPβ was cloned without the upstream region into the PSG5 vector (Utrless SV40-C/EBPβ). The removal of upstream region changed the expression pattern, the truncated version of C/EBPβ was not expressed and the full length form was overexpressed in the K12 cells compared to the WT cells. To analyze the influence of SV40 promoter present in the pSG5 vector on the effect of Hpdcd4, C/EBPβ without upstream region expressed from CMV-promoter in pcDNA3 vector (Utrless CMV-C/EBPβ) was transfected into the WT and K12 cells. The higher molecular weight form of C/EBPβ was overexpressed in the K12 cells compared to the WT cells, but the truncated, lower molecular weight form disappeared in both the cells. The above experiments prove that Hpdcd4 has an inhibitory control over C/EBPβ, which is independent of the promoter. Hpdcd4 may act by controlling C/EBPβ at a different level. In addition, the necessity of the upstream region for producing lower molecular weight forms of C/EBPβ was confirmed.

4.1.6 The search for Novel Molecular Targets of Hpdcd4 – A Proteomic Approach

More than tens of thousands of proteins differing in abundance over six orders of magnitude and different in functions are expressed in the cell. The term proteome describes the entire complement of proteins in a given biological organism, cell or a system at a given time (Wasinger et al., 1995). Proteomics provides a comprehensive approach to the analysis of cellular molecular mechanisms by resolving the protein properties (expression levels, interactions, posttranslational modifications etc.,) of the cells using 2-dimensional-sodium dodecyl sulfate-polyacrylamide gel electrophoresis (2D-SDS-PAGE) followed by mass spectrometry (MS) (Williams and Hochstrasser, 1997; Gorg et al., 2000). Such a holistic approach is essential for finding novel molecular targets of new genes like Pdcd4. Rather than looking for effect of Pdcd4 on specific proteins in 1D-SDS-PAGE which confines and limits the search for novel targets.

The discovery of 2D gels in the 1970s provided the first feasible way of displaying almost 1000 proteins on a single gel (Klose, 1975; O'Farrell, 1975). Identification of those proteins in subpicomolar quantities via MS was made possible by soft ionization techniques like electrospray ionization (Wilm et al., 1996). Eventually, 2D-SDS-PAGE and MS together have become the core elements of the proteomics field.

2D-SDS-PAGE (O'Farrell, 1975) sorts proteins according to two independent properties in two discrete steps. The first dimensional step, isoelectric focusing (IEF), separates proteins according to their isoelectric points (pI); the second dimensional step, SDS-PAGE, separates proteins according to their molecular weights (MW).MS is an analytical technique measures an intrinsic property of a molecule, the mass with high sensitivity, calculates the mass-to-charge ratio of ions and generates a mass spectrum for the sample components. Molecules are first ionized, next separated according to their mass-to-charge ratio (m/z) and finally detected. MS can give sequence data from any Coomassie stained gel spot/band. The proteins are digested enzymatically in the excised gel slice using trypsin and the resulting peptides are extracted and purified by reversed phase chromatography for peptide mapping and sequencing. A characteristic set of peptides is generated for each protein and subsequent mass spectrometric analysis of the generated peptides provides a peptide map or mass fingerprint. The obtained peptide maps are aligned with the standard peptide maps in the database and thus such sequence analysis allows protein identification. Database tools used are protein prospector, Mascot and PROWL. The principle of the mass spectrometric analysis of proteins is explained in the figure 18.

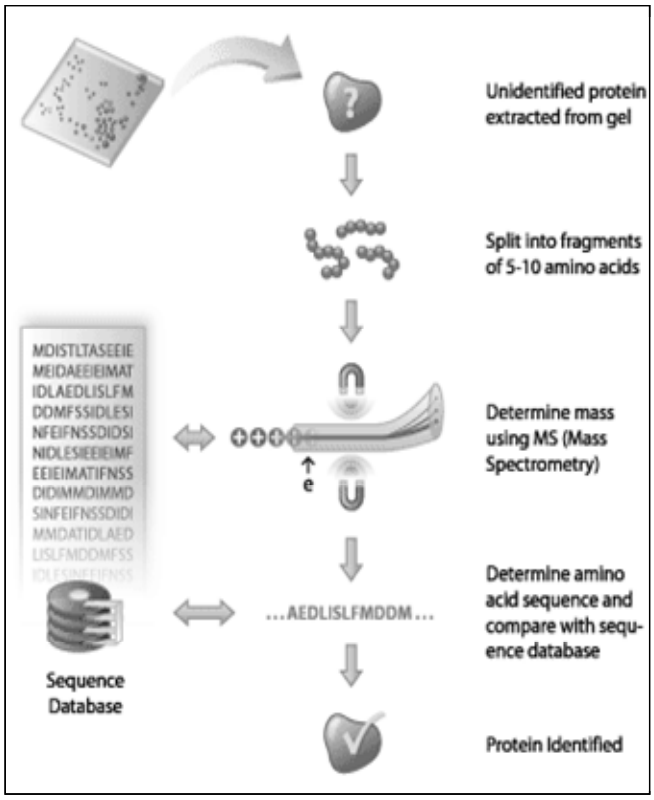

Figure 18: Proteomic analysis by mass spectrometry

The proteins can be digested enzymatically in the excised gel slice using, for example trypsin. The resulting peptides are then extracted and purified for peptide mapping and sequencing. The peptide mass finger print of a sample protein is compared with the database entries and thus the protein is identified.

The 2D-SDS-PAGE Targets

To identify novel targets for Hpdcd4, Hela WT and K12 cells were analyzed by 2D-SDS-PAGE (Fig.19). In the first dimension (1D) different pH ranges like 3-10, 4-7 and 6-11 were used and in the second dimension (2D) 10% SDS-PAGE was performed. Five different proteins were reproducibly differentially expressed in K12 cells compared to WT cells. The five spots corresponding to the unknown proteins were sliced out from the gels and eluted proteins were further analyzed by MS from the proteomic facility available at the integrated functional genomics of IZKF, Muenster.

The protein of spot S1 is overexpressed in the K12 cells compared to the WT cells and was identified as cytokeratin-17 (CK-17). The proteins corresponding to spots S2 and S3 were visible only in the K12 cells but not in the WT cells. They were identified as aldo keto reductase1 (AKR1) family members C2 and C3. There was no quantitative change in the expression level of the protein in spot S4, but two related small spots appeared right next to it. The protein of spot S4 was identified to be cytokeratin-8 (CK-8). The protein of spot S5 was identified to be glutamyl and prolyl bifunctional tRNA synthetase (GluProRS) which was appearing as '5-6 pearls in a string' (this term was coined to better visualize/imagine 5-6 discrete protein spots appear in a row with

uniform interval in less than 1 cm in the 2D-SDS-PAGE) in the K12 cells but as a single spot in WT cells. The following table 3 displays the name of the spots and their differential expression profile in the 2D-SDS-PAGE.

Table 3: The novel molecular targets of Hpdcd4

S.No	HeLa WT	HeLa K12	Name of the target
S1	Less intense	Overexpressed	Cytokeratin–17 (CK-17)
S2	Absent	New spot appears	Aldo Keto Reductase Family member C2 (AKR1C2)
S3	Absent	New spot appears	Aldo Keto Reductase Family member C3 (AKR1C3)
S4	Single spot	2 more related spots appear	Cytokeratin–8 (CK-8)
S5	Single spot	5-6 spots appear as pearls in string	Glutamyl and Prolyl Bifunctional tRNA Synthetase (GluProRS)

The table 4 describes about each target, such as the swissprot database ID, the molecular weight by MS and the functional importance. CK-17 and CK-8 belong to the acidic and basic intermediate filament families, respectively. They both are structural element of normal epithelial cells. They are used as tumor markers for the classification of tumors since their expression is different based on the origin of the tumor. AKR1C2 and C3 reduce aldehydes and ketones to alcohols in normal tissues but are used as tumor markers in a variety of tumors. GluProRS is a bifunctional tRNA synthetase enzyme found to have RNA binding activity, which might carry some significance in the tumor tumor progression.

Table 4: The molecular functions of the novel targets

Swiss Prot ID	Targets	Mol.Wt (KDa)	Molecular Function & Significance
Q04695	CK-17	48.0	Marker of basal cell differentiation
P52895	AKR1C2	36.7	Bile acid & electron transporter, upregulated in cancer
P42330	AKR1C3	36.8	Reduces aldehyde & ketones to alcohol
P05787	CK-8	53.6	Structural & functional protein of intermediate filaments
P07814	GluProRS	163.0	Bifunctional tRNA synthetase

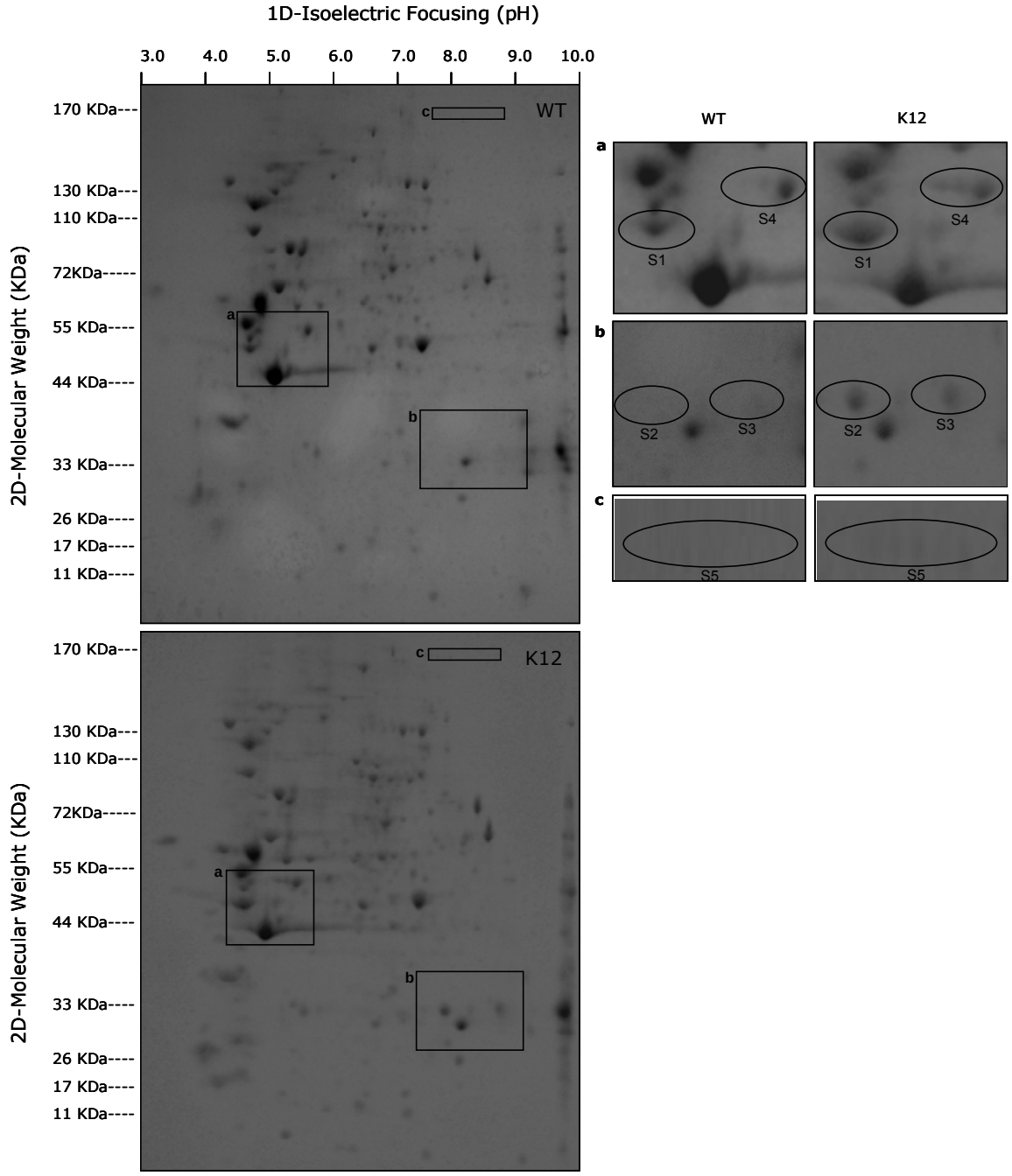

Figure 19: Identification of novel molecular targets of Hpdcd4

1-1.5 X 10^5 cells/ml each from the HeLa WT and K12 cells were seeded and harvested the next day. The proteins were isoelectrically focused in the 1D using immobiline dry pH gel (IPG) strip of pH (3-10) and 10% SDS-PAGE was performed in the 2D. The gels were stained by Coomassie brilliant bule (CBB). The 2D-SDS-PAGE experiment was repeated three times and the reproducibly differentially expressed five spots were named as spot1-spot5 (S1-S5) and further analyzed.

To prove the identity of each individual target, specific monoclonal or polyclonal antibodies were procured. All five targets were tested individually by 1D-SDS-PAGE immunoblotting. The following figure 20 shows the western blotting of WT, K11 and K12 cells probed for the novel molecular targets. In addition, the western blot was probed with rabbit Polyclonal Hpdcd4 antibody to check the expression level of Hpdcd4.

Human aldo keto reductase 1C (AKR1C) isozymes are implicated in the pre-receptor regulation of steroid receptors, nuclear orphan receptors and membrane-bound ligand-gated ion channels (Bauman et al., 2004). AKR1C3 is one of the most interesting isoforms which is involved in the local production of active androgens within the prostate. Its expression in stromal cells is increased with benign and malignant diseases (Penning et al., 2006). Moreover, the tumor molecular profile from studies revealed the overexpression of few proliferative genes including elevated AKR1C3 in certain tumors (Mahadevan et al., 2006) and in prostate carcinoma (Fung et al., 2006). The loss of AKR1C1 and AKR1C2 was observed in breast cancer cells and prostate cancer cells (Ji et al., 2003; Ji et al., 2004). In the current study, AKR1C2 and C3 were highly expressed only in the K12 but not in the WT cells and also not in another knock-down clone, K11. This might be either due to clonal variation or due to the different extent of downregulation and thereby expression of Hpdcd4 in the two different knock-down clones.

CK-17 is expressed in various epithelia (Troyanovsky et al., 1992), including myoepithelial cells, basal layers of transitional and pseudo-stratified epithelia of the respiratory and urinary tracts, and early developmental stages of stratified epithelia. Common characteristics of these cells are contractility and/or frequent changes in shape. Normal adult epidermis does not contain CK-17, but certain pathological states, including psoriasis as well as benign and malignant neoplasms, lead to CK-17 expression (Jiang et al., 1994). Furthermore, CK-17 is identified to be overexpressed in invasive carcinomas (Carrilho et al., 2004) and during wound healing (Coulombe and Omary, 2004). As a rule, defined pairs of keratin proteins are coexpressed, but CK-17 seems to be one of the exceptions to this rule, because its specific coexpression partner has never been found (Jiang et al., 1994). In the present work, CK-17 was found to be overexpressed in the K11 and K12 cells compared to the WT cells.

Human GluProRS is a bifunctional tRNA synthetase enzyme that contains three tandem repeats linking the two catalytic domains and these repeat motifs were shown to be involved in protein-protein and protein-nucleic acid interactions with higher affinity (Jeong et al., 2000). The interest in GluProRS was due to the appearance of new spots as 5-6 pearls in a string in the Coomassie stained 2D-SDS-PAGE of K12 cells. In a 1D-SDS-PAGE, it showed similar level of expression in all three cells (WT, K11 and K12) tested.

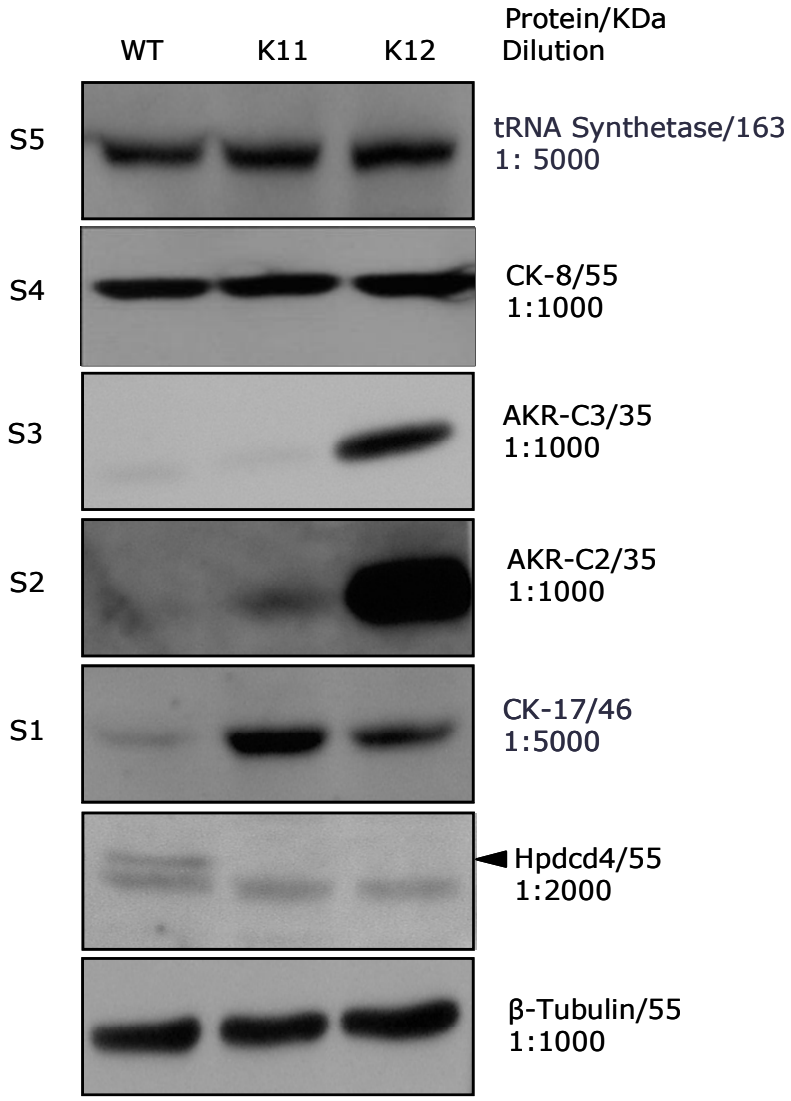

Figure: 20: The novel molecular targets on 1D Immunoblotting

HeLa WT, K11 and K12 cells were harvested, lysed in SDS-Laemmli buffer and samples were electrophoresed on 10% SDS-PAGE followed by western blotting was performed. The blot was probed with specific mouse, rabbit or goat mono/polyclonal antibodies as 1° Ab at the mentioned dilution. Respective HRP conjugated 2° Ab was used. Loading of the cell lysates was normalized by using β-tubulin.

4.1.7 The Effect of Hpdcd4 on the Biochemical Modification of CK-8

CK-8 expression was similar in both WT and clone cells as observed in the 1D-SDS-PAGE (Fig.20), but the interest in further analysis of CK-8 was due to the observation of 2 related spots appearing towards the lower pI side of CK-8 in the 2D-SDS-PAGE which might represent biochemically modified, possibly, phosphorylated forms of CK-8. To study the biochemical modification of CK-8 in detail, the CK-8 related spots were analyzed by 2D-SDS-PAGE and immunoblotting. Firstly, WT, K11 and K12 cells were analyzed in a narrower pH range (4-7) to confirm the appearance of CK-8 related molecular weight spots on the lower pI side of CK-8 in the 2D-SDS-PAGE using CK-8/18 specific antibody, (Fig.21). It was observed that only one spot appeared in the

lower pI side of the CK-8 spot. The second CK-8 related spot has not appeared and therefore might not be related to CK-8. As CK-8 and the related spot were well separated by this particular pH range, for further CK-8 analysis, this pH range was used. Once the reproducibility of the appearance of the spot was proven in the K11 and K12 cells, it was confirmed that this new spot was the result of a biochemical modification by Hpdcd4. The next question was to identify the biochemical modification, which changes the pI of the CK-8 protein but not the molecular weight. As UV treatment is one of the best sources for inducing phosphorylation, the WT and K12 cells were treated with UV followed by 2D-SDS-PAGE. Immunoblotting was performed to check the status of the CK-8 related spot. After the UV treatment, in the WT cells, a new spot was visualized. It was found to be very similar to the spot which appeared in the K12 untreated cells (Fig.22). The UV treated K12 cells did not show any difference in the intensity of the new spot compared to the UV untreated K12 cells (Fig.22).

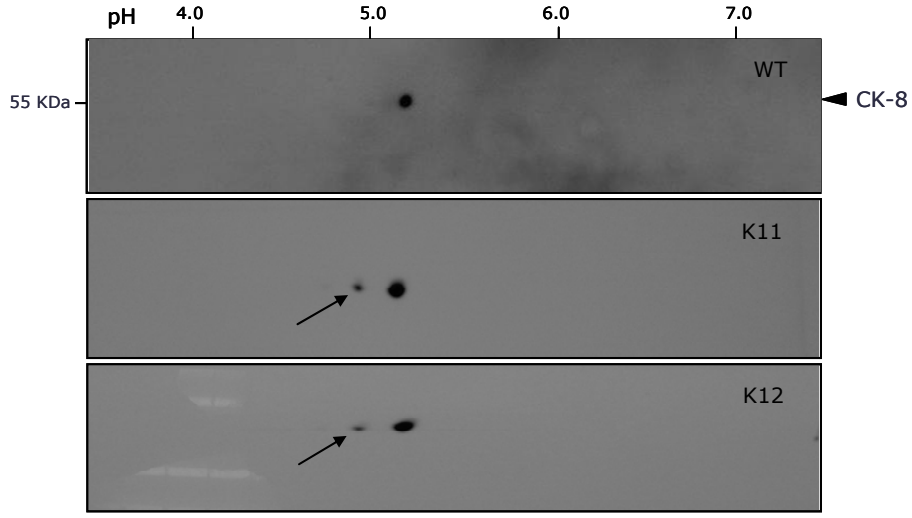

Figure 21: The effect of Hpdcd4 on the biochemical modification of CK-8

HeLa WT, K11 and K12 cells were harvested and the whole protein extract was prepared by calbiochem proteoextraction kit. 1D isoelectric focusing was performed for the pH range of 4-7. In the 2D 10% SDS-PAGE was performed followed by western blotting. The blot was probed with mouse monoclonal CK-8/18 as 1° Ab and then anti-mouse HRP conjugated 2° Ab was used. CK-8 is marked by a thick-short arrow at 55 KDa and the appearance of CK-8 related spot is marked by thin-long arrows at the similar MW in the figure.

It has already been shown that CK-8 can be phosphorylated by protein kinase C (PKC) (Ridge, 2005) or by Jun N-terminal Kinase (JNK) (Jian, 1997). To check the effect of Hpdcd4 on PKC mediated phosphorylation of CK-8, K12 cells were treated with TPA followed by 2D-SDS-PAGE and immunoblotting. The spot suspected to be phosphorylated CK-8 appeared to be more intense in the TPA treated K12 cells than in the DMSO treated control K12 cells (Fig.23). In addition to that two more CK-8 related spots appeared to the right and left of CK-8 in the TPA treated K12 cells, indicated by dashed arrows (Fig.23).

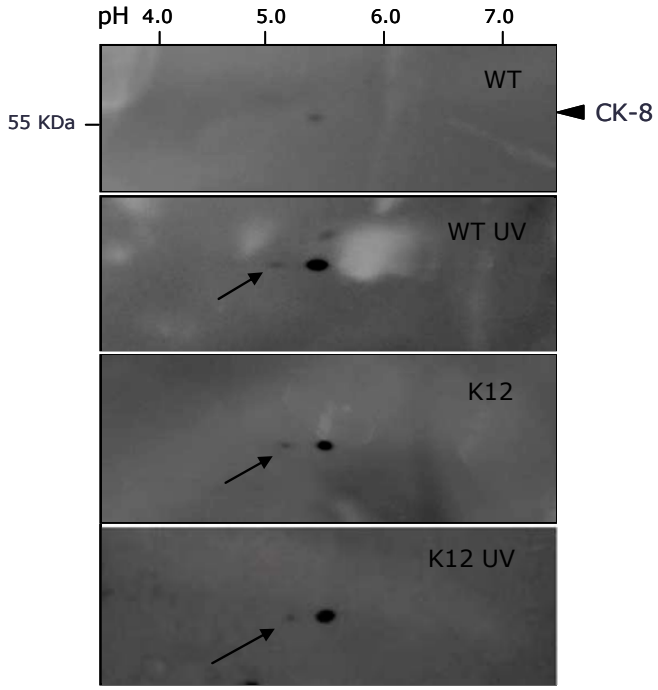

Figure 22: The effect of Hpdcd4 on biochemical modification of CK-8 during UV-induction

HeLa WT, K11 and K12 cells were harvested after UV 100 J/m^2 (10 sec) treatment followed by 6 hrs incubation and the whole protein extract was prepared by calbiochem proteoextraction kit. 1D isoelectric focusing was performed with the pH range of 4-7. In the 2D 10% SDS-PAGE was performed followed by western blotting. The blots were probed with mouse monoclonal CK-8/18 as 1° Ab and then anti-mouse HRP conjugated 2° Ab was used. The appearance of CK-8 related spot is indicated by thin-long arrows in the figure.

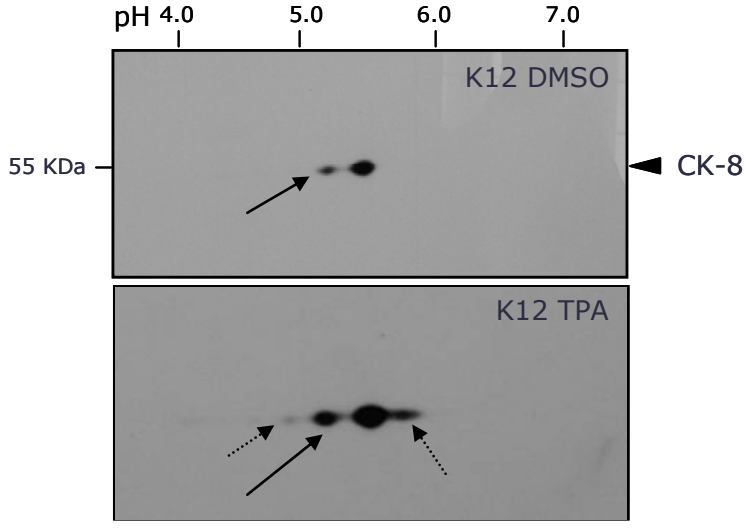

Figure 23: The effect of Hpdcd4 on biochemical modification of CK-8 during TPA treatment

HeLa K12 cells were treated with DMSO (as control) and 250 nm TPA for 1 hr, harvested, and the whole protein extract was prepared by calbiochem proteoextraction kit. In the 1D isoelectric focusing was performed for pH range 4-7 and in the 2D 10% SDS-PAGE was performed followed by western blotting. The blots were probed with mouse monoclonal CK-8/18 as 1° Ab and anti-mouse HRP conjugated 2° Ab was used. The appearance of CK-8 related spot is indicated by a thick arrow in the figure. Two more spots appeared in the TPA treated 2D-SDS-PAGE, as indicated by dashed arrows.

In addition to its suspected role in protein translation, Pdcd4 was also shown to have RNA binding activity which is dependent on RNA binding domain present in the N-terminal part of the protein (Boehm et al., 2003). This raises the possibility of involvement of Hpdcd4 function at RNA level. The analysis of the effect of Hpdcd4 on differential protein expression has revealed a set of cancer related genes which were further analyzed at the RNA level.

PolyA RNA was isolated from the WT and K12 cells and northern blotting was performed to check the effect of Hpdcd4 on c-Jun, c-Myc and CK-17 mRNAs (Fig.24). The respective mRNAs transcripted from the CK-17 and c-Myc genes were highly correlated with their differential protein expression profile except in case of c-Jun. The c-Jun mRNA level was quantitatively equal in both WT and K12 cells. The CK-17 showed higher mRNA levels in the K12 cells compared to the WT cells. In contrast, c-Myc mRNA was expressed less in the K12 cells than in the WT cells.

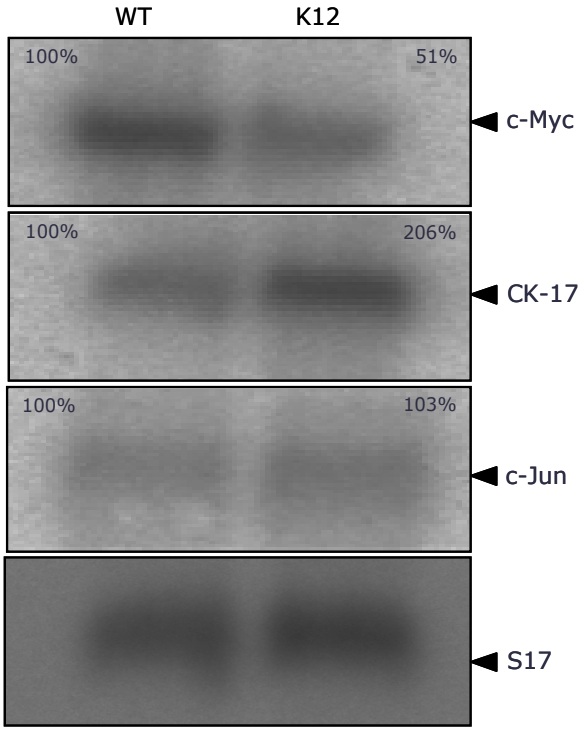

Figure 24: Expression of Pdcd4 targets at the RNA level

HeLa WT and K12 cells were harvested and polyA RNA was isolated using oligo dT cellulose. The samples were electrophoresed on 1% Formaldehyde-Agarose gel, blotted onto a nylon membrane overnight, and hybridized with different probes. The specific DNA fragments were labeled by α-^{32}P-dCTP and probes prepared by nick translation using Amersham G50 columns. S17 was used as a loading control. The specific RNAs are indicated by arrow. The quantitative expression of mRNA is indicated in percentage after normalizing with S17 mRNA.

The effect of Hpdcd4 on CK-17 RNA

The effect of Hpdcd4 on CK-17 was studied in further detail. Because it is possible that the probe used to detect CK-17 RNA also cross reacts with mRNAs of other cytokeratins, CK-17 mRNA was also analyzed by RT-PCR using CK-17 specific primers. Total RNA isolated from both HeLa WT and K12 cells was reverse transcribed and amplified by PCR reaction using β-actin and CK-17 specific primers (Fig.25). CK-17 mRNA expression was higher in the K12 cells compared to the WT cells. This result is consistent with the previous northern blotting experiment (Fig.24).

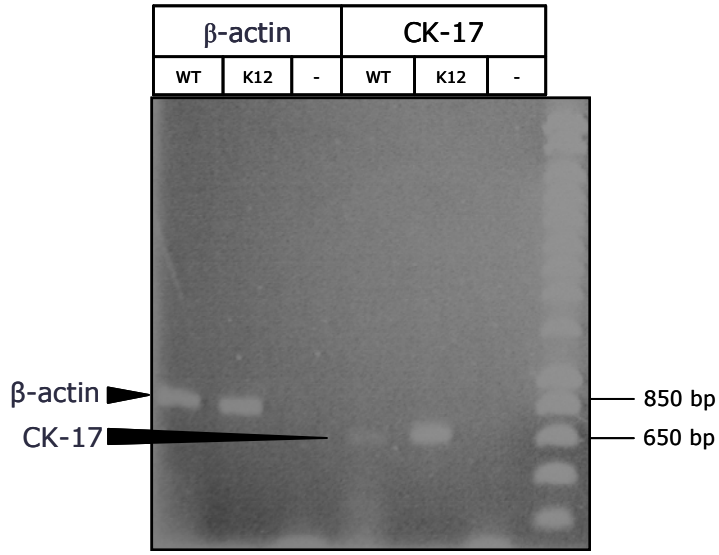

Figure 25: The effect of Hpdcd4 on CK-17 mRNA

HeLa WT and K12 cells were harvested and the total RNA was isolated using Nucleospin total RNA isoloation kit. Reverse transcription was performed using oligo dT primers. PCR amplification of CK-17 was done using ss cDNA as a template and using CK-17 specific primers (at 65°C as annealing temperature and 35 cycles of PCR). B-actin was used as an internal control, β-actin specific primers were used for PCR amplification at 69°C as annealing temperature. – symbol in the figure is negative control without template, to confirm the specificity of the primers. The β-actin (850 bp) and the CK-17 (650 bp) PCR products are marked by arrows.

4.1.9 The effect of Hpdcd4 on mRNA Stability

As Hpdcd4 is affecting the RNA level of CK-17 and c-Myc, it may be regulating the expression of CK-17 and c-Myc at the posttranscriptional level. Gene expression is finely regulated at the posttranscriptional level. Features of the untranslated regions of mRNAs that control their translation, degradation and localization include stem-loop structures, upstream initiation codons and open reading frames, internal ribosome entry sites and various *cis*-acting elements that are bound by RNA binding proteins (Mignone et al., 2002). Multiple mRNA binding proteins that interact specifically with defined regions in posttranscriptionally regulated mRNAs were characterized (Rajagopalan and Malter, 1997). The binding proteins, in turn, are subdivided into

classes that either stabilize or destabilize mRNA. The proteins that regulate mRNA half-lives, affect, in turn, cell growth, differentiation and response to its environment (Ross, 1995). In general the mRNA half-life can be measured by culturing the cells with a transcription inhibitor and harvest at different time points thereafter. The most frequently used transcription inhibitors are actinomycin-D, cordycepin, α-amanitin and 5,6-dichloro-1-β-D-ribofuranosylbenzimidazole (Ross, 1995).

Hpdcd4 binds RNA through its N-terminal RNA binding domain (Bohm et al., 2003). From the previous experiment, it was found that the level of CK-17 and c-Myc mRNAs was increased by Hpdcd4. It is possible that Hpdcd4 is either acting at the promoter level of these genes or is involved in the turn-over and thereby the stability of the mRNAs. To elucidate the effect of Hpdcd4 on the turn-over of CK-17 and c-Myc mRNA transcripts, the HeLa WT and K12 cells were treated with a transcription inhibitor. The cells were harvested at different time points after actinomycin-D treatment. Actinomycin-D forms a stable complex with DNA and blocks the movement of RNA polymerase which interferes with DNA-dependent RNA synthesis. This ensures that the change in the level of mRNA transcript is only due to the stability of the mRNA rather than due to the change in transcription. The following figure (Fig.26) shows the northern blot hybridized with different probes. At the 5 hr time point, no mRNA was seen.

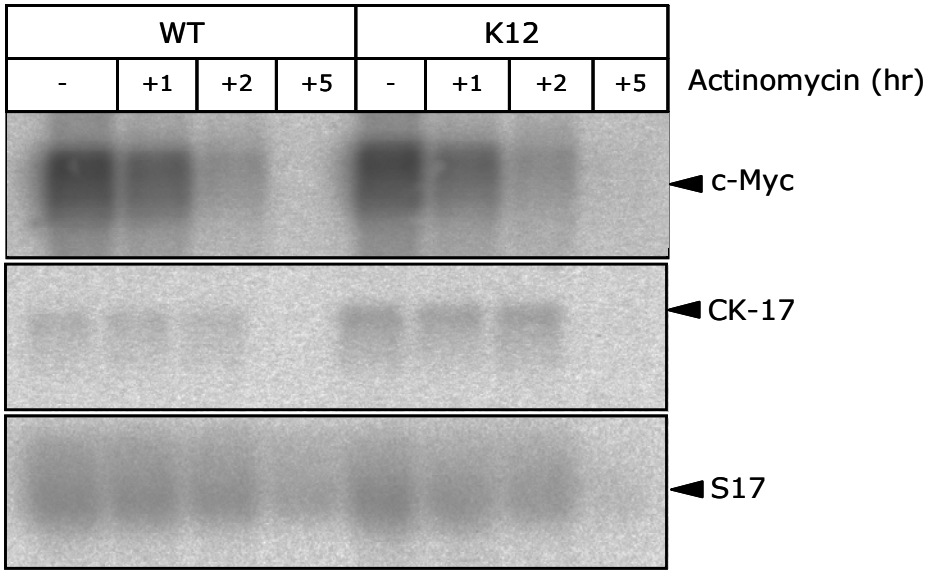

Figure 26: The effect of Hpdcd4 on mRNA stability

HeLa WT and K12 cells were treated with and without actinomycin-D (10 µg/ml), incubated for 1, 2 and 5 hrs and harvested. PolyA RNA was isolated using a oligo dT cellulose column. The RNA was fractionated on a 1% Formaldehyde Agarose gel and blotted onto a nylon membrane overnight. The blot was hybridized with specific α-^{32}P-dCTP labeled probe and S17 mRNA was used as an internal control. The blots were exposed to phosphor imager screen for quantitative analysis. – in the figure refers to actinomycin-D untreated cells.

The northern blot from the previous experiment was quantitated, normalized by S17 mRNA and the data points were plotted (Fig.27). Compared with CK-17, c-Myc mRNA has a shorter half-life and degraded faster, in contrast CK-17 has a longer half-life. In case of both CK-17 and c-Myc, the WT cells degraded the mRNAs faster than the K12 cells.

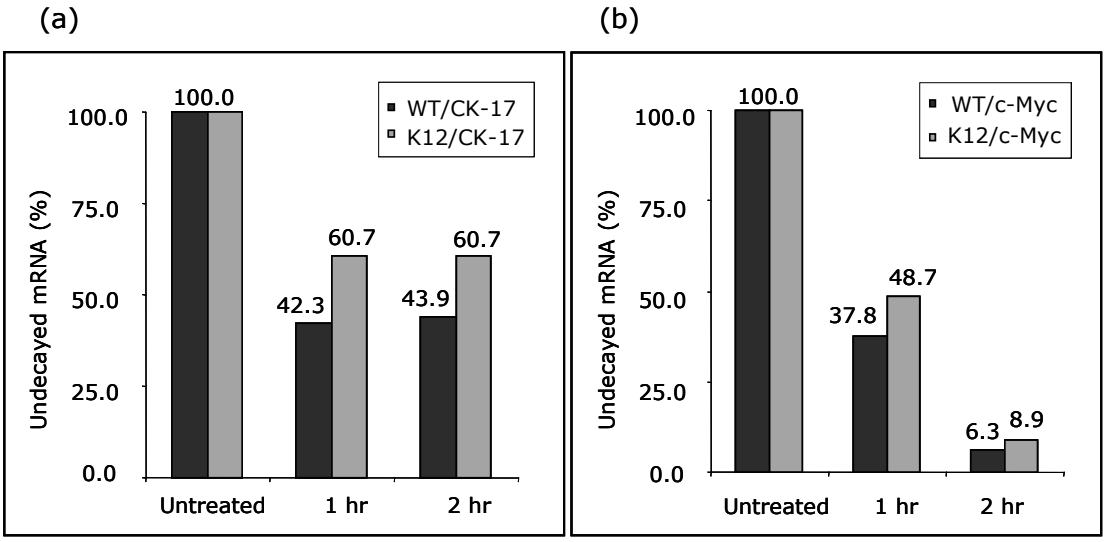

Figure 27: The effect of Hpdcd4 on mRNA stability

The quantified and S17 normalized data from the northern blot shown in the figure 26 was used to plot the graph. The values from the actinomycin-D treated cells were normalized to the values from the untreated cells. The mRNA stability from the untreated cells was arbitrarily expressed as 100% a) CK-17 mRNA and b) c-Myc mRNA.

4.1.10 The effect of Hpdcd4 on Nonsense-Mediated mRNA Decay

In addition to the role of Hpdcd4 on the stability of normal mRNA transcripts, the effect of Hpdcd4 on degradation of mRNAs with a nonsense mutation in the coding region was also analyzed. Accurate gene function depends on a low error rate of each step of the gene expression pathway. The fidelity of gene expression is enhanced further by a phylogenetically widely conserved quality control mechanism against faulty mRNAs with premature translation termination codons (PTC), which has been termed nonsense-mediated mRNA decay (NMD) (Neu-Yilik et al., 2001). In all the organisms, mRNAs are destabilized by 10-fold or more when they contain PTCs (Ross, 1995). In mammals, NMD operates as a posttranscriptional mechanism in the nucleus. The NMD is thought to operate in two possible steps, the abnormal splicing followed by degradation of spliced mRNAs (Hentze and Kulozik, 1999). The β-Globin mRNA is the most stable mRNA having half-life of more than 24 hr and it is subjected to NMD due to the presence of PTC mutations in the 5´proximal exon of its mRNA. To study NMD, the degradation of a β-Globin gene construct with a nonsense mutation at the position of 39 in the exon 2 which is compared to the corresponding WT construct degradation

(Neu-Yilik et al., 2001). The WT and mutant (NS39 at 2nd exon) β-Globin DNA constructs were transfected into the HeLa WT and K12 cells and mRNA was isolated followed by northern blotting using a β-Globin-specific probe (Fig.28). The mutant β-Globin mRNA was found to be degraded almost completely, but the degradation in the WT cells was slightly more efficient compared to the K12 cells, lacking Hpdcd4 (Fig.29).

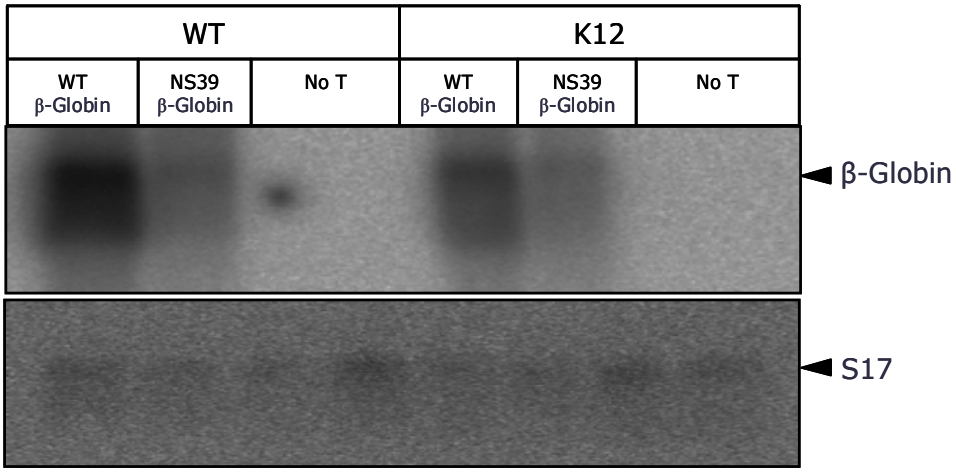

Figure 28: Effect of Hpdcd4 on NMD

The WT and mutant β-Globin DNA were transiently transfected into HeLa WT and K12 cells with pCMV-β-galactosidase to check the transfection efficiency. 48 hrs later, the cells were harvested; PolyA RNA isolation was performed using oligo dT cellulose and northern blotting was performed overnight. The membrane was hybridized with the S17 and the NMD probe (α -^{32}P-dCTP labeled β-Globin full length DNA). The blots were exposed to phosphor imager screen and quantitated. No T: Non-transfected cells. S17 and β-Globin mRNA are marked by arrows.

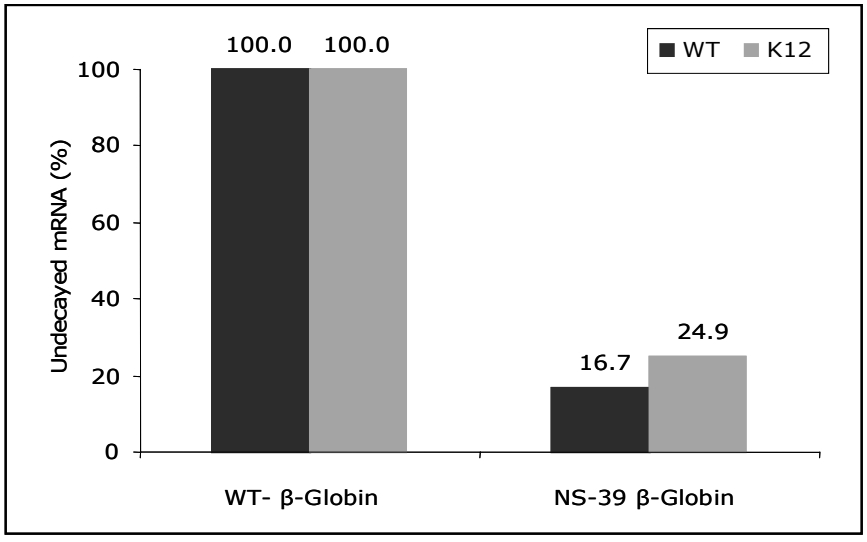

Figure 29: Effect of Hpdcd4 on NMD

The quantitative data from the northern blot was used to plot a graph. The transfection efficiency was normalized by using β-galactosidase values. The northern blot bands were quantified and values of NS-β-Globin were normalized to the values of WT β-Globin. The WT β-Globin values of WT and K12 cells were arbitrarily expressed as 100%.

4.2 Downregulation of Pdcd4 – Knock-Out-System

4.2.1 Targeted Disruption of the Chicken Pdcd4 gene

In nature, homologous recombination is a DNA repair and maintenance pathway that protects chromosomes against damage affecting both strands, such as double strand breaks (DSB) or interstrand cross-links (Jasin, 2000). The recombination machinery has been conserved throughout the evolution, as an essential component of cell survival. This maintenance role of homologous recombination is used as a molecular biology tool in targeting the chromosomal DNA. To perform homologous recombination, the DNA sequence of the gene which will be replaced should be known. With this information, it is possible to replace any gene with a targeting construct containing a selection marker flanked by homologous gene sequences.

DT40 is a chicken pre B lymphoblast suspension cell line, which shows high rates of recombination. Homologous recombination allows the precise replacement of a sequence with another. In order to replace parts of both the functional copies of the chicken Pdcd4 gene (*Cpdcd4*), two different targeting constructs with histidinol and puromycin resistance cassettes were received (Bitomsky, 2003).

By screening a genomic library of chicken DNA with a probe derived from a chicken Pdcd4 (Cpdcd4) cDNA clone (Schlichter et al., 2001a) genomic clones that encompass a major part of the chicken *Pdcd4* gene was isolated (Schlichter et al., 2001b). Two *Cpdcd4* targeting constructs conferring histidinol and puromycin resistance were made by replacing part of the *Cpdcd4* by respective antibiotic resistance cassette (Bitomsky, 2003). Figure 30a shows the schematic diagram of the histidinol targeting construct and the expected fragment pattern of *ApaI* digestion in Southern blotting.

DT40 cells were first transfected with the targeting construct conferring histidinol resistance followed by selection in the presence of 0.5 mg/ml L-histidinol. The resulting clones were then analyzed by Southern blotting for disruption of one copy of *Cpdcd4* using a probe derived from the 5’ end of the gene. A positive clone (K18) was identified in the Southern blotting by the appearance of an ~7 kb novel *Apa*I restriction fragment and retaining a ~13 kb fragment unlike the WT cells, which retains both the ~13 kb fragments of WT Cpdcd4 (Fig.32).

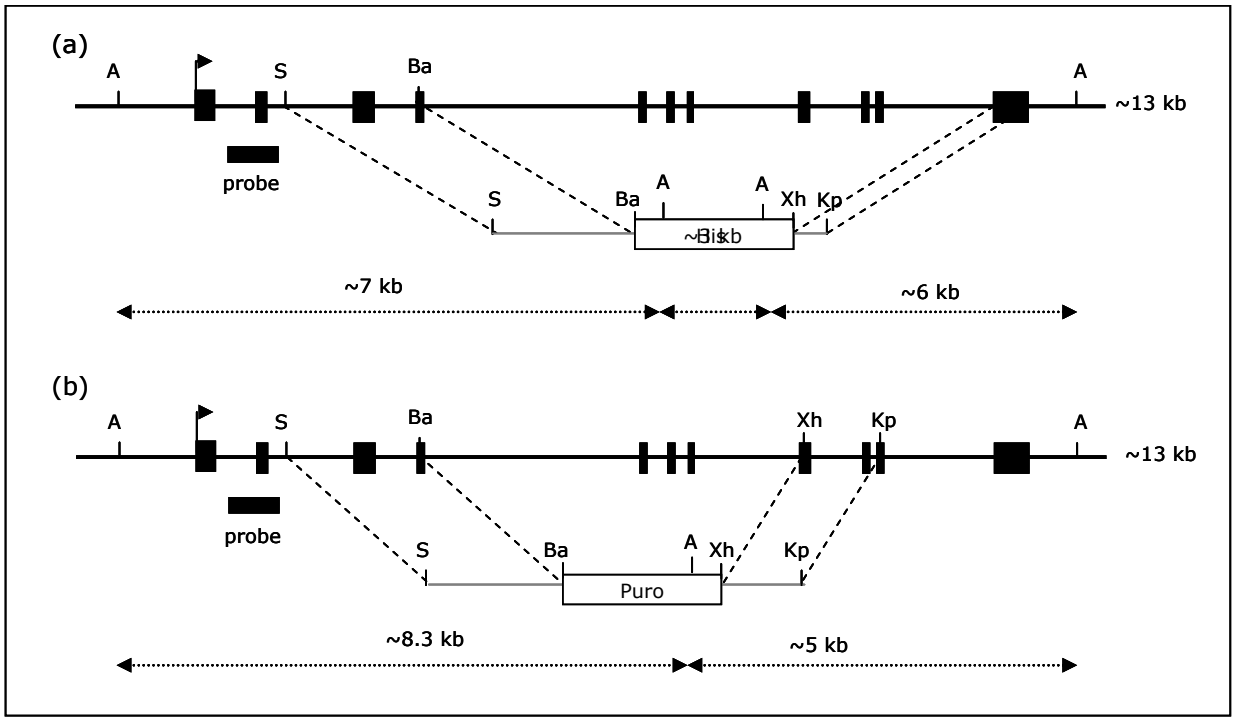

Figure 30: The schematic diagram of the targeting constructs and fragment pattern

(a) and (b) Schematic representation of the *Cpdcd4* locus (thick black line) and the two targeting constructs used (Grey line). The histidinol (His) and puromycin (Puro) resistance genes are marked by white boxes. Relevant *ApaI* (A), *BamHI* (Ba), *KpnI* (Kp), *SacI* (S) and *XhoI* (Xh) restriction sites are shown. The probe fragment is indicated by a black bar. When *ApaI* digestion followed by Southern blotting is performed, the expected fragment pattern is indicated by dashed arrows. *Cpdcd4(+/-)* histidinol resistant clones were expected to give a new approximately 7 Kb fragment and one old ~13 Kb fragment in stead of two WT-~13 Kb fragments. Puromycin resistant clones were expected to give a new ~8.3 kb fragment. As the puromycin construct was targeted to the second copy of the *Cpdcd4(+/-)*, led to the disappearance of both the copies of 13 kb parental *ApaI* fragment and appearance of two novel *ApaI* fragments of ~7 kb and ~8.3 kb from the histidinol and puromycin constructs, respectively.

Among the 36 clones tested, only one clone with one mutated copy of *Cpdcd4*, K18, was identified. Then a second construct with puromycin resistance was transfected and more than 54 resistant clones were analyzed by Southern blotting. There was no double mutant clone identified. It is presumably as the right arm of the puromycin targeting construct made by Bitomsky (2003) was only 600 bp in length, which might target the Pdcd4 inefficiently. Therefore, another targeting construct with a longer right arm of approximately 2.2 kb, conferring puromycin resistance was generated (Fig.31). In the present work, the new puromycin targeting construct and the expected fragment pattern of *ApaI* digestion in Southern blotting is shown in figure 30b. This longer right arm might possibly enhance the specific targeting of *Cpdcd4* by homologous recombination.

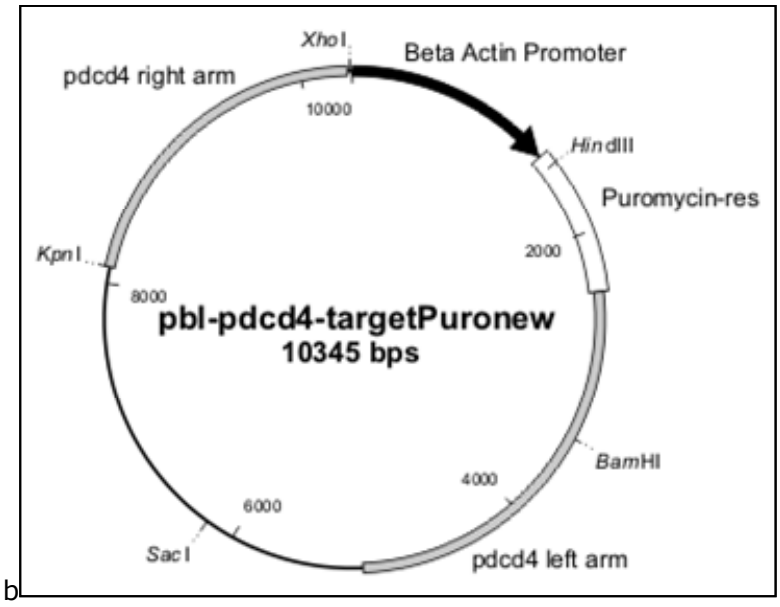

Figure 31: The *Cpdcd4* new puromycin targeting construct

In case of the new puromycin targeting construct, a 2.2 kb fragment containing exons 7 to 9 with the intervening sequences was inserted into the pbl-pdcd4-targetPuro thereby replaced the 600 bp right arm of the targeting construct.

The puromycin targeting construct was transfected into the histidinol resistant clone (K18) by electroporation. After selection in the presence of 1 µg/ml puromycin doubly resistant clones were obtained. These clones were again analyzed by Southern blotting to identify cells in which both copies of *Cpdcd4* had been disrupted. The Southern blot shown in Figure 33 illustrates the successful targeting of both copies of the *Cpdcd4* gene. The Pdcd4 double mutant clones lost both the WT copy of the Pdcd4 (two ~13 kb fragments), in stead they produced two new fragments of ~7 kb and ~8.3 kb, respectively.

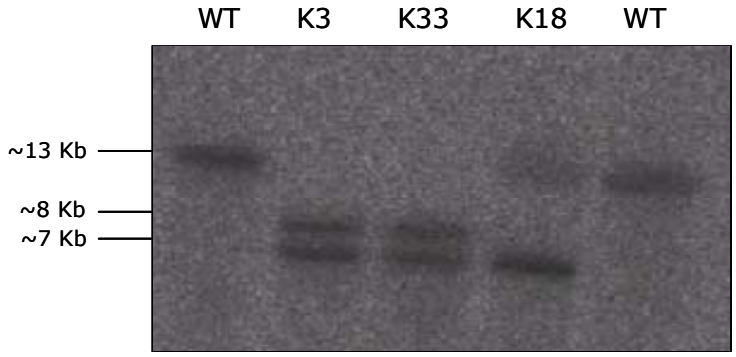

Figure 32: Southern blotting of *Cpdcd4* Knock-out clones

The genomic DNA was isolated from the DT40 WT, *Cpdcd4* single and double mutant clones and digested by *ApaI* overnight. Southern blotting was done and the DNA hybridized with the probe from the 5' side of the *Cpdcd4* gene labeled by α-^{32}P-dCTP. Both the WT copies of the ~13 Kb fragments of *Cpdcd4* were lost in the K3 and K33 clones and two new ~7Kb and ~8.3 Kb fragments appeared.

4.2.2 The effect of the Disruption of Cpdcd4 on the Growth Characteristics

To determine if the absence of *Cpdcd4* affected the proliferation rate of the cells, the growth of *Cpdcd4*(+/+), (+/-) and (-/-) cells were analyzed (Fig.33). All of the cells grew with indistinguishable doubling times of approximately 12 hr. In addition, the cell cycle distribution of the *Cpdcd4(+/+)* and *(-/-)* cell populations by flow cytometry was determined. The fractions of the cells residing in different phases of the cell cycle were similar for each cell population (Fig.34).

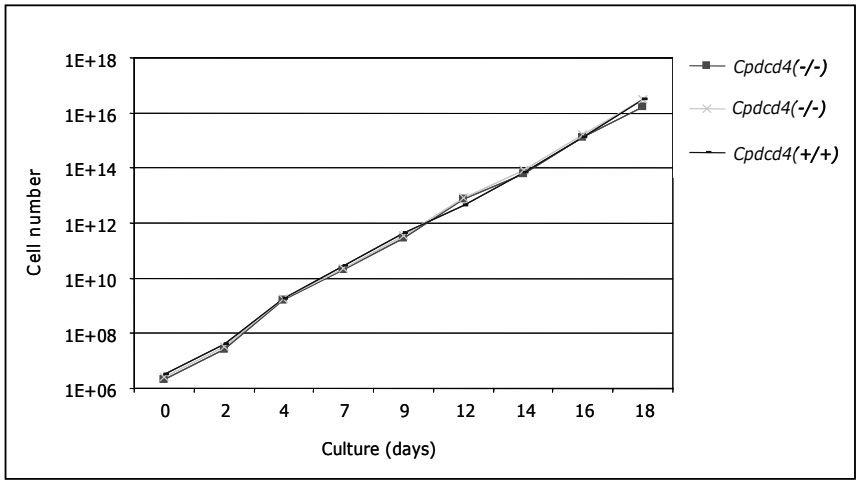

Figure 33: The proliferation rate of DT40 *Cpdcd4(-/-)* and *(+/+)* cells

The cells (K3 and WT) were grown in culture for 18 days and counted.

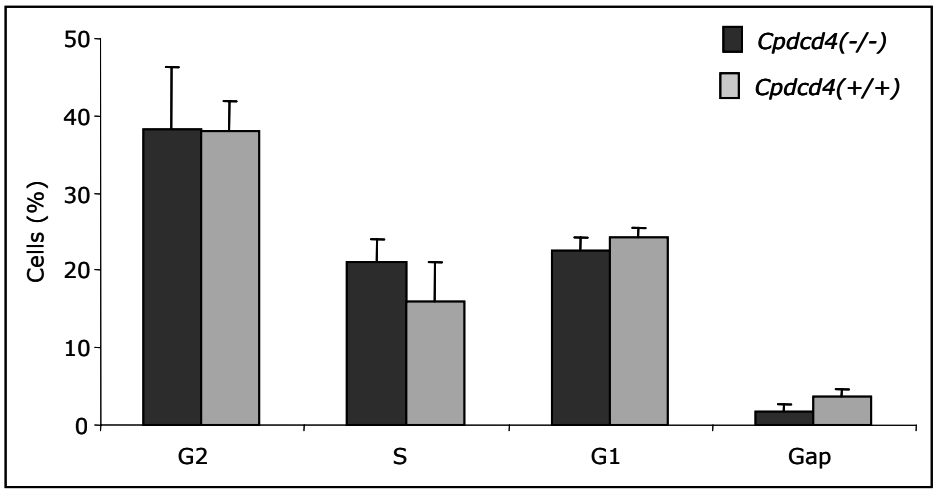

Figure 34: The cell cycle distribution of DT40 *Cpdcd(-/-)* and *(+/+)* cells

The cells (K3 and WT)were grown in the culture, harvested, washed with 1X PBS for 3 times and stained with propidium iodide. Cell cycle analysis was performed using Fluorescence Activated cell Sorting (FACS) instrument. S: DNA synthesis; G1 and G2: Check points before and after S phase, respectively; Gap: Small cells.

4.2.3 The effect of Cpdcd4 on Translation

Previous work has implicated Pdcd4 in the control of translation. Most eucaryotic mRNAs are translated by a cap-dependent mechanism in which eIF4G acts as a scaffold for other proteins, including eIF4A (Gingras et al., 1999). It has been suggested that overexpression of Pdcd4 suppresses translation initiation by interfering with the RNA helicase activity of eIF4A and by preventing its interaction with eIF4G (Yang et al., 2003b).

A subset of cellular mRNAs contains internal ribosomal entry sites (IRES) which mediates cap-independent translation initiation. In general, it was observed that many of the RNAs containing IRES elements are involved in important cellular processes, such as cell cycle, apoptosis, differentiation or development (Vagner et al., 2001; Stoneley and Willis, 2004). As previous studies on the role of Pdcd4 in translation initiation relied exclusively on cells overexpressing Cpdcd4 or on the use of in vitro translation systems it was of interest to assess the effect of the disruption of *Pdcd4* on both mechanisms of translation initiation.

The effect of Cpdcd4 on Cap-Dependent Translation

To measure the overall rate of protein synthesis by labeling DT40 WT and K3 cells were labeled with ^{35}S-methionine for a short time followed by quantification of the radioactivity incorporated into TCA-precipitable material. This experiment measures the overall rate of total protein synthesis, as most of the protein synthesis is cap-dependent when the cells are in the normal conditions. As shown in figure 35a the incorporation of ^{35}S-methionine was very similar in *Cpdcd4(+/+)* and *(-/-)* cells, suggesting that the lack of Pdcd4 has no global effects on cap-dependent protein synthesis.

When the cells were UV induced, the cap-dependent translation is compromised by IRES-dependent translation. To investigate the effect of Cpdcd4 on the cap-independent translation, the cells were treated with UV, labeled with ^{35}S-methionine, shortly after TCA precipitated and the incorporated radioactivity was quantitated (Fig.35b). There was no change in the IRES-dependent translation of WT and K12 cells when they were UV treated.

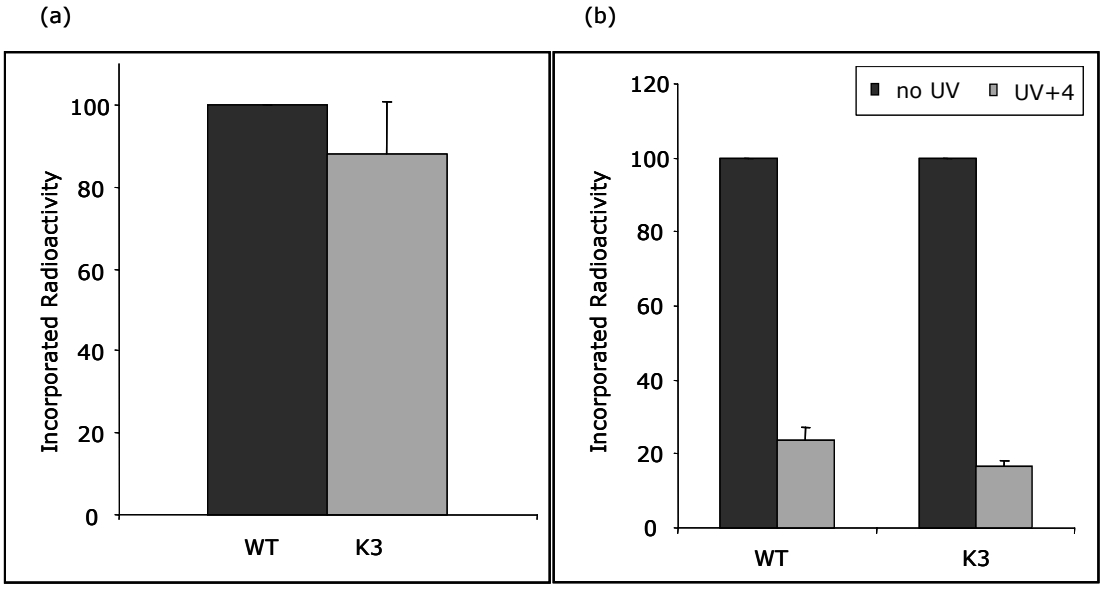

Figure 35: Effect of Cpdcd4 on total protein synthesis

Dt40 *Cpdcd4(+/+)* and *(-/-)* (WT and K3) cells were seeded, grown in the culture and starved without methionine for 30 min. Then cells were fed with ^{35}S-methionine and incubated for 1 hr. Cells were harvested, washed, spotted over whatman filter paper and precipitated by trichloroaceticacid. Then exposed to the phosphorimager screen and quantitated. b) For the UV experiment cells were treated with UV 100 J/m^2 (1 min) or left untreated and incubated for 4 hrs. Then the samples were processed in the similar way mentioned in (a).

To discern the possible effects on IRES-dependent translation bicistronic reporter gene constructs carrying a cap-dependent renilla luciferase gene and an IRES-dependent firefly luciferase gene were employed (Fig.9). The reporter genes containing several previously characterized IRES elements, derived from the c-Myc, N-myc, Apaf-1, Mnt and Xiap genes were used (Stoneley et al., 1998; Jopling and Willis, 2001; Coldwell et al., 2000; Stoneley et al., 2001; Holcik and Korneluk, 2000). The reporter genes were transfected into *Cpdcd4(+/+)* and *(-/-)* cells followed by measurement of the activities of the two luciferases. As illustrated in figure 36, there were only slight increases in the ratio of firefly to renilla luciferase activity in few cases, suggesting that the absence of Cpdcd4 does not have a major impact on the IRES-dependent translation of these genes.

Effect of Pdcd4 on Apaf-1 IRES

The dual luciferase constructs of each gene were also analyzed individually after UV induction. The Apaf-1 IRES was analyzed after different doses of UV treatment and incubation for different times (Fig.37). But no difference in the IRES-dependent translation was observed after UV treatment of the DT40 WT and K3 cells.

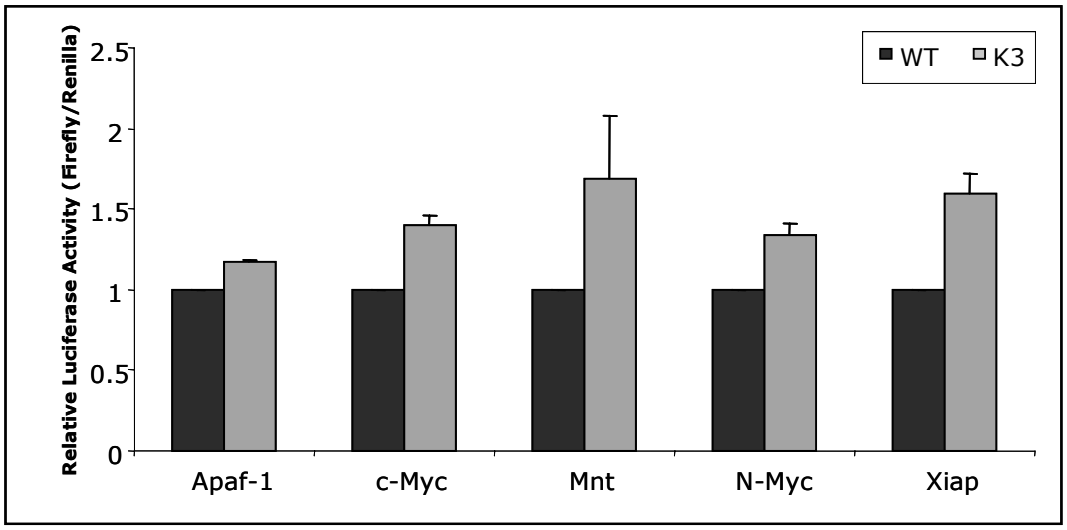

Figure 36: Effect of CPdcd4 on IRES elements

The cells were transiently transfected with pRApaf-1F, pRc-MycF, pRMntF, pRN-MycF, and pRXIAF of each 5µg by electroporation. After 24 hr of transfection, cells were harvested and cell lysate prepared for luciferase assay using the promega dual luciferase assay kit.

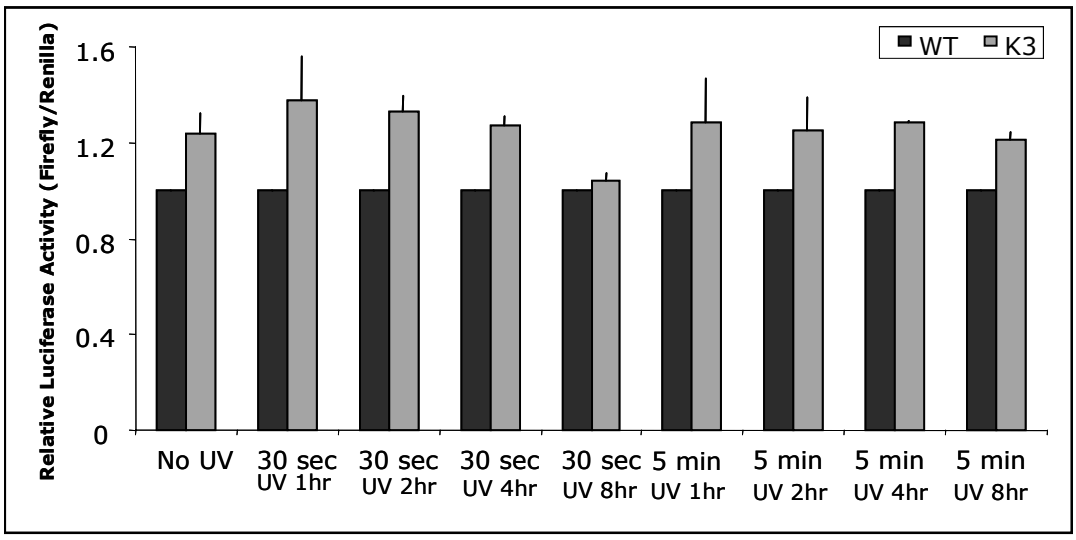

Figure 37: Effect of CPdcd4 on Apaf-1 IRES

The cells were transiently transfected with 5 µg of pRApaf-1F by electroporation, treated with UV 100 J/m^2 (30 sec and 5 min), incubated and harvested after 1 hr, 2 hr, 4 hr and 8 hr. After harvesting, cell lysates were prepared for luciferase assay using the promega dual luciferase assay kit.

Effect of Pdcd4 on N-Myc and Mnt IRES

N-Myc and Mnt IRES were analyzed after inducing with different doses of UV and incubated for different time points (Fig.38 and Fig.39). Though the error bars are large, the N-Myc IRES was affected by UV treatment and with increasing UV dose the IRES-dependent translation also increased. After UV-treatment the N-Myc IRES activity

was higher in the K12 cells compared to the WT cells. The UV treatment has not affected the Mnt IRES-dependent translation.

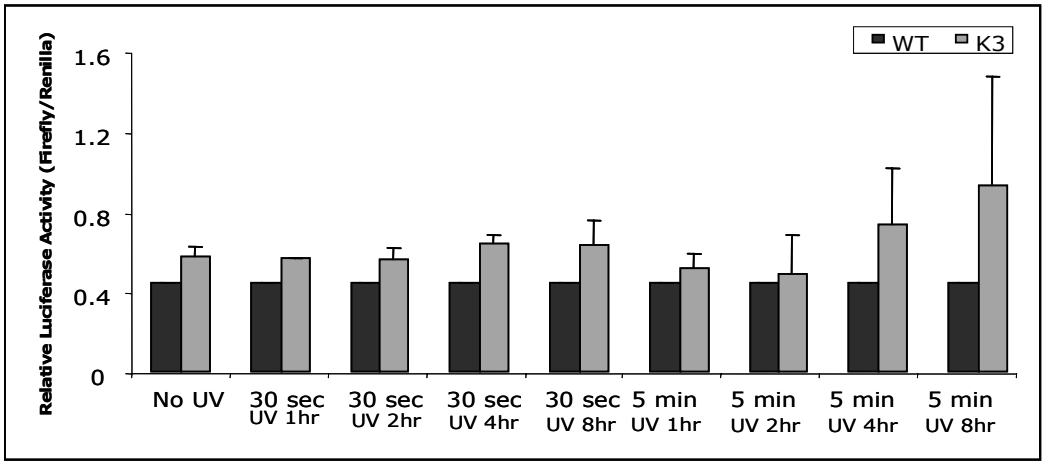

Figure 38: Effect of CPdcd4 on N-Myc IRES

The cells were transiently transfected with 3 µg of pRN-MycF by electroporation and treated with UV 100 J/m^2 (30 sec and 5 min), incubated and harvested after 1 hr, 2 hr, 4 hr and 8 hr. After harvesting, cell lysates were prepared for luciferase assay using the promega dual luciferase assay kit.

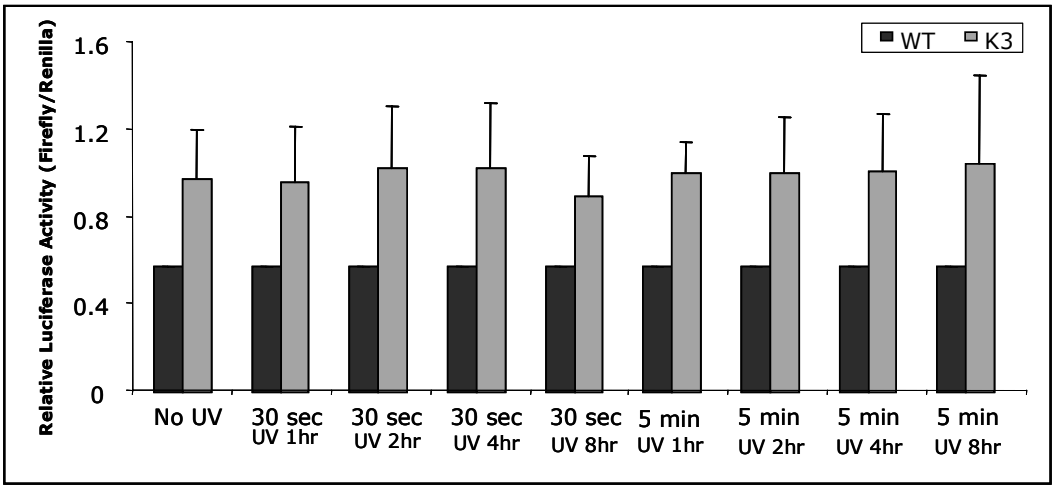

Figure 39: Effect of CPdcd4 on Mnt IRES

The cells were transiently transfected with 3 µg of pRMntF by electroporation and treated with UV 100 J/m^2 (30 sec and 5 min), incubated and harvested after 1 hr, 2 hr, 4 hr and 8 hr. After harvesting, cell lysates were prepared for luciferase assay using the promega dual luciferase assay Kit.

4.2.4 2D-SDS-PAGE Analysis of Cpdcd4 Knock-out Clones

For the comparison of proteomic profile of the DT40 *Cpdcd4(+/+)* and the two *Cpdcd4(-/-)* clones (K3 and K33), 2D-SDS-PAGE was performed. But there was no reproducible difference observed in the expression profile of various proteins (Fig.40).

4.2.4 2D-SDS-PAGE Analysis of Cpdcd4 Knock-out Clones

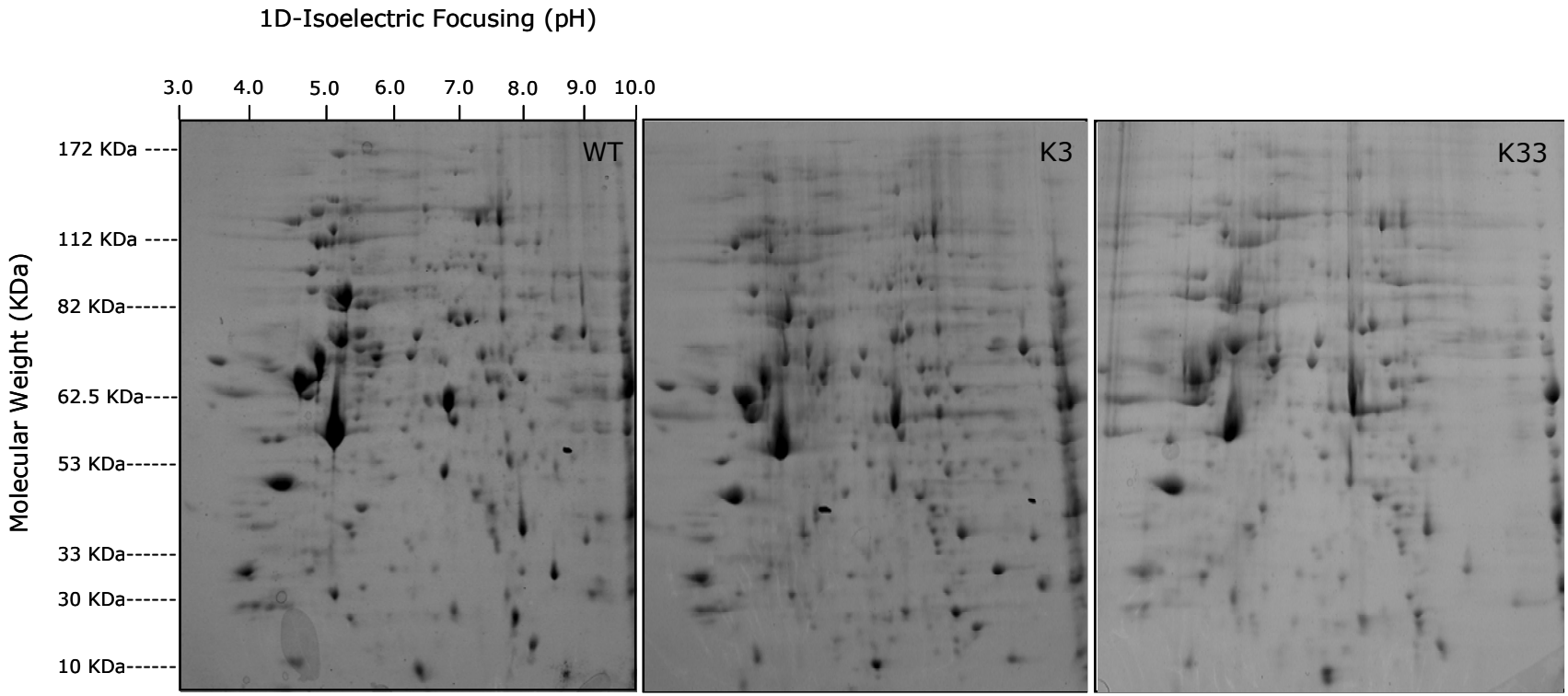

Figure 40: 2D-SDS-PAGE analysis of *Cpdcd4+/+) and (-/-)* cells

1-1.5 X 10^5 cells/ml each from WT, A14 and A19 were seeded and the next day harvested. The total proteome extract was prepared, proteins were isoelectrically focused in the 1D using immobiline pH gel (IPG) strip of pH (3-10) and 10% SDS-PAGE was done in the 2D. The gels were stained by CBB.

4.3 Upregulation of Pdcd4 - Overexpression System

4.3.1 Overexpression of the Human Pdcd4 gene

The human lung carcinoma cell line (A549) was found to express very low amounts of Hpdcd4 (Jansen, 2004). Therefore, A549 cells were chosen to overexpress the Hpdcd4 to study its molecular functions. For this purpose, a Hpdcd4 overexpression construct was made in the pcDNA3 and pcDNA4 vectors. HTB-133, the breast cancer cells, which express high amounts of Pdcd4, were used to generate a full length copy of Hpdcd4 by PCR. Figure 41a shows that an approximately 1500 bp fragment of Hpdcd4, which was amplified by PCR from these cells. The PCR product was then cloned into the TOPO cloning vector, sequenced, and finally cloned into the pcDNA3 (Fig.41b) and pcDNA4 mammalian expression vectors.

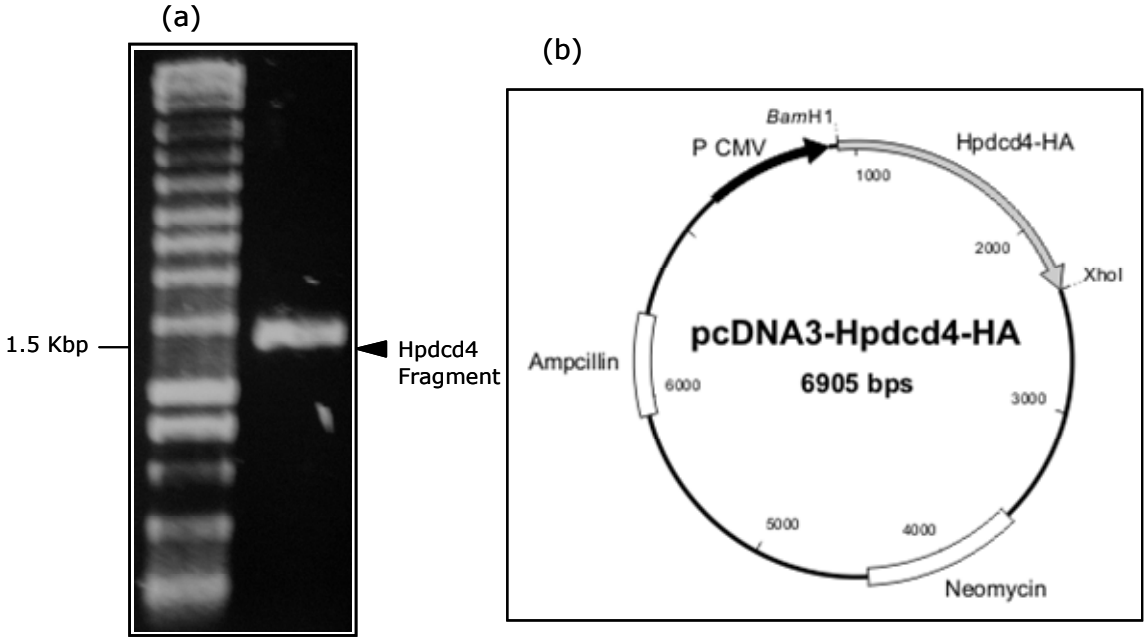

Figure 41: (a) The Hpdcd4 fragment and (b) the overexpression construct

a) The total RNA was isolated from HTB-133, breast carcinoma cell line and ss cDNA was prepared by reverse transcription. PCR amplification of *Hpdcd4* was done using specially designed Hpdcd4 cloning primers, which add a *BamHI* site at the 5' end and HA tag followed by *XhoI* site at the 3' end. The PCR product of 1500 bp fragment was checked in the 1% Agarose gel. *Hpdcd4* fragment is indicated by arrow. b) The 1500 bp fragment of *Hpdcd4* was cloned into the pCR2.1-TOPO cloning vector. The positive clones were sequenced using M13 and T7 primers. The middle *HindIII* fragment of the *Hpdcd4* was subcloned into the pCR2.1-TOPO vector again and sequenced using the same sequencing primers. Then the sequenced *BamHI* and *XhoI* complete fragment was cloned into the pcDNA3 mammalian expression vector.

Transient Transfection

After generating the overexpression construct, transient transfection of Cpdcd4 and Hpdcd4 into QT6 cells was done to check the integrity of the constructs (Fig.42). The Cpdcd4 expression was always higher than Hpdcd4.

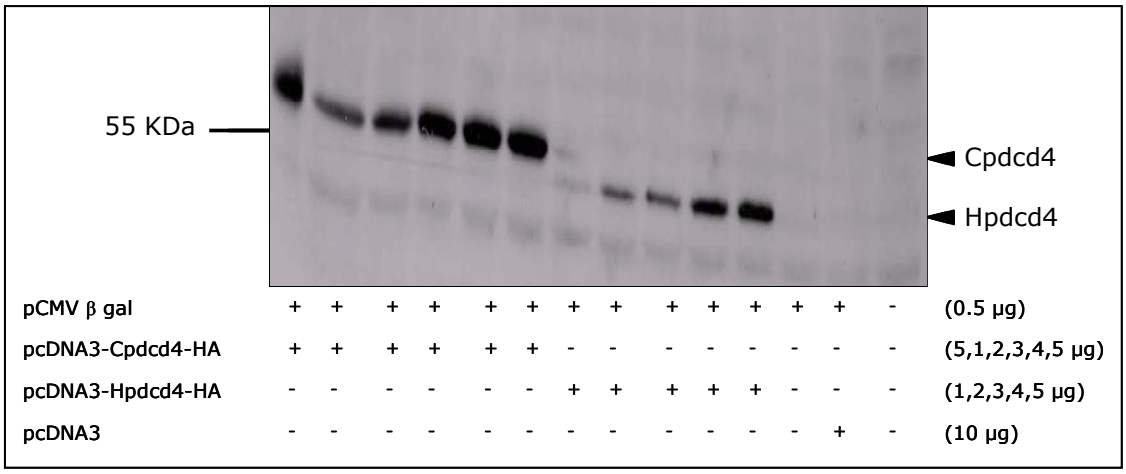

Figure 42: The overexpression of Hpdcd4 by transient transfection

Transient transfection of pcDNA3-Cpdcd4-HA (pcDNA3-i11/6HA) and pcDNA3-Hpdcd4-HA (1-5µg) was done. In addition pCMV-β gal was transfected (0. 5µg). The cells were harvested 24 hrs later and β-galactosidase assay was done to measure the transfection efficiency. The samples have loaded onto a 10% SDS-PAGE followed by western blotting. Mouse monoclonal anti HA antibody was used as a primary antibody, HRP conjugated anti-mouse antibody as secondary. The Cpdcd4 and Hpdcd4 are indicated by arrow.

Stable Transfection

Later the doxycycline inducible Cpdcd4 or Hpdcd4 construct was stably cotransfected with the tetracycline repressor plasmid into the A549 cells for inducibly overexpressing the Pdcd4 using doxycycline (Fig.43). The clones were selected by Blasticidin and Zeocin antibiotics. The stable clones were checked for inducible overexpression of the Pdcd4 protein by western blotting. Hpdcd4 overexpressing clones were not found. However, three Cpdcd4 overexpressing clones (A14, A19 and A20) were identified. These clones were constitutively overexpressing the Cpdcd4 protein, but not inducibly. Further experiments were done with these overexpression clones for the functional analysis of Pdcd4.

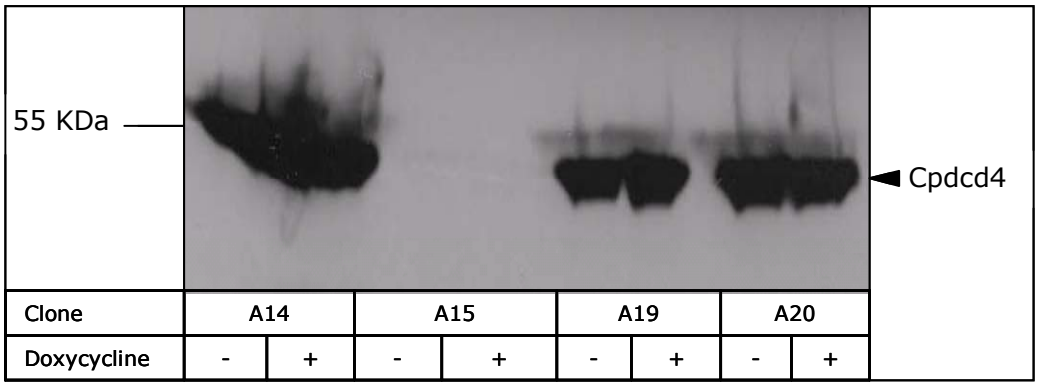

Figure 43: The overexpression of Cpdcd4 by stable transfection

Stable cotransfection of pcDNA4/TO/myc-his-i11/6HA (15 µg) with pcDNA6-TR (20 µg) was done. The clones were selected using blasticidin and zeocin, grown and analyzed. The samples were loaded onto a 10% SDS-PAGE and western blotting was performed. Mouse monoclonal anti HA antibody was used as a primary antibody and HRP conjugated anti-mouse antibody as secondary. The Cpdcd4 is indicated by an arrow at 55 KDa.

4.3.2 2D-SDS-PAGE Analysis of Cpdcd4 Overexpression Clones

2D-SDS-PAGE analysis of A549 WT and Cpdcd4 overexpressing clones (A14 and A19) was performed. Though there was some difference in the expression profile of various proteins, due to lack of reproducibility, no differentially expressed candidates was identified (Fig.44).

The A549 WT and Cpdcd4 overexpressing clones were observed under fluorescence microscopy after staining with fluorescently labeled HA antibodies. It was found that Cpdcd4 was not overexpressed in the cells. It could be that the A549 cells are continuously eliminating the overexpression of Cpdcd4, possibly one of the survival strategies of the cancer cells. In future, for studying the effect of Pdcd4 using overexpression system could be possibly done by generating inducible overexpression clones.

4.3.2 2D-SDS-PAGE Analysis of Cpdcd4 Overexpressing clones

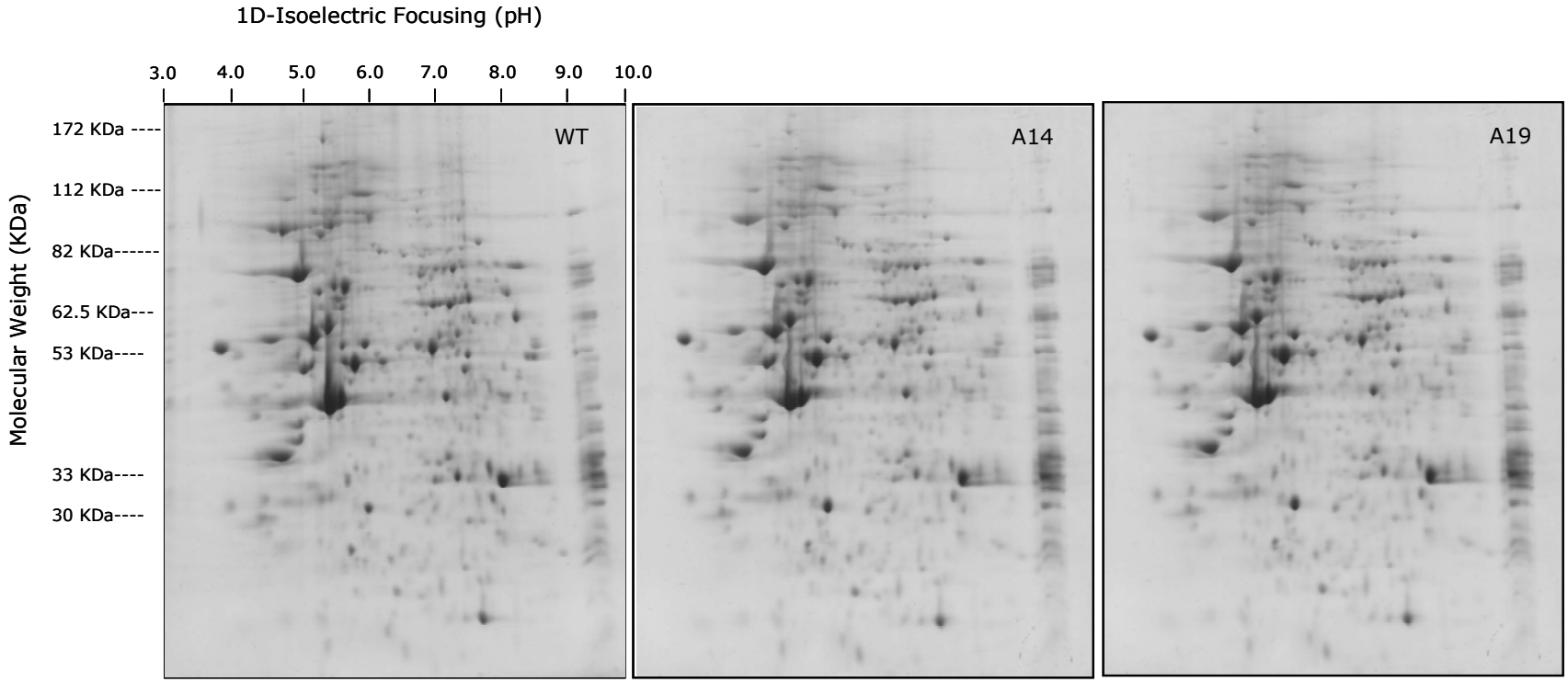

Figure 44: 2D-SDS-PAGE analysis of Cpdcd4 overexpressing clones

1-1.5 X 10^5 cells/ml each from WT, A14 and A19 were seeded and the next day harvested. The total proteome extract was prepared, proteins were isoelectrically focused in the 1D using immobiline pH gel (IPG) strip of pH (3-10) and 10% SDS-PAGE was done in the 2D. The gels were stained by CBB.

5 DISCUSSION

The research summary is shown in the figure 45 followed by a detailed discussion in the subsequent sections.

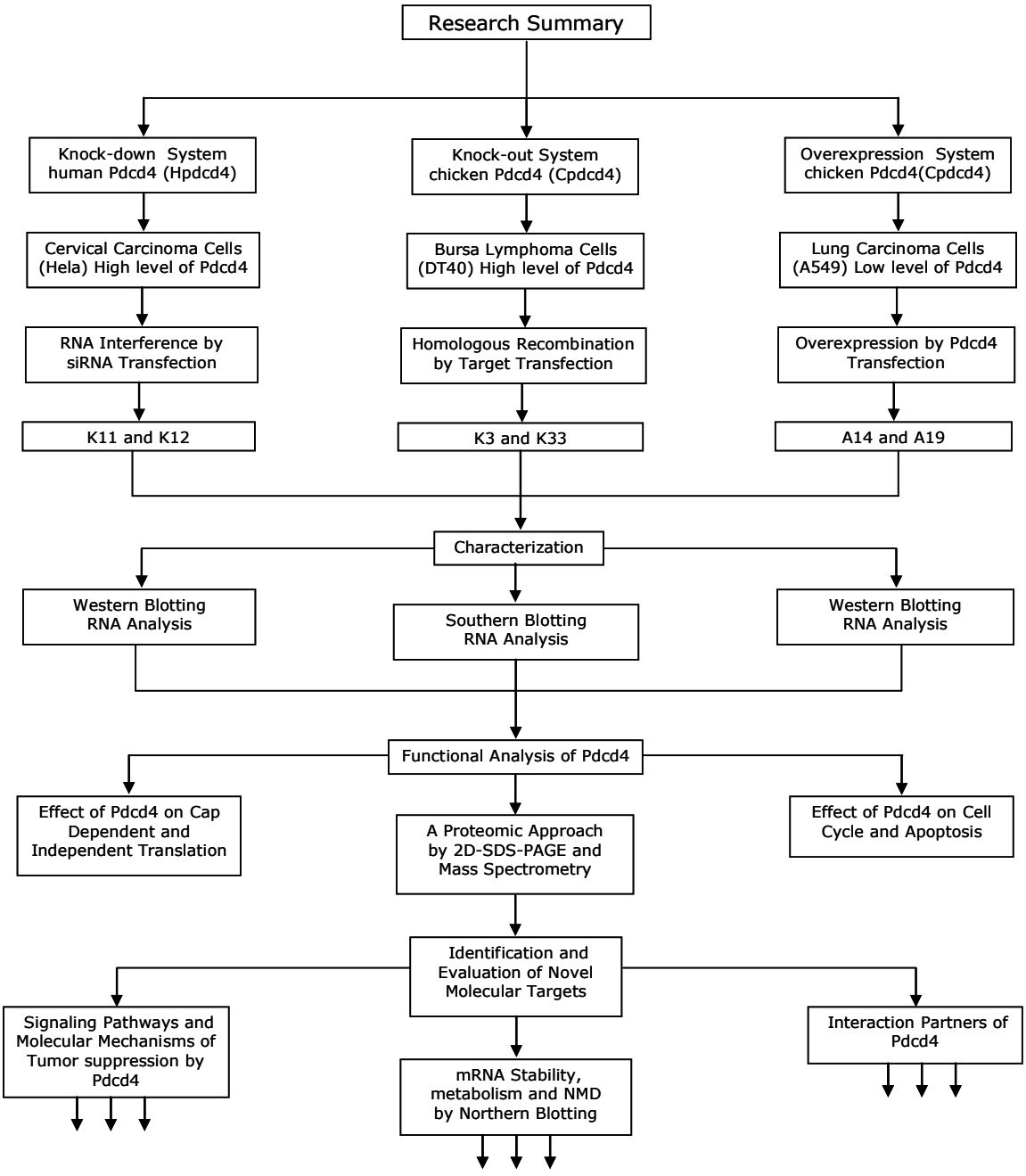

Figure 45: The schematic diagram of the research summary

The schematic diagram outlines the summary of the present work, including the development and characterization of the three Pdcd4 models and the molecular functional analysis of Pdcd4 by utilizing these systems.

5.1 Analysis of Pdcd4 in the HeLa Cells

5.1.1 Downregulation of Human Pdcd4 by siRNA Technology

The whole human genome consisting of three billion base pairs was sequenced by human genome project and it is predicted that the human genome contains about ~35,000-50,000 protein-coding genes. However, the function of approximately half of the genes is yet to be identified. Reverse genetics is the most effective way to study the function of any new gene, provided the sequence is available. Unlike the forward genetics, in this approach the gene of interest is disrupted or modified and then the phenotype is analyzed. RNA mediated interference (RNAi) has emerged as a powerful reverse genetic tool to silence gene expression in plants and in multiple organisms, including *Caenorhabditis elegans* and *Drosophila melanogaster*. RNAi is an evolutionarily conserved phenomenon and a multistep process that involves generation of active small interfering RNA (siRNA) of 21-25 nt fragments *in vivo* through the function of RNase III endonuclease and Dicer on RNA. The formed siRNA binds to several proteins to form a complex called the RNA-induced silencing complex (RISC). siRNA is unzipped by an ATP-dependent process, which activates the RISC to bind and cleave the targeted mRNA (Elbashir et al., 2001b; Bernstein et al., 2001; Ishizuka et al., 2002).

During this decade, the discovery of synthetic double-stranded, 21 nt siRNA triggering gene-specific silencing in mammalian cells has further expanded the utility of RNAi in mammalian systems (Elbazhir et al., 2001a; Caudy et al., 2002). Given the ability to knock down the homologous gene of interest, RNAi using siRNAs has generated a great deal of interest in both basic and applied biology. There is an increase in the number of genes being studied by applying siRNA technology.

Pdcd4 is a novel gene identified only in the last decade. While there is accumulating evidence that Pdcd4 is a tumor suppressor gene (Cmarik et al., 1999; Chen et al., 2003; Jansen et al., 2005; Zhang et al., 2006) its molecular function is presently not well understood. This may be due to the lack of a well-characterized cell system to study the functions of Pdcd4. In the present work, to facilitate the analysis of functions of human Pdcd4 (Hpdcd4), a Hpdcd4 knock down system was developed by employing RNAi technology. Two different siRNAs targeting Hpdcd4 mRNA at two different positions were designed which were together stably transfected into the HeLa cells. Two stable knock down clones, K11 and K12, were used for the functional analysis of Hpdcd4.

5.1.2 Hpdcd4 inhibits Translation of Secondary Structured RNAs

It has been shown that Pdcd4 inhibits translation of 5´UTR structured mRNAs approximately two fold in primary keratinocytes overexpressing Pdcd4 (Jansen et al., 2005). A reporter gene construct producing structured mRNA was transfected into the HeLa wild-type (WT) and K12 cells, the translation was almost 50% higher in the absence of Hpdcd4. This suggests that Hpdcd4 has an inhibitory control over the RNA secondary structures. This observation is consistent with the results of a Pdcd4 overexpression system by another group (Jansen et al., 2005). Moreover, the fold reduction in the translation due to the introduction of RNA secondary structure upstream of the gene was higher in the WT cells compared to the K12 cells, which again demonstrates the inhibitory effect of Hpdcd4 on mRNA secondary structures. For example, cyclin dependent kinase 4 (CDK4) and ornithinedecarboxlase (ODC) are controlled partially at the level of translation due to 5' structured UTRs (Clemens, 1999). Protein levels of CDK4 and ODC in Pdcd4 overexpressing primary keratinocytes were decreased by 40 and 46%, respectively (Jansen et al., 2005) as their mRNAs contain 5´structured UTRs.

5.1.3 Hpdcd4 inhibits IRES-Dependent Translation

In the present work, it was procured that the dual luciferase constructs containing IRES regions for four genes (*Apaf-1, c-Myc, Mnt* and *N-Myc*) which are involved in cell proliferation and programmed cell death (Coldwell et al., 2000; Stoneley et al., 1998; Stoneley et al., 2001; Jopling and Willis, 2001) were used to assess the effect of Hpdcd4 on IRES-dependent translation. The IRES dependent translation was 2.5 times higher in the K12 cells compared to the WT cells. This suggests that the Hpdcd4 has a direct or indirect negative control over these IRES elements. Comparing the RNA and protein levels of genes containing IRES elements would be the next necessary experiment to confirm the inhibitory effect of Hpdcd4 on these IRES elements.

The internal ribosome entry mechanism requires the formation of a complex RNA structural element with the recruited ribosome in the presence of IRES-trans-acting factors (ITAFs). The interactions of several ITAFs with IRESs have been investigated in detail, and several mechanisms of action have been noted, including an action as chaperones or stabilization and remodelling of the RNA structure (Spriggs et al., 2005). Structural remodelling by the polypyrimidne tract-binding protein (PTB) was studied in detail and it was shown that PTB is able to facilitate recruitment of the ribosome to several IRESs by causing previously occluded sites to become more accessible (Mitchell et al., 2001). From the present work, it is reasonable to speculate that Hpdcd4 might be acting as an inhibitor of an ITAF, possibly by hindering the binding of PTB to IRES.

The effect of Hpdcd4 on specific IRES element is discussed in detail below. Apaf-1, the apoptotic protease activating factor plays a central role in apoptosis and interaction of this protein with the procaspase-9 leads to cleavage and activation of the initiator caspase (Coldwell et al., 2000). The 578 nt long 5´ UTR contains a 233 nt long IRES and translation initiation of the mRNA is dependent on this IRES element. The Apaf-1 IRES is active in almost all human cell types tested, including HeLa cells (Coldwell et al., 2000). Because of Hpdcd4 showed inhibitory control over this proapoptotic element, it is reasonable to speculate that Hpdcd4 may act as an anti-apoptotic element.

The Apaf-1 IRES requires two *trans*-acting factors for its function. In addition to PTB, it also requires upstream of N-ras (unr), to attain the correct structural conformation of the IRES (Mitchell et al., 2001). Based on these evidence, there are many possible mechanisms can be proposed to explain by which Hpdcd4 might inhibit the IRES-dependent translation (e.g.) Hpdcd4 might directly bind to the mRNA secondary structure and thus inhibiting the binding of ITAFs to the mRNA, or interfere with the interaction between ITAFs in enhancing the IRES-dependent translation. In the future, investigation of Hpdcd4 binding to the apoptosis related mRNAs (Apaf-1, Bcl-2, Bag-1 and DAP5) and binding partners of Hpdcd4 in regulating the IRES dependent translation of these genes might unravel the role of Hpdcd4 in apoptosis.

The second IRES element found to be inhibited by Hpdcd4 was the c-Myc IRES. The *myc* gene family comprises of c-, N- and L-*myc,* and gives rise to nuclear phosphoproteins which function as transcription factors. In accordance with the stimulatory effect of the Myc proteins on cell growth, their overexpression is associated with a number of different cancers (Jopling and Willis, 2001). In the present work, it was shown that Hpdcd4 has a negative control over the IRES-element of c-*myc* and N-*myc* oncogenes thereby uncovering a possible mode of action of its tumor suppressor activity. Checking specifically on c-Myc protein level made only by the IRES-dependent translation is mandatory to confirm the effect of Hpdcd4 on IRES-dependent translation of c-Myc. Further, coimmunoprecipitation experiments could help to map the Hpdcd4 binding region in the c-Myc and N-Myc IRES and to identify interaction partners for Hpdcd4 in regulating the IRES dependent translation of c-Myc proteins.

Furthermore, Hpdcd4 also inhibits Mnt IRES element. Mnt is a transcriptional repressor related to the Myc/Mad family of transcription factors, expressed in proliferating, resting as well as differentiating cells and believed to antagonize the function of Myc (Stoneley et al., 2001). Mnt is involved in the control of cell proliferation, differentiation, apoptosis and tumor progression. In the present experiments, it was

shown that Hpdcd4 inhibited the Mnt IRES suggesting that Mnt is one of the target of Hpdcd4. Hpdcd4 may inhibit the IRES-dependent translation of both Myc and the Myc repressor Mnt. At first sight, it may be contradictory to explain the tumor suppressor behavior of Hpdcd4. However, a hypothesis could be postulated to explain these observations. Hpdcd4 is a primary threshold point which most cancer-prone cells have to disrupt to enter or progress to the cancerous state. Thereby activating the subsequent cancerous genes, this stimulates the aberrant cell growth and thus increases cell survival in their microenvironment. For the above reason, cells also have many second level defenses or failsafe mechanisms activated beyond Hpdcd4. A schematic diagram shows the activation of failsafe mechanisms by Hpdcd4 (Fig.46).

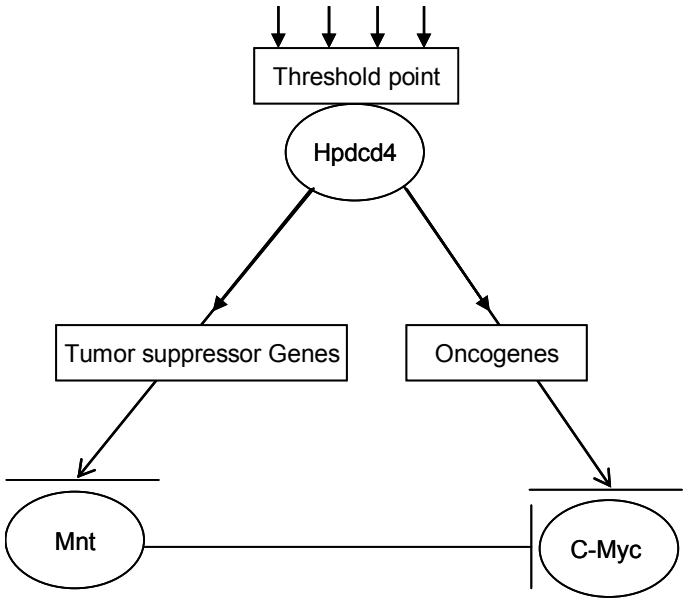

Figure 46: Hpdcd4 – A primary threshold point in tumorigenesis

As a consequence of disruption of critical check points like Hpdcd4, secondary level failsafe mechanisms could be triggered through various tumor suppressor genes like Mnt, to balance or nullify the effect of activated oncogenes like c-Myc.

It has been shown that IRESs are important to maintain protein expression under conditions when cap-dependent translation initiation is compromised; for example, during mitosis, apoptosis and under conditions of cell stress (Spriggs et al., 2005). Induction of stress also results in a large reduction in global protein synthesis rates. It was therefore also investigated whether the c-Myc IRES was active following DNA damage (Subkhankulova et al., 2001). After UV-irradiation, the HeLa WT cells showed increased c-Myc IRES-dependent translation. In contrast, there was no increase in the c-Myc IRES-dependent translation of the K12 cells. Moreover, there was no difference in the c-Myc IRES-dependent translation of the WT and K12 cells. It suggests that in

the absence of Hpdcd4, the cells might not be able to react to the UV-irradiation. This could imply that Hpdcd4 is a significant component of DNA-damage response.

5.1.4 Novel Molecular Targets of Hpdcd4

By 1D-SDS-PAGE several transcription factors were examined as potential targets for Hpdcd4. While c-Myc was downregulated, c-Jun was significantly overexpressed and phosphorylation of ATF-2 and c-Jun was less efficient in the K12 cells compared to the WT cells. In addition to such a reductionist approach, a holistic approach was applied to identify additional molecular targets of Hpdcd4.

Proteomics is a high throughput and holistic approach to screen all the proteins of a cell or organism expressed at a particular time. It requires stringently controlled 2D-SDS-PAGE, image detection and analysis and spot identification through mass spectrometry (MS) followed by database searches. 2D-SDS-PAGE is a technique (O'Farrell 1975), in which proteins are separated according to their charge by isoelectric focusing (IEF) in the first dimension and molecular weight by SDS-PAGE in the second dimension. It provides a two dimensional array, in which each spot corresponds to a single protein species in the sample. The highly purified single protein spots are analyzed by MS and identified by database search.

Functional proteomics aims at the characterization of multiprotein complexes and signaling pathways. For example, a study was carried out previously to identify cellular targets regulated by the MKK/ERK cascade and 25 targets of this signaling pathway were identified (Lewis et al., 2000). Alternatively, expression proteomics aims to measure up- and downregulation of proteins (Mann et al., 2001). Such strategy has been employed in several studies (Wasinger et al., 1995; Dencher et al., 2006; Welham et al., 2006). In the present study, a comparable strategy was applied to identify several novel molecular targets of Hpdcd4 using the 2D-SDS-PAGE followed by MS. The molecular targets are: Cytokeratin-17 (CK-17), aldo keto reductase1 (AKR1) family members C2 and C3, Cytokeratin-8 (CK-8) and Glutamyl Prolyl tRNA synthetase (GluProRS). CK-17 and AKR1C2 and C3 were overexpressed in the K12 cells compared to the WT cells. Furthermore, biochemically modified CK-8 and GluProRS related similar molecular weight spots appeared on the lower pH side of the respective mother spot, only in the absence of Hpdcd4.

5.1.5 Expression of c-Myc is lower in the Absence of Hpdcd4

The transcription factor c-Myc is one of the targets for Hpdcd4, shown to be downregulated in the absence of Hpdcd4. Myc genes comprise a small, multi-gene

family and are implicated in the development of different human tumors (Adhikary et al., 2005). To some degree most of the major processes such as proliferation, growth, differentiation, apoptosis and metabolism are regulated by c-Myc (Liu et al., 2006). The deregulation of these processes, in turn, influences the level of c-Myc expression as well as diverse pathophysiological signals which are directed to act on the c-Myc level by activating various proteins. Enhanced expression of Myc genes promotes and contributes to many aspects of the tumor cell phenotype. The present work has shown that in the absence of the tumor suppressor gene Hpdcd4, c-Myc expression is decreased. It is rational to assume that Hpdcd4 maintains c-Myc oncoprotein level in normal conditions. But, when Hpdcd4 is inactivated during many cancers, inhibition of c-Myc might occur due to the activation of failsafe mechanisms. The c-Myc RNA level was lower in the absence of Pdcd4 as well as the turn-over rate. This suggests that the reduced amount of c-Myc mRNA might not be due to the effect of Pdcd4 on the turn-over of mRNA but could be the other mechanisms operating at different level.

5.1.6 Phosphorylation of ATF-2 is decreased in the Absence of Hpdcd4

Another transcription factor affected by Hpdcd4 is ATF-2. ATF-2 is a bZip transcription factor which has been implicated in the regulation of a wide set of cAMP-response element (CRE)-dependent target genes. The transcriptional activity of ATF-2 requires homo or heterodimerization with other members of the bZip family, such as c-Jun. Moreover, it is stimulated by phosphorylation of threonine residues (T69 and T71) which is mediated by the JNK and p38 protein kinases (Livngstone et al., 1995). Furthermore, it has been shown that ATF-2 has an intrinsic histone acetyltransferase (HAT) activity that is controlled by phosphorylation. Phosphorylation of ATF-2 enhances its HAT activity, subsequently specific acetylation of H2B and H4 followed by CRE-dependent transcription (Kawasaki et al., 2000).

In the present experiments it was observed that after UV exposure, ATF-2 expression and the extent of ATF-2 phosphorylation was lower in the absence of Hpdcd4 than in its presence. Several studies have implicated the phosphorylation of ATF-2 in regulating repair of DNA-damage caused by different agents, such as ionizing or UV radiation or cisplatin (Potapova et al., 1997; Potapova et al., 2001; Kabuyama et al., 2002; Hayakawa et al., 2003; Bhoumik et al., 2005). Hayakawa et al. (2004) have identified a set of genes whose expression is coordinately induced by activated ATF-2 following genotoxic stress. Many of these genes are involved in DNA-damage-repair, suggesting that the genotoxic stress response occurs at least partially via activation of ATF-2, leading to increased expression of DNA-damage repair genes. Therefore, it is logical to assume that in the absence of Hpdcd4, the ATF-2 phosphorylation is less efficient and

thus the response to DNA-damage. C-Myc induces the phosphorylation of ATF-2 at Thr-69 and Thr-71 to prolong the half-life of ATF-2 (Miethe et al., 2001). This raises the possibility that in the absence of Hpdcd4 the c-Myc protein is less abundant and as a consequence the phosphorylation of ATF-2 is also decreased.

A study correlated the phosphorylation of ATF-2 by p38 and the cyclin D1 transcription in MCF-7 breast cancer cells (Lewis et al., 2005). D type cyclins are major downstream targets of extracellular signaling pathways which act to integrate mitogenic signals to the cell cycle machinery (Sherr, 1995). Future investigation of the effect of Hpdcd4 on the level of cyclin D1 may reveal the possible role of Hpdcd4 in tumor cell cycle progression.

5.1.7 Expression of C/EBPβ is increased in the absence of Hpdcd4

The ability of C/EBPβ to bind specific DNA sequences and to mediate protein-protein interactions makes it a bona fide transcription factor. C/EBPβ plays a pivotal role in numerous cellular responses, including proliferation, differentiation, inflammatory response, apoptosis, and control of metabolism. Several C/EBPβ isoforms corresponding to full length and amino-terminally truncated proteins were observed (Calkoven et al., 2000). These isoforms display contrasting functions in gene activation and cell proliferation (Descombes and Schibler, 1991). Moreover, various experiments have shown that the ratio of different isoforms influences various cellular processes including tumorigenic conversion (Raught et al., 1996).

The present work showed that C/EBPβ was expressed stronger in the absence of Hpdcd4, when an expression vector for full length C/EBPβ was transfected. This raised the possibility that Hpdcd4 inhibits the expression of C/EBPβ by binding to its upstream region. However, higher expression level of full length C/EBPβ isoform in the absence of Hpdcd4 was also observed, when expression vectors for C/EBPβ without upstream region were transfected. This shows that Hpdcd4 does not act on the upstream region but that the inhibitory effect is operating at a different level.

5.1.8 Biochemical Modification of Cytokeratin-8 in the absence of Hpdcd4

The Cytokeratin Family

Although in various literatures the intermediate filaments are represented by different conventions (Keratin-8, cytokeratin-8, k8, k-8, ck8 and ck-8 etc.,), in the present work, cytokeratins are mentioned e.g. as CK-8 to enable a clear distinction between the conventions used to represent cytokeratins and the generated Pdcd4 clones.

Eucaryotic cells contain up to three families of cytoskeletal proteins that are responsible for the spatial organization of the cell. The three types are differentiated by the diameter of the filament and include thick microtubules (25 nm), thin actin filaments (7 nm), and intermediate filaments (IF, 10-12 nm). More than twenty cytokeratin intermediate filament proteins are expressed in a cell type preferential manner (Knap and Franke, 1989).

The large cytokeratin multigene family can produce more than 20 unique keratin gene products (CK1-CK20) which are characterized and classified into type I-Acidic (CK9-CK20) and type II-Basic (CK1-CK8) intermediate filaments (Coulombe et al., 2002). An equimolar ratio (1:1) of each Type I and Type II keratin forms a noncovalent obligate heteropolymers either in a soluble tetrameric form or in a core complex filamentous cytoskeletal form. Since the cooperation of one member of each family is necessary for mutual costabilization and cytoskeletal assembly, defined pairs of keratin proteins are coexpressed. For example, it was coexpressed that the CK-8 and CK-18 in simple epithelia, CK-5 and CK-14 in basal layers of multilayered epithelia, and CK-1 and CK-10 in differentiated layers of the epidermis (Steinert, 1988).

Cytokeratin expression is a persistent phenotype which is used in diagnosing cancers, enabling identification of tumor type, metastatic tumor origin, and stage of disease (Nagle et al., 1993; Moll et al., 1982a). Tumors may either begin to express a novel cytokeratin or, alternatively, may reduce/cease the expression of cytokeratins which are normally present in this tissue. Furthermore, changes in the pattern of expression of cytokeratins during tumor progression can also involve a reversion to the simple epithelial from the CK-8/18 dimer (Moll, 1982b). These particular cytokeratins are also preferentially expressed in many carcinoma cell lines (Chan et al., 1986).

Posttranslational Modification of CK-8

Keratin posttranslational modifications like glycosylation, phosphorylation and transglutamination, are thought to modulate K8/K18 functions. Glycosylation via O-GlcNAc, is a dynamic modification conclusively identified in three keratins including CK-8 (Omary et al., 1998). Phosphorylation is an important regulatory modification of keratins and in this regard many keratin family members were studied in detail. CK-8/18 phosphorylation also affects their functional assembly state and has been suggested to play a role in cell signaling (Ku et al., 1996a). Serine is the major physiological phosphorylated keratin residue (Oshima, 1982). In the case of CK-8/18, phosphorylation regulates filament reorganization *in vivo*, enhances keratin solubility, plays a role in dictating the localization in specific cellular compartments, regulates the

association with the 14-3-3 protein family and is associated with a variety of physiological stresses (Ku et al., 1996a).

Phosphorylation of K8 was studied upon activation of the epidermal growth factor receptor (Baribault et al., 1989) and pro-urokinase stimulation (Busso et al., 1994). Drug-induced hepatotoxic stress, induced by feeding mice with a griseofulvin-supplemented diet resulted in a dramatic CK-8/18 hyperphosphorylation (Ku et al., 1996b). Pervanadate-mediated tyrosine phosphorylation of CK-8 and CK-19 in a p38 kinase-dependent pathway was reported (Feng et al., 1999). Furthermore, it has been shown that cultured HT-29 cells were induced by anisomycin or etoposide and it was shown that hyperphosphorylation of CK-8 at Ser-73 was linked to apoptosis.

So far, three *in vivo* CK-8 phosphorylation sites have been described. The first site, Ser-23 is located in the head domain of CK-8. This site is conserved in all type II keratins and phosphorylated by purified cAMP-dependent protein kinase (Ando et al., 1996). The second site, Ser-431 is located in the tail domain of CK-8 and is phosphorylated after stimulation of cells by epidermal growth factor and is presumably a member of the mitogen-activated protein kinase family (MAPK) (Ku and Omary, 1997). The third site, Ser-73 is phosphorylated either by p38 stress-activated protein kinase or by c-Jun N-terminal kinase (JNK) in a context-dependent manner (He et al., 2002; Ku et al., 2002).

It has been shown that in shear-stressed alveolar epithelial cells CK-8 S73 phosphorylation occurs in a time-dependent manner by protein kinase Cδ (PKCδ) (Ridge et al., 2005). Protein kinase C is a family of well studied serine-threonine protein kinases, which is involved in many cellular functions, including proliferation, differentiation, apoptosis, and gene expression. Receptor-mediated activation of phospholipase C induces the generation of the second messengers calcium and diacyglycerol which contribute to the activation of PKC (Li et al., 2005). As a cellular target for the tumor-promoting phorbol esters, PKC has been implicated in tumor development for decades. Among the 12 members of PKC isozymes, PKCα and PKCε have been implicated in cell proliferation, whereas PKCδ and PKCη have been associated with apoptosis and terminal differentiation (Li et al., 2005).

In a recent study CK-8 was identified as a cytoplasmic target for JNK during Fas receptor-mediated signaling (He et al., 2002). The MAPK family which is composed of the mitogen-activated (MAPK/ERK) and the stress-activated protein kinases (SAPK). They both are involved in cellular responses to physical stresses, inflammatory cytokines and apoptosis. The JNK belongs to the subgroup of SAPK family.

In the present experiments, in the 2D-SDS-PAGE analysis there appeared two similar molecular weight spots on the acidic side of the CK-8 spot. These unidentified spots were visible only in the K12 cells but not in the WT cells. Therefore, it was interesting to study the relationship between Hpdcd4 and the appearance of the CK-8 related spots. When 2D-immunoblotting was performed using CK-8 specific antibodies only one CK-8 related spot was observed. The second CK-8 related spot might be an unrelated protein. Another Hpdcd4 knock down clone, K11, also showed the additional CK-8 related spot which was similar to the one observed in the K12 cells. The appearance of a CK-8 related spot was also confirmed by a different pH range (4-7) in the 2D-SDS-PAGE.

To elucidate the identity of the CK-8 related spot, the WT and K12 cells were treated with UV. When stress is induced by UV treatment, the cells are provided with activated protein kinases. The CK-8 related spots also appeared in the WT cells after UV-induction which confirmed that this spot could be due to the phosphorylation of CK-8. When K12 cells were induced with tumor promoter TPA, the CK-8 related spot became more prominent. These two experiments suggest that the spot might be due to phosphorylation of CK-8.

Modulation of keratin phosphorylation occurs during multiple stimuli, including stress, apoptosis and mitosis with resultant regulation of keratin filament organization and keratin interaction with its binding partners (Ku et al., 1999). Furthermore, it has been shown that phosphorylation of CK-8 induces depolymerization of CK-8/18 pairs which enabled tumor progression (Ku et al., 1996). From the present experiments and other evidences it is reasonable to speculate that in the absence of tumor suppressor protein Hpdcd4, the phosphorylation of CK-8 and subsequently the disentanglement of CK-8 from its bound partner may confer to the tumor cells an evolutionary advantage for tumor progression (Fig.47). Thence, it is essential to check whether Hpdcd4 inhibits phosphorylation of CK-8 by PKC or JNK as previous studies have shown that CK-8 is phosphorylated by PKC (Cadrin et al., 1992) and by JNK (He et al., 2002). This future experiment might provide interesting insight into the molecular mechanism of tumor suppression by Hpdcd4.

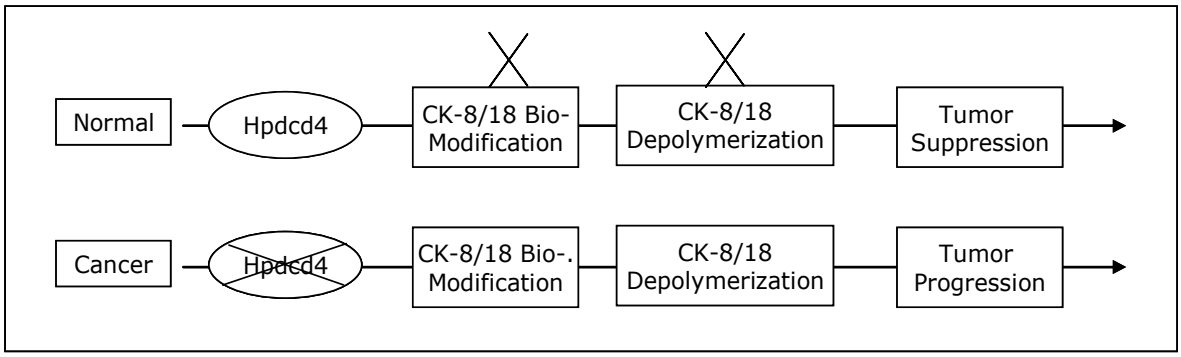

Figure 47: An extremely simplified schematic diagram outlines the possible molecular mechanism behind the tumor suppressor function of Hpdcd4 through CK-8.

5.1.9 Expression of Cytokeratin-17 is higher in the absence of Hpdcd4

Most of the earlier functional studies about keratins revealed that their major role is to protect the cell by providing cytological support. Later it has been shown that they are also suitable as tumor markers. But recent studies shed light on how this structural support is modulated to meet the changing needs of cells, and reveal a novel role whereby intermediate filaments influence the cell growth and death through dynamic interactions with non-structural proteins (Coulombe et al., 2004). Other emerging functions of cytokeratins, in particular of CK-17 includes roles in cell signaling, the stress response and apoptosis (Coulombe and Omary, 2002).

In the present work, it was shown that the CK-17 RNA and protein level is increased in the Hela K12 cells compared to the WT cells, suggesting that Hpdcd4 inhibits the CK-17 expression. A previous study has revealed that the CK-17 is a target of interferon signaling. Interferons influence the gene expression by activating transcription factors, which in turn bind to specific DNA sequences known as interferon-stimulated response elements thereby activating transcription of nearby genes. It was found that interferon-γ (IFN-γ) strongly and specifically induced the promoter of the CK-17 gene (Jiang et al., 1994). The IFN-γ-activated sequence (GAS) was characterized in the CK-17 promoter. IFN-γ activates another protein, STAT-91 (signal-transducing activator of transcription), one of the four components of ISGF3 (the primary IFN-α responsive transcription factor). The activated STAT-91 binds to the CK-17 GAS and in turn, activates the transcription of CK-17.

A recent study has shown that CK-17 has a role in cell growth. Cell growth is a highly regulated cellular event, by which the cells gain mass and size. The Akt/mTOR signaling pathway has a central role in the control of protein synthesis and thus the growth of cells, tissues and organisms (Kozma and Thomas, 2002). Three keratins (CK-6, CK-16

and CK-17) were rapidly upregulated in wound-activated skin epithelial cells, and the signaling pathway following CK-17 induction was studied in detail (Coulombe et al., 2006). Moreover, the Akt (protein kinase B) serine/threonine kinase is a key mediator of phosphoinositide-2-kinase pathway involved in the regulation of cell proliferation, survival, and growth. It has been shown that Pdcd4 is phosphorylated by Akt kinase in two sites, at Ser-67 and Ser-457, both *in vitro* and *in vivo* (Palamarchuk et al., 2005).

From these evidences it is logical to speculate that the role of Hpdcd4 in inhibiting CK-17 expression could possibly be extended to the cell growth through the mTOR signaling pathway (Fig.48). The phosphorylation of Hpdcd4 by Akt kinase might be one step among the multistep pathway. Furthermore, phosphorylation of Hpdcd4 might activate/inhibit its effect on CK-17. Further elucidating the role of Hpdcd4 on mTOR pathway will reveal the molecular mechanisms of Hpdcd4 in cell growth and thereby tumor suppression.

From the current study, the finding of inhibition of CK-17 expression by Hpdcd4 raises many possibilities for the mechanism of action of Hpdcd4. Hpdcd4 could directly bind to the CK-17 promoter, thereby inhibiting the CK-17 expression. It would be interesting to generate a CK-17 promoter-reporter gene construct and check its activity in the Hela WT and K12 cells. Alternative to the direct binding to the CK-17 promoter, Hpdcd4 could interfere with CK-17 activator proteins. Based on the above mentioned study (Jiang et al., 1994) Hpdcd4 could possibly hinder either the activation of STAT-91 or the binding of STAT-91 on the GAS of the CK-17 promoter. These future experiments may confirm the significance of the effect of Hpdcd4 on the structural element CK-17 in mTOR or IFN signaling and thereby the molecular mechanisms of tumor suppressor function of Hpdcd4.

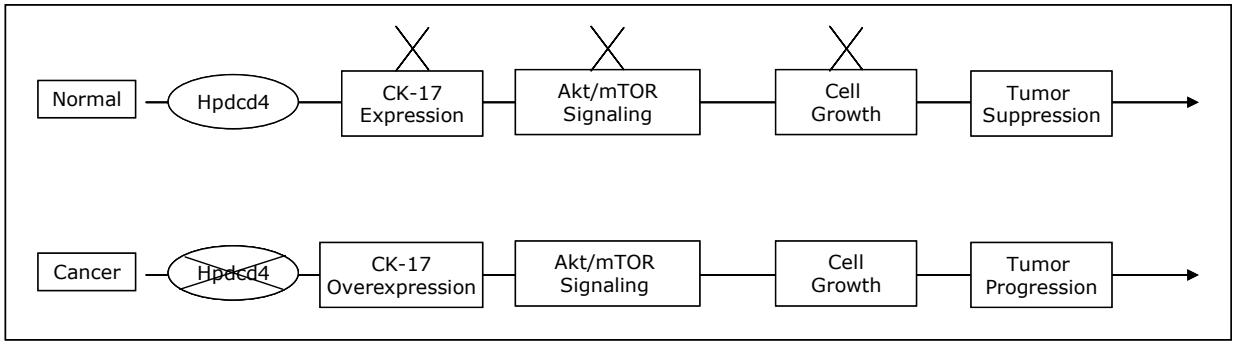

Figure 48: An extremely simplified schematic diagram outlines the possible molecular mechanism behind the tumor suppressor function of Hpdcd4 through CK-17.

5.1.10 Expression of AKR1C2 and C3 are higher in the absence of Hpdcd4

In the present study, when Hpdcd4 is silenced, AKR1C2 and C3 were found to be upregulated. The human aldo keto reductases (AKR) superfamily contains four isoforms of 3α_hydroxysteroid dehydrogenase (3 α-HSD). The enzymes correspond to type 1-type 4 share at least 84% amino acid sequence identity. All enzymes act as NADPH-dependent 3-, 17- and 20-ketosteroid reductases and as 3α-, 17β- and 20α-hydroxysteroid oxidases. The functional plasticity of these isoforms highlights their ability to modulate the levels of active androgens, oestrogens and progestins (Penning, 2000).

AKR1 family members have been the basis for tumor classification since few decades. Reduced levels of AKR1C2 and AKR1C3 were observed in breast carcinoma cells (Lewis et al., 2004). Moreover, it was also reported that the overexpression of AKR1C3 in myeloid leukemia cell lines prevents the cells from undergoing differentiation. Although they are well-characterized tumor markers, the molecular mechanism by which their altered expression is manifested in cancer is not yet clarified. However, a recent study on parathyroid hormone-related protein (PTHrP) revealed a molecular mechanism of the linkage of AKR1C2 and C3 to cancer (Tsigelney et al., 2005). PTHrP is known as the factor responsible for humoral hypercalcemia of malignancy. It regulates cell growth, apoptosis, cytokine production and angiogenesis in cancer cells and contributes to cancer progression and metastasis. In the present study, it was interesting, as AKR1C2 and C3 were found to be upregulated in the absence of Hpdcd4. It partially reveals a mutual molecular mechanism by which AKR1 family members or Hpdcd4 might be involved in tumorigenesis. However, AKR1C2 and C3 were expressed differently in both the Hpdcd4 knock down clones, an observation which questions the identity of these genes as true Hpdcd4 targets.

Similarly, although, both knock-down clones (K11 and K12) overexpress CK-17 compared to the WT, the degree of overexpression varied between these clones. It is possible that these clones are either genetically different or that they vary in the extent of silencing of Hpdcd4. In the future, it will be important to confirm the effect of Hpdcd4 on AKR1C2 and C3. Conceivably, the identity of the AKR1C2 and C3 as targets of Hpdcd4 could be confirmed by reexpression of Hpdcd4 in the knock-down clones and assessing the expression of them.

5.1.11 Biochemical Modification of GluProRS in the absence of Hpdcd4

Glutamyl Prolyl Bifunctional tRNA Synthetase (GluProRS) appeared as 5-6 spots on a string in the absence of Hpdcd4, but as a single spot in the presence of Hpdcd4. GluProRS catalyzes the ligation of amino acids to the tRNAs during translation. It has divergent functions in protein synthesis. In the multisynthetase complex, its aminoacylation activity supports global translation, but phosphorylation and thus translocation of GluProRS to an inflammation responsive mRNAP causes gene-specific translational silencing (Sampath et al., 2004). The appearance of GluProRS as 5-6 spots as pearls on a string at the molecular weight of 163 KDa in the absence of Hpdcd4 suggests a possibility that the GluProRS is biochemically modified in the absence of Hpdcd4. However, further, 2D-SDS-PAGE imunoblotting using a 3-10 pI range is necessary to confirm the identity of GluProRS related spots in the absence of Hpdcd4.

5.1.12 Potential Role of Hpdcd4 in mRNA Stability

The function of Hpdcd4 at the protein level was traced back to the RNA level of the identified targets. Furthermore, in the present work, it was also found that Hpdcd4 may play a role in posttranscriptional level control of gene expression. Every eucaryotic cell contains the same 35,000-50,000 genes. The remarkable diversity in cell specialization is achieved through the tightly controlled expression and regulation of a precise subset of these genes in each cell lineage. The regulation of mRNA turn-over plays a major role in the posttranscriptional level control of gene expression (Saini et al., 1990) as there is a vast difference in the mammalian mRNA half-lives from 15-30 min to more than 24 hr (Sylke, 2004). The half-life of an mRNA represents a balance between the transcriptional activity and intracellular degradative processes. Half-life can be modulated by the presence of specific *cis*- and *trans*-acting elements in the mRNA (Ross, 1995).

A mRNA can be stabilized or destabilized as a result of the combined actions of different *trans*-acting regulatory factors. There are some RNA-binding proteins which protect mRNA from degradation whereas, some mRNA-binding proteins tag mRNA for degradation (Ross, 1995). For example, PolyA-binding protein, proteins that bind to AU-rich elements (ARE), iron regulatory protein, ribonucleotide reductase mRNA-binding proteins and c-Myc coding region determinant-binding protein stabilize the mRNAs.

The present northern blotting experiments confirmed the effect of Hpdcd4 on CK-17 and c-Myc mRNA. In the absence of Hpdcd4, the CK-17 and c-Myc mRNA transcript levels increase. This could be a consequence of an increase in the transcription or the stability of these mRNAs. The mRNA stability studies revealed that in the absence of Hpdcd4 the mRNA degradation was slightly less efficient for CK-17 and c-Myc mRNA than in the presence of Hpdcd4. This suggests that Hpdcd4 decreases the stability of the CK-17 and the c-Myc mRNA transcripts. However, this effect might be either general, affecting all mRNAs, or specific for Hpdcd4-functionally relevant mRNAs. Apparently, the S17 mRNA was unaffected by Hpdcd4, further confirming the specificity of the effect of Hpdcd4. The observations suggest a possible role of Hpdcd4 in the stability of mRNAs.

It has been shown that Pdcd4 has an N-terminal RNA binding domain (Boehm et al., 2003). Furthermore, it has been shown that the mRNA binding proteins that bind to AREs of mRNA are predominantly nuclear but shuttle between the nucleus and the cytoplasm (Katz et al., 1994; Shim et al., 2002). Hpdcd4 has been also shown to be predominantly a nuclear protein and to shuttle between the nucleus and cytoplasm during serum withdrawal (Boehm et al., 2003). These observations support the assumption that Hpdcd4 might be binding RNAs and possibly plays a role in mRNA stability.

It was somewhat contradictory that c-Myc mRNA is degraded faster but the c-Myc protein expression was higher in the presence of Hpdcd4. A possible explanation might be that in normal conditions, Hpdcd4 enables degradation of c-Myc mRNA but in most of the cancers when Hpdcd4 is downregulated, possibly some other not yet identified failsafe mechanisms acting to still lower the level of c-Myc oncoprotein.

From the previous experiments, the effect of Hpdcd4 on IRES-dependent translation shows that Hpdcd4 negatively regulated the translation of specific mRNAs having secondary structures in the 5’ UTR. It is possible that Hpdcd4 also affect the secondary structured elements present in the 3’ UTR of mRNAs. The mode by which Hpdcd4 facilitates the mRNA degradation, the significance and the interaction partners of Hpdcd4 that are involved in RNA metabolism are yet to be elucidated.

5.1.13 Potential role of Hpdcd4 in Nonsense-Mediated mRNA Decay

From the present study, the role of Hpdcd4 on mRNA stability was further extended to the metabolism of mRNAs having nonsense-mutations. When β-Globin mRNA with a nonsense mutation was expressed in the HeLa WT and knock-down cells, NMD

operated slightly lower in the absence of Hpdcd4. This suggests a possible role of Hpdcd4 in NMD. A correlation of sequence and structural motifs with several other proteins involved in RNA metabolism was made. Pdcd4 contains two conserved MA-3 domains in the region of amino acids 164-275 and 329-440, respectively (Fig.2). Surprisingly, the MA-3 domain present in Pdcd4 is highly homologous to the domains present in proteins of several other eucaryotic proteins involved in translation and mRNA processing (Ponting, 1992). However, further experiments are necessary to confirm the role of Hpdcd4 in NMD. Moreover, among the two MA-3 domains of Hpdcd4 which is interacting or how both are coordinately interacting with the known members of the mRNA processing machinery like NMD pathway could be studied by generating deletion mutants of Hpdcd4 gene.

5.2. Analysis of Pdcd4 in the DT40 Cells

5.2.1 Downregulation of Chicken Pdcd4 by Homologous Recombination

The chicken pre-B cell line DT40 has exceptionally high rate of homologous recombination and because of that it is an extremely useful model system to study the role of genes that perform general cellular functions or that play specific roles in B-lymphoid cells. In chickens, Pdcd4 (Cpdcd4) is expressed in many tissues with particularly high levels found in hematopoietic tissues, such as the bursa and the thymus (Schlichter et al., 2001a). Therefore, DT40 cell line was chosen to explore the role of the tumor suppressor, Cpdcd4 gene (*Cpdcd4)* by knocking out both the copies of Cpdcd4. Among the generated and characterized 5 *Cpdcd4(-/-)* clones, two clones (K3 and K33) were further characterized and used for the functional analysis of Cpdcd4.

5.2.2 Growth Characteristics are unaffected by Cpdcd4

The analysis of the growth properties of the Cpdcd4 knock-out cells showed that the disruption of *Cpdcd4* does not cause a detectable distortion of the cell cycle or a change in the proliferation rate of these cells. Thus it appears that Cpdcd4 does not play an essential role during cell proliferation, at least under normal growth conditions.

These findings are at variance with the recent reports that have used overexpression of Pdcd4 to address its role in cell proliferation. It was observed that overexpression of Pdcd4 causes growth inhibition in the human carcinoid cell line Bon-1 (Lankat-Buttgereit et al., 2004). Goke et al. (2002) reported that overexpression of Pdcd4 in HEK-293 cells causes resistance to apoptosis while Afonja et al. (2004) showed that Pdcd4 induces apoptosis in certain breast cancer cells. Pdcd4 overexpression reveals no effect on proliferation or apoptosis in HEK-293 cells (Bitomsky et al., 2004). One potential explanation for these divergent observations could be that the actual outcome of Pdcd4 overexpression might be highly dependent on the cell type used for the experiments. Since each cell line may have their own basal level of Pdcd4 expression which could influence apoptosis to various extents. In addition to that fact, the degree of overexpression of Pdcd4 might vary between different systems which could affect the response of the cells.

5.2.3 Cpdcd4 has no Effect on Total Protein Synthesis

Previous work has implicated Pdcd4 in the control of translation initiation. The majority of eucaryotic translation is cap-dependent and involves the association of the cap-binding complex (consisting of eIF4G, eIF4A and eIF4E) with the 5'-m7G cap structure of mRNAs (Gingras et al., 1999; Gebauer and Hentze, 2004). It has been suggested that Pdcd4 interferes with the function of eIF4A and eIF4G by binding itself to these proteins and by inhibiting the helicase activity of eIF4A (Yang et al., 2003b).

The present experimental results showed that the disruption of the *Cpdcd4* has no significant effect on total protein synthesis. Therefore, Cpdcd4 does not appear to exert a general inhibitory effect on cap-dependent translation. It is possible, however, that the inhibition of cap-dependent translation by Cpdcd4 is restricted to specific mRNAs, which cannot be detected by a global labeling approach. Further analysis of the role of Cpdcd4 in cap-dependent translation might be progressed through assessing the mRNA targets identified in the HeLa system.

5.2.4 Cpdcd4 has no Effect on Cap-Independent Translation

In an alternative translation initiation mechanism translation can be initiated at internal ribosomal entry sites (IRES) (Vagner et al., 2001; Stoneley and Willis, 2004; Gebauer and Hentze, 2004). Originally, IRES sequences were identified in viral mRNAs and later detected in a subset of cellular mRNAs. It is thought that IRES elements permit translation of mRNAs under conditions when cap-dependent translation is inhibited. Several IRES elements containing genes were transfected into the DT40 system to study the effect of Cpdcd4 on IRES dependent translation. However, similar to cap-dependent translation it was found that the disruption of Cpdcd4 had no major effects on translation initiation mediated by IRES elements. The experiment on the effect of Hpdcd4 on IRES-dependent translation offered no consistent results between the HeLa knock-down and DT40 knock-out systems. This might be explained by an observation that the IRESs can show marked difference in the activity when transfected into different cell lines, and stimulated by different exogenous proteins (Coldwell et al., 2000; Coldwell et al., 2001). As avian and human cell lines differ in many aspects this could explain the variance in the effect of Hpdcd4 on the IRES dependent translation between the two different systems. 2D-SDS-PAGE experiments performed with DT40 WT and Cpdcd4 knock-out clones failed to identify novel targets.

5.3 Analysis of Pdcd4 in A549 Cells

In addition to the Pdcd4 knock-down and knock-out system, a Pdcd4 overexpression system was also generated by stably expressing the chicken Pdcd4 in the lung tumor cells. However, after few generations of cells in the culture, it was found that Pdcd4 was no longer overexpressed in these cells. Probably the tumor cells evolve to continuously eliminate the tumor suppressor proteins. In such case, a Pdcd4 inducible overexpression system might be used in future to study the functions of Pdcd4.

6 FUTURE PERSPECTIVES

In the future, concerning the role of Hpdcd4 on IRES-dependent translation, more apoptosis related genes having IRES elements have to be tested to confirm the effect of Pdcd4 on IRES-dependent translation of stress related genes and thereby on apoptosis. It would be interesting to find an effect of Hpdcd4 on IRES-dependent translation of a gene which is unrelated to apoptosis to prove the specificity of this effect.

Regarding the ATF-2 and c-Jun, it might be interesting to study that the enzyme by which Hpdcd4 is phosphorylating these transcription factors to further elucidate the role of Hpdcd4 in DNA-damage response.

As CK-8 is proved to be biochemically modified in the absence of Hpdcd4, it is essential to confirm the nature of the biochemical modification of CK-8 and the enzyme(s) mediating it. This might reveal the possible mechanism of tumor suppressor function of Hpdcd4 via inhibition of CK-8 biochemical modification. In addition, as CK-8 is the molecular target of Hpdcd4, the binding partner CK-18 might be also a potential target of Hpdcd4. In the future, the effect of Hpdcd4 on CK-18 should also be tested. Further, 2D-SDS-PAGE imunoblotting using a 3-10 pH range is necessary to confirm the biochemical modification of GluProRS in the absence of Hpdcd4.

The effect of Pdcd4 on CK-17 could be studied in detail at the promoter level. Besides, it would be interesting to explore the effect of Hpdcd4 on the structural element CK-17 in connection to mTOR or IFN signaling and thereby the molecular mechanisms of tumor suppressor function of Hpdcd4. Conceivably, the identity of the AKR1C2 and C3 as targets of Hpdcd4 could be confirmed by reexpression of Hpdcd4 in the knock-down clones and assessing their expression.

Furthermore, the binding of Hpdcd4 to AU rich elements (ARE) might be checked, as Hpdcd4 has been shown to have some effects already on the IRES elements present in the 5’ untranslated region (UTR). As AREs are present in the 3’ UTR of the mRNA transcripts and play roles in the stability of mRNAs, the effect of Hpdcd4 on ARE might reveal the mechanism of Hpdcd4 role in mRNA stability. The experiment on NMD has to be repeated to confirm the potential role of Hpdcd4 on NMD.

7 REFERENCES

Adhikary, S., and Eilers, M. (2005). Transcriptional regulation and transformation by Myc proteins. Nat Rev Mol Cell Biol *6*, 635-645.

Adler, V., Polotskaya, A., Kim, J., Dolan, L., Davis, R., Pincus, M., and Ronai, Z. (1996). Dose rate and mode of exposure are key factors in JNK activation by UV irradiation. Carcinogenesis *17*, 2073-2076.

Afonja, O., Juste, D., Das, S., Matsuhashi, S., and Samuels, H. H. (2004). Induction of PDCD4 tumor suppressor gene expression by RAR agonists, antiestrogen and HER-2/neu antagonist in breast cancer cells. Evidence for a role in apoptosis. Oncogene *23*, 8135-8145.

Ahlbory, D. (2005) Investigation of function of B-Myb and c-Myb in DT40 cells, University of Muenster, Muenster.
Alderson, T. (1965). Chemically induced delayed germinal mutation in Drosophila. Nature *207*, 164-167.

Alberts, B., Johnson, A., Lewis, J., Raf, M., Roberts, K., and Walter, P. (2002). Chapter 23. Cancer. In The molecular biology of THE CELL (4th Edition), (Garland Science Taylor and Francis Group), pp. 1333-1361.

Ando, S., Tokui, T., Yano, T., and Inagaki, M. (1996). Keratin 8 phosphorylation in vitro by cAMP-dependent protein kinase occurs within the amino- and carboxyl-terminal end domains. Biochem Biophys Res Commun *221*, 67-71.

Angel, P., Hattori, K., Smeal, T., and Karin, M. (1988). The jun proto-oncogene is positively autoregulated by its product, Jun/AP-1. Cell *55*, 875-885.

Appl, H., and Klempnauer, K. H. (2002). Targeted disruption of c-myb in the chicken pre B-cell line DT40. Oncogene *21*, 3076-3081.

Azzoni, L., Zatsepina, O., Abebe, B., Bennett, I. M., Kanakaraj, P., and Perussia, B. (1998). Differential transcriptional regulation of CD161 and a novel gene, 197/15a, by IL-2, IL-15, and IL-12 in NK and T cells. J Immunol *161*, 3493-3500.

Baer, M., Williams, SC., Dillner, A., Schwartz, RC., and Johnson, PF. (1998). Autocrine signals control CCAAT/enhancer binding protein beta expression, localization, and activity in macrophages. Blood *92*, 4353-65.

Baribault, H., Blouin, R., Bourgon, L., and Marceau, N. (1989). Epidermal growth factor-induced selective phosphorylation of cultured rat hepatocyte 55-kD cytokeratin before filament reorganization and DNA synthesis. J Cell Biol *109*, 1665-1676.

Bauer, C., Diesinger, I., Brass, N., Steinhart, H., Iro, H., and Meese, E. U. (2001). Translation initiation factor eIF-4G is immunogenic, overexpressed, and amplified in patients with squamous cell lung carcinoma. Cancer *92*, 822-829.

Bauman, D. R., Steckelbroeck, S., and Penning, T. M. (2004). The roles of aldo-keto reductases in steroid hormone action. Drug News Perspect *17*, 563-578.

Beck, K. (2004) The Transcription factor C/EBPbeta triggers phosphorylation of the coactivator p300 - a new mechanism of cross-talk between transcription factors and coactivators, University of Muenster, Muenster.

Bernstein, E., Caudy, A. A., Hammond, S. M., and Hannon, G. J. (2001). Role for a bidentate ribonuclease in the initiation step of RNA interference. Nature *409*, 363-366.

Berthonneau, E., and Mirande, M. (2000). A gene fusion event in the evolution of aminoacyl-tRNA synthetases. FEBS Lett *470*, 300-304.

Bhoumik, A., Takahashi, S., Breitweiser, W., Shiloh, Y., Jones, N., and Ronai, Z. (2005). ATM-dependent phosphorylation of ATF2 is required for the DNA damage response. Mol Cell *18*, 577-587.

Bitomsky, N. (2003) Inactivation of transformation suppressor gene *PDCD4* through siRNA and homologous recombination, Dissertation, University of Muenster, Muenster.

Bitomsky, N., Bohm, M., and Klempnauer, K. H. (2004). Transformation suppressor protein Pdcd4 interferes with JNK-mediated phosphorylation of c-Jun and recruitment of the coactivator p300 by c-Jun. Oncogene *23*, 7484-7493.

Boehm, M. (2005) The transformation suppressor protein Pdcd4: New realizations for teh physiological function of programmed cell death 4 protein as tumor suppressor and RNA-binding protein, University of Muenster, Muenster.

Boehm, M., Sawicka, K., Siebrasse, J. P., Brehmer-Fastnacht, A., Peters, R., and Klempnauer, K. H. (2003). The transformation suppressor protein Pdcd4 shuttles between nucleus and cytoplasm and binds RNA. Oncogene *22*, 4905-4910.

Bouck, N., Stellmach, V., and Hsu, S. C. (1996). How tumors become angiogenic. Adv Cancer Res *69*, 135-174.

Brummelkamp, T. R., Bernards, R., and Agami, R. (2002). A system for stable expression of short interfering RNAs in mammalian cells. Science *296*, 550-553.

Bryan, T. M., and Cech, T. R. (1999). Telomerase and the maintenance of chromosome ends. Curr Opin Cell Biol *11*, 318-324.

Bryan, T. M., Englezou, A., Gupta, J., Bacchetti, S., and Reddel, R. R. (1995). Telomere elongation in immortal human cells without detectable telomerase activity. Embo J *14*, 4240-4248.

Busso, N., Nicodeme, E., Chesne, C., Guillouzo, A., Belin, D., and Hyafil, F. (1994). Urokinase and type I plasminogen activator inhibitor production by normal human hepatocytes: modulation by inflammatory agents. Hepatology *20*, 186-190.

Cadrin, M., McFarlane-Anderson, N., Aasheim, L. H., Kawahara, H., Franks, D. J., Marceau, N., and French, S. W. (1992). Differential phosphorylation of CK8 and CK18 by 12-O-tetradecanoyl-phorbol-13-acetate in primary cultures of mouse hepatocytes. Cell Signal *4*, 715-722.

Cahuzac, B., Berthonneau, E., Birlirakis, N., Guittet, E., and Mirande, M. (2000). A recurrent RNA-binding domain is appended to eucaryotic aminoacyl-tRNA synthetases. Embo J *19*, 445-452.

Calkhoven, C. F., and Ab, G. (1996). Multiple steps in the regulation of transcription-factor level and activity. Biochem J *317 (Pt 2)*, 329-342.

Calkhoven, C. F., Muller, C., and Leutz A. (2000). Tranlational control of C/EBPalpha and C/EBPbeta isoforms expression. Genes Dev *14*, 1920-1932.

Carinci, F., Lo Muzio, L., Piattelli, A., Rubini, C., Chiesa, F., Ionna, F., Palmieri, A., Maiorano, E., Pastore, A., Laino, G.*, et al.* (2005). Potential markers of tongue tumor progression selected by cDNA microarray. Int J Immunopathol Pharmacol *18*, 513-524.

Carrilho, C., Alberto, M., Buane, L., and David, L. (2004). Keratins 8, 10, 13, and 17 are useful markers in the diagnosis of human cervix carcinomas. Hum Pathol *35*, 546-551.

Caudy, A. A., Myers, M., Hannon, G. J., and Hammond, S. M. (2002). Fragile X-related protein and VIG associate with the RNA interference machinery. Genes Dev *16*, 2491-2496.

Chan, R., Rossitto, P. V., Edwards, B. F., and Cardiff, R. D. (1986). Presence of proteolytically processed keratins in the culture medium of MCF-7 cells. Cancer Res *46*, 6353-6359.

Chen, Y., Knosel, T., Kristiansen, G., Pietas, A., Garber, M. E., Matsuhashi, S., Ozaki, I., and Petersen, I. (2003). Loss of PDCD4 expression in human lung cancer correlates with tumour progression and prognosis. J Pathol *200*, 640-646.

Clemens, M. J., and Bommer, U. A. (1999). Translational control: the cancer connection. Int J Biochem Cell Biol *31*, 1-23.

Cmarik, J. L., Min, H., Hegamyer, G., Zhan, S., Kulesz-Martin, M., Yoshinaga, H., Matsuhashi, S., and Colburn, N. H. (1999). Differentially expressed protein Pdcd4 inhibits tumor promoter-induced neoplastic transformation. Proc Natl Acad Sci U S A *96*, 14037-14042.

Cohen, P. (2000). The regulation of protein function by multisite phosphorylation--a 25 year update. Trends Biochem Sci *25*, 596-601.

Coldwell, M. J., deSchoolmeester, M. L., Fraser, G. A., Pickering, B. M., Packham, G., and Willis, A. E. (2001). The p36 isoform of BAG-1 is translated by internal ribosome entry following heat shock. Oncogene *20*, 4095-4100.

Coldwell, M. J., Mitchell, S. A., Stoneley, M., MacFarlane, M., and Willis, A. E. (2000). Initiation of Apaf-1 translation by internal ribosome entry. Oncogene *19*, 899-905.

Cole, M. D., and Mango, S. E. (1990). cis-acting determinants of c-myc mRNA stability. Enzyme *44*, 167-180.

Coulombe, P. A., and Omary, M. B. (2002). 'Hard' and 'soft' principles defining the structure, function and regulation of keratin intermediate filaments. Curr Opin Cell Biol *14*, 110-122.

Coulombe, P. A., Tong, X., Mazzalupo, S., Wang, Z., and Wong, P. (2004). Great promises yet to be fulfilled: defining keratin intermediate filament function in vivo. Eur J Cell Biol *83*, 735-746.

Counter, C. M., Avilion, A. A., LeFeuvre, C. E., Stewart, N. G., Greider, C. W., Harley, C. B., and Bacchetti, S. (1992). Telomere shortening associated with chromosome instability is arrested in immortal cells which express telomerase activity. Embo J *11*, 1921-1929.

De Benedetti, A., and Harris, A. L. (1999). eIF4E expression in tumors: its possible role in progression of malignancies. Int J Biochem Cell Biol *31*, 59-72.

Dencher, N. A., Goto, S., Reifschneider, N. H., Sugawa, M., and Krause, F. (2006). Unraveling age-dependent variation of the mitochondrial proteome. Ann N Y Acad Sci *1067*, 116-119.

Descombes, P., and Schibler, U. (1991). A liver-enriched transcriptional activator protein, LAP, and a transcriptional inhibitory protein, LIP, are translated from the same mRNA. Cell *67*, 569-579.

Dhar, A., Young, M. R., and Colburn, N. H. (2002). The role of AP-1, NF-kappaB and ROS/NOS in skin carcinogenesis: the JB6 model is predictive. Mol Cell Biochem *234-235*, 185-193.

Eberle, J., Krasagakis, K., and Orfanos, C. E. (1997). Translation initiation factor eIF-4A1 mRNA is consistently overexpressed in human melanoma cells in vitro. Int J Cancer *71*, 396-401.

Elbashir, S. M., Lendeckel, W., and Tuschl, T. (2001a). RNA interference is mediated by 21- and 22-nucleotide RNAs. Genes Dev *15*, 188-200.

Elbashir, S. M., Martinez, J., Patkaniowska, A., Lendeckel, W., and Tuschl, T. (2001b). Functional anatomy of siRNAs for mediating efficient RNAi in Drosophila melanogaster embryo lysate. Embo J *20*, 6877-6888.

Elbirt, K. K., and Bonkovsky, H. L. (1999). Heme oxygenase: recent advances in understanding its regulation and role. Proc Assoc Am Physicians *111*, 438-447.

Fekete, L. F., and Bick, R. L. (1976). Laboratory modalities for assessing hemostasis during cardiopulmonary bypass. Semin Thromb Hemost *3*, 83-89.

Feng, L., Zhou, X., Liao, J., and Omary, M. B. (1999). Pervanadate-mediated tyrosine phosphorylation of keratins 8 and 19 via a p38 mitogen-activated protein kinase-dependent pathway. J Cell Sci *112 (Pt 13)*, 2081-2090.

Fisher, G. J., Talwar, H. S., Lin, J., Lin, P., McPhillips, F., Wang, Z., Li, X., Wan, Y., Kang, S., and Voorhees, J. J. (1998). Retinoic acid inhibits induction of c-Jun protein by ultraviolet radiation that occurs subsequent to activation of mitogen-activated protein kinase pathways in human skin in vivo. J Clin Invest *101*, 1432-1440.

Folkman, J. (1997). Angiogenesis and angiogenesis inhibition: an overview. Exs *79*, 1-8.

Foulds, L. (1954). The experimental study of tumor progression: a review. Cancer Res *14*, 327-339.

Fuchs, S. Y., Fried, V. A., and Ronai, Z. (1998). Stress-activated kinases regulate protein stability. Oncogene *17*, 1483-1490.

Fung, K. M., Samara, E. N., Wong, C., Metwalli, A., Krlin, R., Bane, B., Liu, C. Z., Yang, J. T., Pitha, J. V., Culkin, D. J.*, et al.* (2006). Increased expression of type 2 3alpha-hydroxysteroid dehydrogenase/type 5 17beta-hydroxysteroid dehydrogenase (AKR1C3) and its relationship with androgen receptor in prostate carcinoma. Endocr Relat Cancer *13*, 169-180.

Gebauer, F., and Hentze, M. W. (2004). Molecular mechanisms of translational control. Nat Rev Mol Cell Biol *5*, 827-835.

Gerdes, M. J., Myakishev, M., Frost, N. A., Rishi, V., Moitra, J., Acharya, A., Levy, M. R., Park, S. W., Glick, A., Yuspa, S. H., and Vinson, C. (2006). Activator protein-1 activity regulates epithelial tumor cell identity. Cancer Res *66*, 7578-7588.

Gingras, A. C., Raught, B., and Sonenberg, N. (1999). eIF4 initiation factors: effectors of mRNA recruitment to ribosomes and regulators of translation. Annu Rev Biochem *68*, 913-963.

Goke, A., Goke, R., Knolle, A., Trusheim, H., Schmidt, H., Wilmen, A., Carmody, R., Goke, B., and Chen, Y. H. (2002). DUG is a novel homologue of translation initiation factor 4G that binds eIF4A. Biochem Biophys Res Commun *297*, 78-82.

Goke, R., Barth, P., Schmidt, A., Samans, B., and Lankat-Buttgereit, B. (2004b). Programmed cell death protein 4 suppresses CDK1/cdc2 via induction of p21(Waf1/Cip1). Am J Physiol Cell Physiol *287*, C1541-1546.

Goke, R., Gregel, C., Goke, A., Arnold, R., Schmidt, H., and Lankat-Buttgereit, B. (2004a). Programmed cell death protein 4 (PDCD4) acts as a tumor suppressor in neuroendocrine tumor cells. Ann N Y Acad Sci *1014*, 220-221.

Gorg, A., Obermaier, C., Boguth, G., Harder, A., Scheibe, B., Wildgruber, R., and Weiss, W. (2000). The current state of two-dimensional electrophoresis with immobilized pH gradients. Electrophoresis *21*, 1037-1053.

Green, D. R., and Reed, J. C. (1998). Mitochondria and apoptosis. Science *281*, 1309-1312.

Gronbaek, K., and Guldberg, P. (2006). [Acquired mutations--basic cancer biology]. Ugeskr Laeger *168*, 2335-2338.

Hammond, S. M., Bernstein, E., Beach, D., and Hannon, G. J. (2000). An RNA-directed nuclease mediates post-transcriptional gene silencing in Drosophila cells. Nature *404*, 293-296.

Hammond, S. M., Boettcher, S., Caudy, A. A., Kobayashi, R., and Hannon, G. J. (2001). Argonaute2, a link between genetic and biochemical analyses of RNAi. Science *293*, 1146-1150.

Hanahan, D., and Folkman, J. (1996). Patterns and emerging mechanisms of the angiogenic switch during tumorigenesis. Cell *86*, 353-364.

Hanahan, D., and Weinberg, R. A. (2000). The hallmarks of cancer. Cell *100*, 57-70.

Hanukoglu, I., and Fuchs, E. (1983). The cDNA sequence of a Type II cytoskeletal keratin reveals constant and variable structural domains among keratins. Cell *33*, 915-924.

Harris, C. C. (1996). p53 tumor suppressor gene: from the basic research laboratory to the clinic--an abridged historical perspective. Carcinogenesis *17*, 1187-1198.

Hayakawa, J., Depatie, C., Ohmichi, M., and Mercola, D. (2003). The activation of c-Jun NH2-terminal kinase (JNK) by DNA-damaging agents serves to promote drug resistance via activating transcription factor 2 (ATF2)-dependent enhanced DNA repair. J Biol Chem *278*, 20582-20592.

Hayakawa, J., Mittal, S., Wang, Y., Korkmaz, K. S., Adamson, E., English, C., Ohmichi, M., McClelland, M., and Mercola, D. (2004). Identification of promoters bound by c-Jun/ATF2 during rapid large-scale gene activation following genotoxic stress. Mol Cell *16*, 521-535.

Hayflick, L. (1997). Mortality and immortality at the cellular level. A review. Biochemistry (Mosc) *62*, 1180-1190.

He, T., Stepulak, A., Holmstrom, T. H., Omary, M. B., and Eriksson, J. E. (2002). The intermediate filament protein keratin 8 is a novel cytoplasmic substrate for c-Jun N-terminal kinase. J Biol Chem *277*, 10767-10774.

Hellen, C. U., and Sarnow, P. (2001). Internal ribosome entry sites in eucaryotic mRNA molecules. Genes Dev *15*, 1593-1612.

Henriksson, M., and Luscher, B. (1996). Proteins of the Myc network: essential regulators of cell growth and differentiation. Adv Cancer Res *68*, 109-182.

Hentze, M. W., and Kulozik, A. E. (1999). A perfect message: RNA surveillance and nonsense-mediated decay. Cell *96*, 307-310.

Herbert, T. P., Kilhams, G. R., Batty, I. H., and Proud, C. G. (2000). Distinct signalling pathways mediate insulin and phorbol ester-stimulated eucaryotic initiation factor 4F assembly and protein synthesis in HEK 293 cells. J Biol Chem *275*, 11249-11256.

Herr, I., van Dam, H., and Angel, P. (1994). Binding of promoter-associated AP-1 is not altered during induction and subsequent repression of the c-jun promoter by TPA and UV irradiation. Carcinogenesis *15*, 1105-1113.

Hirohashi, S., and Kanai, Y. (2003). Cell adhesion system and human cancer morphogenesis. Cancer Sci *94*, 575-581.

Hirst, T. R. a. D. G. (2003). Transcriptional targeting in cancer gene therapy. Journal of Biomedicine and Biotechnology *2*, 110-137.

Holcik, M., and Korneluk, R. G. (2000). Functional characterization of the X-linked inhibitor of apoptosis (XIAP) internal ribosome entry site element: role of La autoantigen in XIAP translation. Mol Cell Biol *20*, 4648-4657.

Hooker, C. W., and Hurlin, P. J. (2006). Of Myc and Mnt. J Cell Sci *119*, 208-216.

Hsu, H. Y., and Twu, Y. C. (2000). Tumor necrosis factor-alpha -mediated protein kinases in regulation of scavenger receptor and foam cell formation on macrophage. J Biol Chem *275*, 41035-41048.

Hsu, T. C., Young, M. R., Cmarik, J., and Colburn, N. H. (2000). Activator protein 1 (AP-1)- and nuclear factor kappaB (NF-kappaB)-dependent transcriptional events in carcinogenesis. Free Radic Biol Med *28*, 1338-1348.

Hunter, T., and Karin, M. (1992). The regulation of transcription by phosphorylation. Cell *70*, 375-387.

In Data for Biochemical Research, (1986), pp. 260-261.

Ishizuka, A., Siomi, M. C., and Siomi, H. (2002). A Drosophila fragile X protein interacts with components of RNAi and ribosomal proteins. Genes Dev *16*, 2497-2508.

Jansen, A. P., Camalier, C. E., and Colburn, N. H. (2005). Epidermal expression of the translation inhibitor programmed cell death 4 suppresses tumorigenesis. Cancer Res *65*, 6034-6041.

Jansen, A. P., Camalier, C. E., Stark, C., and Colburn, N. H. (2004). Characterization of programmed cell death 4 in multiple human cancers reveals a novel enhancer of drug sensitivity. Mol Cancer Ther *3*, 103-110.

Jasin, M. (2000). Chromosome breaks and genomic instability. Cancer Invest *18*, 78-86.

Jeong, E. J., Hwang, G. S., Kim, K. H., Kim, M. J., Kim, S., and Kim, K. S. (2000). Structural analysis of multifunctional peptide motifs in human bifunctional tRNA synthetase: identification of RNA-binding residues and functional implications for tandem repeats. Biochemistry *39*, 15775-15782.

Ji, Q., Chang, L., VanDenBerg, D., Stanczyk, F. Z., and Stolz, A. (2003). Selective reduction of AKR1C2 in prostate cancer and its role in DHT metabolism. Prostate *54*, 275-289.

Jiang, C. K., Flanagan, S., Ohtsuki, M., Shuai, K., Freedberg, I. M., and Blumenberg, M. (1994). Disease-activated transcription factor: allergic reactions in human skin cause nuclear translocation of STAT-91 and induce synthesis of keratin K17. Mol Cell Biol *14*, 4759-4769.

Jin, H., Kim, T. H., Hwang, S. K., Chang, S. H., Kim, H. W., Anderson, H. K., Lee, H. W., Lee, K. H., Colburn, N. H., Yang, H. S*., et al.* (2006). Aerosol delivery of urocanic acid-modified chitosan/programmed cell death 4 complex regulated apoptosis, cell cycle, and angiogenesis in lungs of K-ras null mice. Mol Cancer Ther *5*, 1041-1049.

Johannes, G., and Sarnow, P. (1998). Cap-independent polysomal association of natural mRNAs encoding c-myc, BiP, and eIF4G conferred by internal ribosome entry sites. Rna *4*, 1500-1513.

Jopling, C. L., and Willis, A. E. (2001). N-myc translation is initiated via an internal ribosome entry segment that displays enhanced activity in neuronal cells. Oncogene *20*, 2664-2670.

Jorgensen, R. (1990). Altered gene expression in plants due to trans interactions between homologous genes. Trends Biotechnol *8*, 340-344.

Jurisicova, A., Latham, K. E., Casper, R. F., and Varmuza, S. L. (1998a). Expression and regulation of genes associated with cell death during murine preimplantation embryo development. Mol Reprod Dev *51*, 243-253.

Jurisicova, A., Rogers, I., Fasciani, A., Casper, R. F., and Varmuza, S. (1998b). Effect of maternal age and conditions of fertilization on programmed cell death during murine preimplantation embryo development. Mol Hum Reprod *4*, 139-145.

Kabuyama, Y., Homma, M. K., Kurosaki, T., and Homma, Y. (2002). Early signaling events induced by 280-nm UV irradiation. Eur J Biochem *269*, 664-670.

Kang, M. J., Ahn, H. S., Lee, J. Y., Matsuhashi, S., and Park, W. Y. (2002). Up-regulation of PDCD4 in senescent human diploid fibroblasts. Biochem Biophys Res Commun *293*, 617-621.

Katz, D. A., Theodorakis, N. G., Cleveland, D. W., Lindsten, T., and Thompson, C. B. (1994). AU-A, an RNA-binding activity distinct from hnRNP A1, is selective for AUUUA repeats and shuttles between the nucleus and the cytoplasm. Nucleic Acids Res *22*, 238-246.

Kawasaki, H., Taira, K., and Yokoyama, K. (2000). Histone acetyltransferase (HAT) activity of ATF-2 is necessary for the CRE-dependent transcription. Nucleic Acids Symp Ser, 259-260.

Kim, S., Wong, P., and Coulombe, P. A. (2006). A keratin cytoskeletal protein regulates protein synthesis and epithelial cell growth. Nature *441*, 362-365.

Kinzler, K. W., and Vogelstein, B. (1996). Lessons from hereditary colorectal cancer. Cell *87*, 159-170.

Klose, J. (1975). Protein mapping by combined isoelectric focusing and electrophoresis of mouse tissues. A novel approach to testing for induced point mutations in mammals. Humangenetik *26*, 231-243.

Knapp, A. C., and Franke, W. W. (1989). Spontaneous losses of control of cytokeratin gene expression in transformed, non-epithelial human cells occurring at different levels of regulation. Cell *59*, 67-79.

Kowenz-Leutz, E., Twamley, G., Ansieau, S., and Leutz, A. (1994). Novel mechanism of C/EBP beta (NF-M) transcriptional control: activation through derepression. Genes Dev *8*, 2781-2791.

Kozak, M. (1989). Circumstances and mechanisms of inhibition of translation by secondary structure in eucaryotic mRNAs. Mol Cell Biol *9*, 5134-5142.

Kozma, S. C., and Thomas, G. (2002). Regulation of cell size in growth, development and human disease: PI3K, PKB and S6K. Bioessays *24*, 65-71.

Ku, N. O., Azhar, S., and Omary, M. B. (2002). Keratin 8 phosphorylation by p38 kinase regulates cellular keratin filament reorganization: modulation by a keratin 1-like disease causing mutation. J Biol Chem *277*, 10775-10782.

Ku, N. O., Liao, J., Chou, C. F., and Omary, M. B. (1996a). Implications of intermediate filament protein phosphorylation. Cancer Metastasis Rev *15*, 429-444.

Ku, N. O., Michie, S. A., Soetikno, R. M., Resurreccion, E. Z., Broome, R. L., Oshima, R. G., and Omary, M. B. (1996b). Susceptibility to hepatotoxicity in transgenic mice that express a dominant-negative human keratin 18 mutant. J Clin Invest *98*, 1034-1046.

Ku, N. O., and Omary, M. B. (1997). Phosphorylation of human keratin 8 in vivo at conserved head domain serine 23 and at epidermal growth factor-stimulated tail domain serine 431. J Biol Chem *272*, 7556-7564.

Ku, N. O., Zhou, X., Toivola, D. M., and Omary, M. B. (1999). The cytoskeleton of digestive epithelia in health and disease. Am J Physiol *277*, G1108-1137.

Lankat-Buttgereit, B., and Goke, R. (2003). Programmed cell death protein 4 (pdcd4): a novel target for antineoplastic therapy? Biol Cell *95*, 515-519.

Lankat-Buttgereit, B., Gregel, C., Knolle, A., Hasilik, A., Arnold, R., and Goke, R. (2004). Pdcd4 inhibits growth of tumor cells by suppression of carbonic anhydrase type II. Mol Cell Endocrinol *214*, 149-153.

Latonen, L., and Laiho, M. (2005). Cellular UV damage responses--functions of tumor suppressor p53. Biochim Biophys Acta *1755*, 71-89.

Lee, S., Bang, S., Song, K., and Lee, I. (2006). Differential expression in normal-adenoma-carcinoma sequence suggests complex molecular carcinogenesis in colon. Oncol Rep *16*, 747-754.

Levine, A. J. (1997). p53, the cellular gatekeeper for growth and division. Cell *88*, 323-331.

Lewis, J. D., and Izaurralde, E. (1997). The role of the cap structure in RNA processing and nuclear export. Eur J Biochem *247*, 461-469.

Lewis, J. S., Vijayanathan, V., Thomas, T. J., Pestell, R. G., Albanese, C., Gallo, M. A., and Thomas, T. (2005). Activation of cyclin D1 by estradiol and spermine in MCF-7 breast cancer cells: a mechanism involving the p38 MAP kinase and phosphorylation of ATF-2. Oncol Res *15*, 113-128.

Lewis, M. J., Wiebe, J. P., and Heathcote, J. G. (2004). Expression of progesterone metabolizing enzyme genes (AKR1C1, AKR1C2, AKR1C3, SRD5A1, SRD5A2) is altered in human breast carcinoma. BMC Cancer *4*, 27.

Lewis, T. S., Hunt, J. B., Aveline, L. D., Jonscher, K. R., Louie, D. F., Yeh, J. M., Nahreini, T. S., Resing, K. A., and Ahn, N. G. (2000). Identification of novel MAP kinase pathway signaling targets by functional proteomics and mass spectrometry. Mol Cell *6*, 1343-1354.

Li, L., Sampat, K., Hu, N., Zakari, J., and Yuspa, S. H. (2006). Protein kinase C negatively regulates Akt activity and modifies UVC-induced apoptosis in mouse keratinocytes. J Biol Chem *281*, 3237-3243.

Liao, J., Ku, N. O., and Omary, M. B. (1997). Stress, apoptosis, and mitosis induce phosphorylation of human keratin 8 at Ser-73 in tissues and cultured cells. J Biol Chem *272*, 17565-17573.
Liu, J., and Levens, D. (2006). Making myc. Curr Top Microbiol Immunol *302*, 1-32.

Livingstone, C., Patel, G., and Jones, N. (1995). ATF-2 contains a phosphorylation-dependent transcriptional activation domain. Embo J *14*, 1785-1797.

Ma, G., Guo, K. J., Zhang, H., Ozaki, I., Matsuhashi, S., Zheng, X. Y., and Dong, M. (2005). [Expression of programmed cell death 4 and its clinicopathological significance in human pancreatic cancer]. Zhongguo Yi Xue Ke Xue Yuan Xue Bao *27*, 597-600.

Macleod, K. (2000). Tumor suppressor genes. Curr Opin Genet Dev *10*, 81-93.

Mahadevan, D., Dimento, J., Croce, K. D., Riley, C., George, B., Fuchs, D., Mathews, T., Wilson, C., and Lobell, M. (2006). Transcriptosome and serum cytokine profiling of an atypical case of myelodysplastic syndrome with progression to acute myelogenous leukemia. Am J Hematol *81*, 779-786.

Mann, M., Hendrickson, R. C., and Pandey, A. (2001). Analysis of proteins and proteomes by mass spectrometry. Annu Rev Biochem *70*, 437-473.

Meyer, S., Temme, C., and Wahle, E. (2004). Messenger RNA turnover in eucaryotes: pathways and enzymes. Crit Rev Biochem Mol Biol *39*, 197-216.

Miethe, J., Schwartz, C., Wottrich, K., Wenning, D., and Klempnauer, K. H. (2001). Crosstalk between Myc and activating transcription factor 2 (ATF2): Myc prolongs the half-life and induces phosphorylation of ATF2. Oncogene *20*, 8116-8124.

Mignone, F., Gissi, C., Liuni, S., and Pesole, G. (2002). Untranslated regions of mRNAs. Genome Biol *3*, REVIEWS0004.

Mink, S., Kerber, U. and Klempnauer, K. H. (1996). Interaction of v-Myb is required for synergistic activation fo the mim-1 gene. Mol Cell Biol *16*, 1316-1325.

Mink, S., Haenig, B., and Klempnauer, K. H. (1997). Interaction and functional collaboration of p300 and C/EBPbeta. Mol Cell Biol *17*, 6609-6617.

Mitchell, S. A., Brown, E. C., Coldwell, M. J., Jackson, R. J., and Willis, A. E. (2001). Protein factor requirements of the Apaf-1 internal ribosome entry segment: roles of polypyrimidine tract binding protein and upstream of N-ras. Mol Cell Biol *21*, 3364-3374.

Modesti, M., and Kanaar, R. (2001). Homologous recombination: from model organisms to human disease. Genome Biol *2*, REVIEWS1014.

Moll, R., and Franke, W. W. (1982b). Intermediate filaments and their interaction with membranes. The desmosome-cytokeratin filament complex and epithelial differentiation. Pathol Res Pract *175*, 146-161.

Moll, R., Franke, W. W., Schiller, D. L., Geiger, B., and Krepler, R. (1982a). The catalog of human cytokeratins: patterns of expression in normal epithelia, tumors and cultured cells. Cell *31*, 11-24.

Nagle, R. B., McDaniel, K. M., Clark, V. A., and Payne, C. M. (1983). The use of antikeratin antibodies in the diagnosis of human neoplasms. Am J Clin Pathol *79*, 458-466.

Nanbru, C., Lafon, I., Audigier, S., Gensac, M. C., Vagner, S., Huez, G., and Prats, A. C. (1997). Alternative translation of the proto-oncogene c-myc by an internal ribosome entry site. J Biol Chem *272*, 32061-32066.

Nanbru, C., Prats, A. C., Droogmans, L., Defrance, P., Huez, G., and Kruys, V. (2001). Translation of the human c-myc P0 tricistronic mRNA involves two independent internal ribosome entry sites. Oncogene *20*, 4270-4280.

Neu-Yilik, G., Gehring, N. H., Thermann, R., Frede, U., Hentze, M. W., and Kulozik, A. E. (2001). Splicing and 3' end formation in the definition of nonsense-mediated decay-competent human beta-globin mRNPs. Embo J *20*, 532-540.

Nevins, T. A., Harder, Z. M., Korneluk, R. G., and Holcik, M. (2003). Distinct regulation of internal ribosome entry site-mediated translation following cellular stress is mediated by apoptotic fragments of eIF4G translation initiation factor family members eIF4GI and p97/DAP5/NAT1. J Biol Chem *278*, 3572-3579.

Norcum, M. T., and Dignam, J. D. (1999). Immunoelectron microscopic localization of glutamyl-/ prolyl-tRNA synthetase within the eucaryotic multisynthetase complex. J Biol Chem *274*, 12205-12208.

Nowell, P. C. (1976). The clonal evolution of tumor cell populations. Science *194*, 23-28.

Nykanen, A., Haley, B., and Zamore, P. D. (2001). ATP requirements and small interfering RNA structure in the RNA interference pathway. Cell *107*, 309-321.

O'Farrell, P. H. (1975). High resolution two-dimensional electrophoresis of proteins. J Biol Chem *250*, 4007-4021.

Omary, M. B., Ku, N. O., Liao, J., and Price, D. (1998). Keratin modifications and solubility properties in epithelial cells and in vitro. Subcell Biochem *31*, 105-140.

Onishi, Y., Hashimoto, S., and Kizaki, H. (1998). Cloning of the TIS gene suppressed by topoisomerase inhibitors. Gene *215*, 453-459.

Orphanides, G., and Reinberg, D. (2002). A unified theory of gene expression. Cell *108*, 439-451.

Oshima, R. G. (1982). Developmental expression of murine extra-embryonic endodermal cytoskeletal proteins. J Biol Chem *257*, 3414-3421.

Ossipow, V., Descombes, P., and Schibler, U. (1993). CCAAT/enhancer-binding protein mRNA is translated into multiple proteins with different transcription activation potentials. Proc Natl Acad Sci U S A *90*, 8219-8223.

Palamarchuk, A., Efanov, A., Maximov, V., Aqeilan, R. I., Croce, C. M., and Pekarsky, Y. (2005). Akt phosphorylates and regulates Pdcd4 tumor suppressor protein. Cancer Res *65*, 11282-11286.

Papassava, P., Gorgoulis, V. G., Papaevangeliou, D., Vlahopoulos, S., van Dam, H., and Zoumpourlis, V. (2004). Overexpression of activating transcription factor-2 is required for tumor growth and progression in mouse skin tumors. Cancer Res *64*, 8573-8584.

Penning, T. M., Steckelbroeck, S., Bauman, D. R., Miller, M. W., Jin, Y., Peehl, D. M., Fung, K. M., and Lin, H. K. (2006). Aldo-keto reductase (AKR) 1C3: role in prostate disease and the development of specific inhibitors. Mol Cell Endocrinol *248*, 182-191.

Ponting, C. P. (2000). Novel eIF4G domain homologues linking mRNA translation with nonsense-mediated mRNA decay. Trends Biochem Sci *25*, 423-426.

Ponzielli, R., Katz, S., Barsyte-Lovejoy, D., and Penn, L. Z. (2005). Cancer therapeutics: targeting the dark side of Myc. Eur J Cancer *41*, 2485-2501.

Potapova, O., Basu, S., Mercola, D., and Holbrook, N. J. (2001). Protective role for c-Jun in the cellular response to DNA damage. J Biol Chem *276*, 28546-28553.

Potapova, O., Haghighi, A., Bost, F., Liu, C., Birrer, M. J., Gjerset, R., and Mercola, D. (1997). The Jun kinase/stress-activated protein kinase pathway functions to regulate DNA repair and inhibition of the pathway sensitizes tumor cells to cisplatin. J Biol Chem *272*, 14041-14044.

Powell, D. J., Hajduch, E., Kular, G., and Hundal, H. S. (2003). Ceramide disables 3-phosphoinositide binding to the pleckstrin homology domain of protein kinase B (PKB)/Akt by a PKCzeta-dependent mechanism. Mol Cell Biol *23*, 7794-7808.

Prendergast, G. C. (1999). Mechanisms of apoptosis by c-Myc. Oncogene *18*, 2967-2987.

Pyronnet, S., Pradayrol, L., and Sonenberg, N. (2000). A cell cycle-dependent internal ribosome entry site. Mol Cell *5*, 607-616.
Quon, K. C., and Berns, A. (2001). Haplo-insufficiency? Let me count the ways. Genes Dev *15*, 2917-2921.

Rajagopalan, L. E., and Malter, J. S. (1997). Regulation of eucaryotic messenger RNA turnover. Prog Nucleic Acid Res Mol Biol *56*, 257-286.

Ramaswamy, N. T., Ronai, Z., and Pelling, J. C. (1998). Rapid activation of JNK1 in UV-B irradiated epidermal keratinocytes. Oncogene *16*, 1501-1505.

Raught, B., Liao, W. S., and Rosen, J. M. (1995). Developmentally and hormonally regulated CCAAT/enhancer-binding protein isoforms influence beta-casein gene expression. Mol Endocrinol *9*, 1223-1232.

Ricote, M., Garcia-Tunon, I., Bethencourt, F., Fraile, B., Onsurbe, P., Paniagua, R., and Royuela, M. (2006). The p38 transduction pathway in prostatic neoplasia. J Pathol *208*, 401-407.

Ridge, K. M., Linz, L., Flitney, F. W., Kuczmarski, E. R., Chou, Y. H., Omary, M. B., Sznajder, J. I., and Goldman, R. D. (2005). Keratin 8 phosphorylation by protein kinase C delta regulates shear stress-mediated disassembly of keratin intermediate filaments in alveolar epithelial cells. J Biol Chem *280*, 30400-30405.

Rizner, T. L., Smuc, T., Rupreht, R., Sinkovec, J., and Penning, T. M. (2006). AKR1C1 and AKR1C3 may determine progesterone and estrogen ratios in endometrial cancer. Mol Cell Endocrinol *248*, 126-135.

Ross, J. (1995). mRNA stability in mammalian cells. Microbiol Rev *59*, 423-450.

Saini, K. S., Summerhayes, I. C., and Thomas, P. (1990). Molecular events regulating messenger RNA stability in eucaryotes. Mol Cell Biochem *96*, 15-23.

Salonen, T., Jarvela, I., Peltonen, L., and Jalanko, A. (2000). Detection of eight novel palmitoyl protein thioesterase (PPT) mutations underlying infantile neuronal ceroid lipofuscinosis (INCL;CLN1). Hum Mutat *15*, 273-279.

Sampath, P., Mazumder, B., Seshadri, V., Gerber, C. A., Chavatte, L., Kinter, M., Ting, S. M., Dignam, J. D., Kim, S., Driscoll, D. M., and Fox, P. L. (2004). Noncanonical function of glutamyl-prolyl-tRNA synthetase: gene-specific silencing of translation. Cell *119*, 195-208.

Schlichter, U., Burk, O., Worpenberg, S., and Klempnauer, K. H. (2001a). The chicken Pdcd4 gene is regulated by v-Myb. Oncogene *20*, 231-239.

Schlichter, U., Kattmann, D., Appl, H., Miethe, J., Brehmer-Fastnacht, A., and Klempnauer, K. H. (2001b). Identification of the myb-inducible promoter of the chicken Pdcd4 gene. Biochim Biophys Acta *1520*, 99-104.

Shatkin, A. J. (1976). Capping of eucaryotic mRNAs. Cell *9*, 645-653.

Shay, J. W. (1997). Telomerase in human development and cancer. J Cell Physiol *173*, 266-270.
Sherr, C. J. (1995). D-type cyclins. Trends Biochem Sci *20*, 187-190.

Sherr, C. J. (2004). Principles of tumor suppression. Cell *116*, 235-246.

Shibahara, K., Asano, M., Ishida, Y., Aoki, T., Koike, T., and Honjo, T. (1995). Isolation of a novel mouse gene MA-3 that is induced upon programmed cell death. Gene *166*, 297-301.

Shim, J., Lim, H., R Yates, J., and Karin, M. (2002). Nuclear export of NF90 is required for interleukin-2 mRNA stabilization. Mol Cell *10*, 1331-1344.

Simmons, H. M., Ruis, B. L., Kapoor, M., Hudacek, A. W., and Conklin, K. F. (2005). Identification of NOM1, a nucleolar, eIF4A binding protein encoded within the chromosome 7q36 breakpoint region targeted in cases of pediatric acute myeloid leukemia. Gene *347*, 137-145.

Smith, L., Dahler, A. L., Cavanagh, L. L., Popa, C., Barnes, L. M., Serewko-Auret, M. M., Fai Wong, C., and Saunders, N. A. (2004). Modulation of proliferation-specific and differentiation-specific markers in human keratinocytes by SMAD7. Exp Cell Res *294*, 356-365.

Society, A. C. (2005). Oncogenes and tumor suppressor genes.

Soejima, H., Miyoshi, O., Yoshinaga, H., Masaki, Z., Ozaki, I., Kajiwara, S., Niikawa, N., Matsuhashi, S., and Mukai, T. (1999). Assignment of the programmed cell death 4 gene (PDCD4) to human chromosome band 10q24 by in situ hybridization. Cytogenet Cell Genet *87*, 113-114.

Sporn, M. B. (1996). The war on cancer. Lancet *347*, 1377-1381.

Spriggs, K. A., Bushell, M., Mitchell, S. A., and Willis, A. E. (2005). Internal ribosome entry segment-mediated translation during apoptosis: the role of IRES-trans-acting factors. Cell Death Differ *12*, 585-591.

Stalberg, P., Lopez-Egido, J. R., Wang, S., Gobl, A., Oberg, K., and Skogseid, B. (2001). Differentially expressed cDNAs in PLCbeta3-induced tumor suppression in a human endocrine pancreatic tumor cell line: activation of the human mismatch repair protein 3 gene. Biochem Biophys Res Commun *281*, 227-231.

Stalberg, P., Wang, S., Larsson, C., Weber, G., Oberg, K., Gobl, A., and Skogseid, B. (1999). Suppression of the neoplastic phenotype by transfection of phospholipase C beta 3 to neuroendocrine tumor cells. FEBS Lett *450*, 210-216.

Steinert, P. M. (1988). The dynamic phosphorylation of the human intermediate filament keratin 1 chain. J Biol Chem *263*, 13333-13339.

Stoneley, M., Chappell, S. A., Jopling, C. L., Dickens, M., MacFarlane, M., and Willis, A. E. (2000a). c-Myc protein synthesis is initiated from the internal ribosome entry segment during apoptosis. Mol Cell Biol *20*, 1162-1169.

Stoneley, M., Paulin, F. E., Le Quesne, J. P., Chappell, S. A., and Willis, A. E. (1998). C-Myc 5' untranslated region contains an internal ribosome entry segment. Oncogene *16*, 423-428.

Stoneley, M., Spencer, J. P., and Wright, S. C. (2001). An internal ribosome entry segment in the 5' untranslated region of the mnt gene. Oncogene *20*, 893-897.

Stoneley, M., Subkhankulova, T., Le Quesne, J. P., Coldwell, M. J., Jopling, C. L., Belsham, G. J., and Willis, A. E. (2000b). Analysis of the c-myc IRES; a potential role for cell-type specific trans-acting factors and the nuclear compartment. Nucleic Acids Res *28*, 687-694.

Stoneley, M., and Willis, A. E. (2004). Cellular internal ribosome entry segments: structures, trans-acting factors and regulation of gene expression. Oncogene *23*, 3200-3207.

Subkhankulova, T., Mitchell, S. A., and Willis, A. E. (2001). Internal ribosome entry segment-mediated initiation of c-Myc protein synthesis following genotoxic stress. Biochem J *359*, 183-192.

Sui, G., Soohoo, C., Affar, E. B., Gay, F., Shi, Y., Forrester, W. C., and Shi, Y. (2002). A DNA vector-based RNAi technology to suppress gene expression in mammalian cells 10.1073/pnas.082117599. PNAS *99*, 5515-5520.

Tamaoki, T., Nomoto, H., Takahashi, I., Kato, Y., Morimoto, M., and Tomita, F. (1986). Staurosporine, a potent inhibitor of phospholipid/Ca++dependent protein kinase. Biochem Biophys Res Commun *135*, 397-402.

Thornberry, N. A., and Lazebnik, Y. (1998). Caspases: enemies within. Science *281*, 1312-1316.

Ting, S. M., and Dignam, J. D. (1994). Post-transcriptional regulation of glutamyl-prolyl-tRNA synthetase in rat salivary gland. J Biol Chem *269*, 8993-8998.

Troyanovsky, S. M., Leube, R. E., and Franke, W. W. (1992). Characterization of the human gene encoding cytokeratin 17 and its expression pattern. Eur J Cell Biol *59*, 127-137.

Tsigelny, I., Burton, D. W., Sharikov, Y., Hastings, R. H., and Deftos, L. J. (2005). Coherent expression chromosome cluster analysis reveals differential regulatory functions of amino-terminal and distal parathyroid hormone-related protein domains in prostate carcinoma. J Biomed Biotechnol *2005*, 353-363.

Ueda, K., and Komano, T. (1984). Sequence-specific DNA damage induced by reduced mitomycin C and 7-N-(p-hydroxyphenyl)mitomycin C. Nucleic Acids Res *12*, 6673-6683.

Vagner, S., Galy, B., and Pyronnet, S. (2001). Irresistible IRES. Attracting the translation machinery to internal ribosome entry sites. EMBO Rep *2*, 893-898.

van Dam, H., Wilhelm, D., Herr, I., Steffen, A., Herrlich, P., and Angel, P. (1995). ATF-2 is preferentially activated by stress-activated protein kinases to mediate c-jun induction in response to genotoxic agents. Embo J *14*, 1798-1811.

van de Wetering, M., Oving, I., Muncan, V., Pon Fong, M. T., Brantjes, H., van Leenen, D., Holstege, FC., Brummelkamp, TR., Agami, R., and Clevers, H. (2003) Specific inhibition of gene expression using a stably integrated, inducible small-interfering-RNA vector. EMBO Rep. *4*, 609-615.

Wang, S. Y., Iordanov, M., and Zhang, Q. (2006). c-Jun NH2-terminal kinase promotes apoptosis by down-regulating the transcriptional co-repressor CtBP. J Biol Chem (in press).

Wasinger, V. C., Cordwell, S. J., Cerpa-Poljak, A., Yan, J. X., Gooley, A. A., Wilkins, M. R., Duncan, M. W., Harris, R., Williams, K. L., and Humphery-Smith, I. (1995). Progress with gene-product mapping of the Mollicutes: Mycoplasma genitalium. Electrophoresis *16*, 1090-1094.

Waters, L. C., Bohm, M., Veverka, V., Muskett, F. W., Frenkiel, T. A., Kelly, G. P., Prescott, A., Dosanjh, N. S., Klempnauer, K. H., and Carr, M. D. (2006). NMR Assignment and Secondary Structure Determination of the C-terminal MA-3 Domain of the Tumour Suppressor Protein Pdcd4. J Biomol NMR (in press).

Welham, N. V., Marriott, G., and Bless, D. M. (2006). Proteomic profiling of rat thyroarytenoid muscle. J Speech Lang Hear Res *49*, 671-685.

Welm, A. L., Kim, S., Welm, B. E., and Bishop, J. M. (2005). MET and MYC cooperate in mammary tumorigenesis. Proc Natl Acad Sci U S A *102*, 4324-4329.

WHO (2006). WHO Cancer Control Programme.

Williams, K. L., and Hochstrasser, D. F. (1997). Introduction to the proteome. In Proteome Research: New Frontiers in Functional Genomics, In (Berlin: Springer-Verlag), pp. 1-12.

Wilm, M., Shevchenko, A., Houthaeve, T., Breit, S., Schweigerer, L., Fotsis, T., and Mann, M. (1996). Femtomole sequencing of proteins from polyacrylamide gels by nano-electrospray mass spectrometry. Nature *379*, 466-469.

Wisdom, R., and Lee, W. (1991). The protein-coding region of c-myc mRNA contains a sequence that specifies rapid mRNA turnover and induction by protein synthesis inhibitors. Genes Dev *5*, 232-243.

Wyllie, A. H., Kerr, J. F., and Currie, A. R. (1980). Cell death: the significance of apoptosis. Int Rev Cytol *68*, 251-306.

Xu, N., Chen, C. Y., and Shyu, A. B. (1997). Modulation of the fate of cytoplasmic mRNA by AU-rich elements: key sequence features controlling mRNA deadenylation and decay. Mol Cell Biol *17*, 4611-4621.

Yan, J. X., Tonella, L., Sanchez, J. C., Wilkins, M. R., Packer, N. H., Gooley, A. A., Hochstrasser, D. F., and Williams, K. L. (1997). The Dictyostelium discoideum proteome--the SWISS-2DPAGE database of the multicellular aggregate (slug). Electrophoresis *18*, 491-497.

Yang, H. S., Cho, M. H., Zakowicz, H., Hegamyer, G., Sonenberg, N., and Colburn, N. H. (2004). A novel function of the MA-3 domains in transformation and translation suppressor Pdcd4 is essential for its binding to eucaryotic translation initiation factor 4A. Mol Cell Biol *24*, 3894-3906.

Yang, H. S., Jansen, A. P., Komar, A. A., Zheng, X., Merrick, W. C., Costes, S., Lockett, S. J., Sonenberg, N., and Colburn, N. H. (2003b). The transformation suppressor Pdcd4 is a novel eucaryotic translation initiation factor 4A binding protein that inhibits translation. Mol Cell Biol *23*, 26-37.

Yang, H. S., Jansen, A. P., Nair, R., Shibahara, K., Verma, A. K., Cmarik, J. L., and Colburn, N. H. (2001). A novel transformation suppressor, Pdcd4, inhibits AP-1 transactivation but not NF-kappaB or ODC transactivation. Oncogene *20*, 669-676.

Yang, H. S., Knies, J. L., Stark, C., and Colburn, N. H. (2003a). Pdcd4 suppresses tumor phenotype in JB6 cells by inhibiting AP-1 transactivation. Oncogene *22*, 3712-3720.

Yang, H. S., Matthews, C. P., Clair, T., Wang, Q., Baker, A. R., Li, C. C., Tan, T. H., and Colburn, N. H. (2006). Tumorigenesis suppressor Pdcd4 down-regulates mitogen-activated protein kinase kinase kinase kinase 1 expression to suppress colon carcinoma cell invasion. Mol Cell Biol *26*, 1297-1306.
Yang, Y. (2003). Tumor suppressor gene database.

Yano, T., Tokui, T., Nishi, Y., Nishizawa, K., Shibata, M., Kikuchi, K., Tsuiki, S., Yamauchi, T., and Inagaki, M. (1991). Phosphorylation of keratin intermediate filaments by protein kinase C, by calmodulin-dependent protein kinase and by cAMP-dependent protein kinase. Eur J Biochem *197*, 281-290.

Yoshinaga, H., Matsuhashi, S., Fujiyama, C., and Masaki, Z. (1999). Novel human PDCD4 (H731) gene expressed in proliferative cells is expressed in the small duct epithelial cells of the breast as revealed by an anti-H731 antibody. Pathol Int *49*, 1067-1077.

Young, M. R., Yang, H. S., and Colburn, N. H. (2003). Promising molecular targets for cancer prevention: AP-1, NF-kappa B and Pdcd4. Trends Mol Med *9*, 36-41.

Zakowicz, H., Yang, H. S., Stark, C., Wlodawer, A., Laronde-Leblanc, N., and Colburn, N. H. (2005). Mutational analysis of the DEAD-box RNA helicase eIF4AII characterizes its interaction with transformation suppressor Pdcd4 and eIF4GI. Rna *11*, 261-274.

Zhang, H., Ozaki, I., Mizuta, T., Hamajima, H., Yasutake, T., Eguchi, Y., Ideguchi, H., Yamamoto, K., and Matsuhashi, S. (2006a). Involvement of programmed cell death 4 in transforming growth factor-beta1-induced apoptosis in human hepatocellular carcinoma. Oncogene *25*, 6101-6112.

Zhang, Y., Ohyashiki, J. H., Takaku, T., Shimizu, N., and Ohyashiki, K. (2006b). Transcriptional profiling of Epstein-Barr virus (EBV) genes and host cellular genes in nasal NK/T-cell lymphoma and chronic active EBV infection. Br J Cancer *94*, 599-608.

Zhang, Z., and DuBois, R. N. (2001). Detection of differentially expressed genes in human colon carcinoma cells treated with a selective COX-2 inhibitor. Oncogene *20*, 4450-4456.

The Websites

1) http://www.ncbi.nlm.nih.gov/

2) http://www.oligoengine.com/

3) http://www.who.int/cancer/en/

8 APPENDIX

8.1 Clone Charts

The following constructs have been made during the work

Clone Chart	pbl-pdcd4-targetPuronew
Description	Eucaryotic expression vector codes for the targeting construct directed against chicken Pdcd4
Size	~ 10.3 Kb
Vector	~3.0 Kb
Insert	~7.3 Kb
Promoter	--
Resistance	Puromycin, expressed under β-actin promoter
Construction	This vector derived from the pbl-pdcd4-targetPuro vector (Bitomsky, 2003). The right arm (600 bp) of the targeting construct was replaced by a 2.2 Kb fragment derived from the exon 7-9 of the chicken Pdcd4. For this purpose, first the pUC18#141 was made by cloning the 2.2 Kb fragment (from *KpnI/XbaI* digest of the vector p15-1.6x/#141) into the same sites of pUC18 vector. The 2.2 Kb fragment of *KpnI/SalI* digest (from pUC18#141 vector) was cloned into the *KpnI/XhoI* sites of pbl-pdcd4-targetPuro vector by replacing the 600 bp right arm.

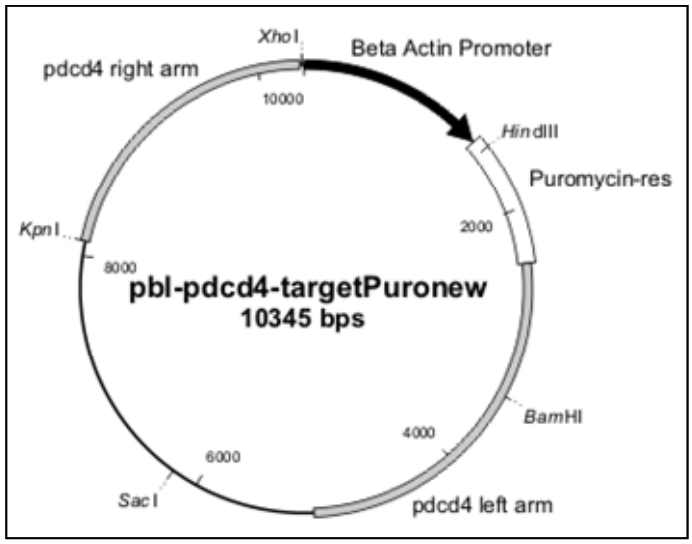

Clone Chart	pCR2.1-TOPO-Hpdcd4-HA
Description	T/A cloning vector
Size	~5.4 Kb
Vector	~3.9 Kb
Insert	~1.5 Kb
Promoter	--
Resistance	Ampicillin and kanamycin
Construction	Total RNA was isolated from HTB-133 cells and human Pdcd4 (Hpdcd4) was amplified by using designed HPdcd4 cloning primers (human_pdcd4_cp_for and human_pdcd4_cp_rev). The primers insert *BamHI* site and KOZAK in the 5' end and HA tag followed by *XhoI* site in the 3' end). This PCR fragment (~1.5 Kb) was cloned into the pCR2.1-TOPO cloning vector (I*nvitrogen*) by T/A cloning protocol. The positive clones (clone2 and clone5) were sequenced using M13 reverse and T7 primers. The clone 2 and 5 are cut with *HindIII* and the middle fragment was subcloned into the pCR2.1-TOPO vector again and sequenced using the same primers from both the sides. The clone5 codes for the full length Hpdcd4-HA tagged.

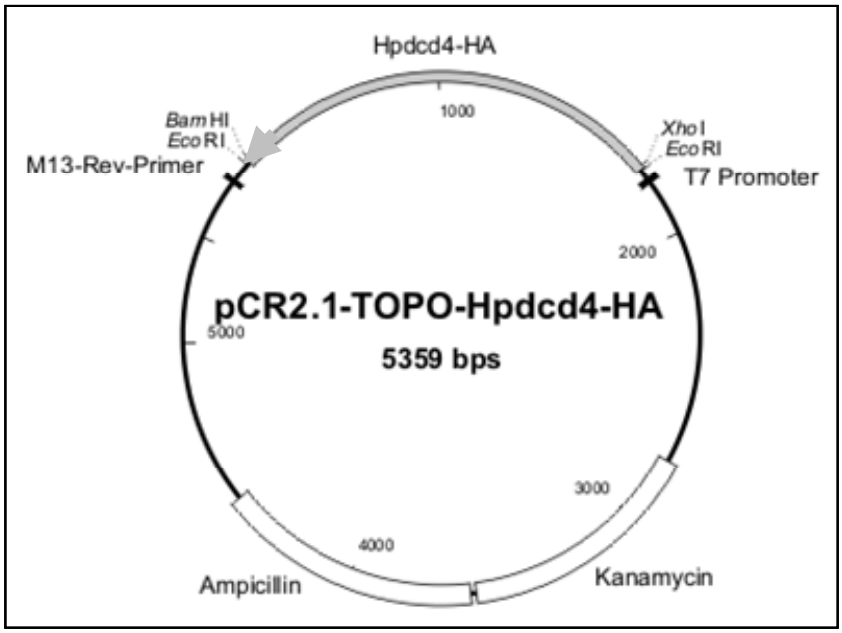

Clone Chart	pcDNA3-Hpdcd4-HA
Description	Eucaryotic expression vector codes for the human Pdcd4-HA
Size	~6.9 Kb
Vector	~5.4 Kb
Insert	~1.5 Kb
Promoter	CMV
Resistance	Ampicillin and neomycin
Construction	The pCR2.1-TOPO-Hpdcd4-HA construct, codes for the correct Hpdcd4-HA tagged sequence was double digested with *BamHI/XhoI* and cloned into the same restriction sites of pcDNA3 (*Invitrogen*).

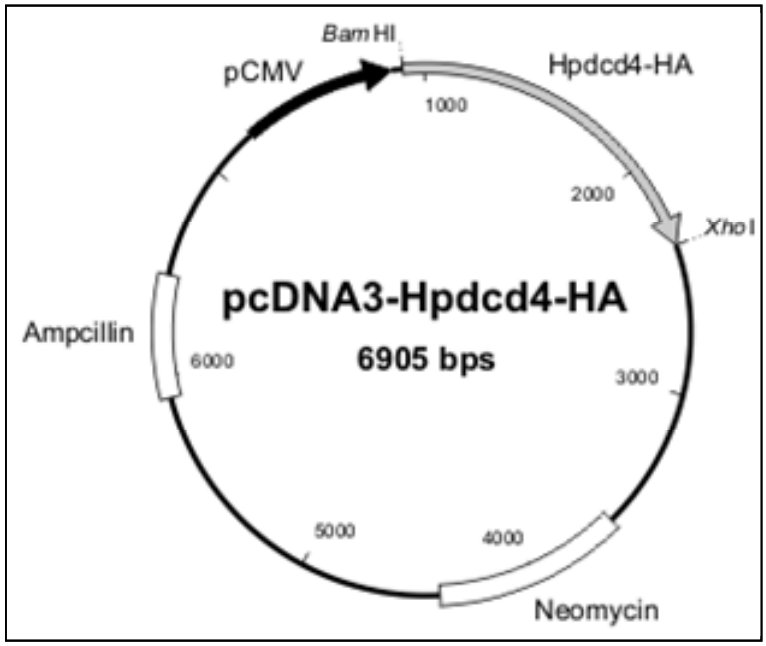

Clone Chart	pcDNA4-Hpdcd4-HA
Description	Eucaryotic expression vector code for the human Pdcd4-HA
Size	~6.6 Kb
Vector	~5.1 Kb
Insert	~1.5 Kb
Promoter	CMV-Tetracycline Operator
Resistance	Ampicillin and zeocin
Construction	The pCR2.1-TOPO-Hpdcd4-HA construct, codes for the correct Hpdcd4-HA tagged sequence was double digested with *BamH1/XhoI* and cloned into the same restriction sites of pcDNA4/TO/*myc*-His (*Invitrogen*).

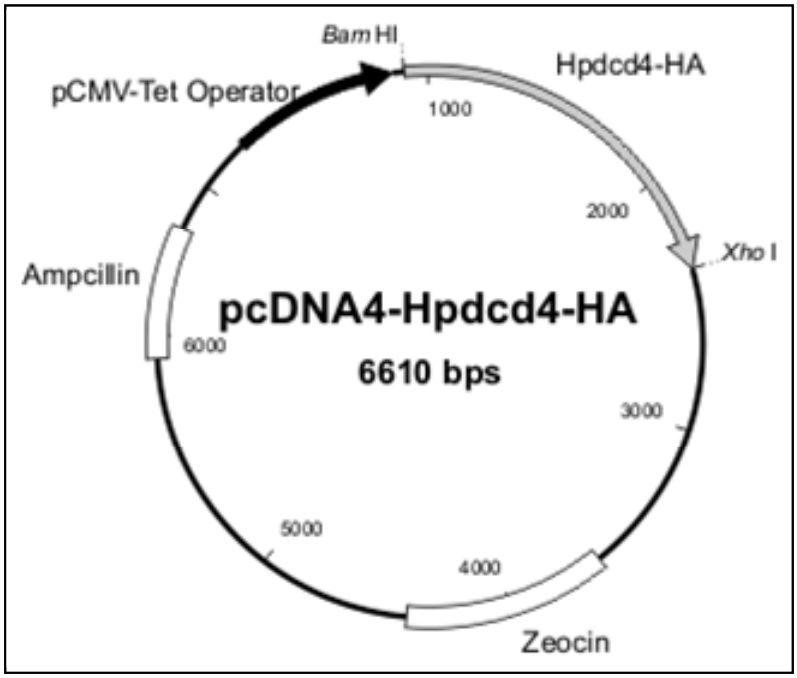

Clone Chart	Utrless-pSG5-C/EBPβ
Description	Eucaryotic expression vector code for the C/EBPβ without upstream region
Size	~5.1 Kb
Vector	~4.1 Kb
Insert	~1.0 Kb
Promoter	SV40
Resistance	Ampicillin
Construction	For cloning the utrless C/EBPβ into the pSG5 vector, the *EcoRI/NarI* fragment (425 bp) from pcDNA3-CCR vector and the *NarI/BamHI* fragment (712 bp) from pSG5-NFM#16.3 vector were cloned into the *EcoRI/BamHI* fragment (~4.1 Kb) from the pSG5-NFM#16.3 construct (*Stratagene*).

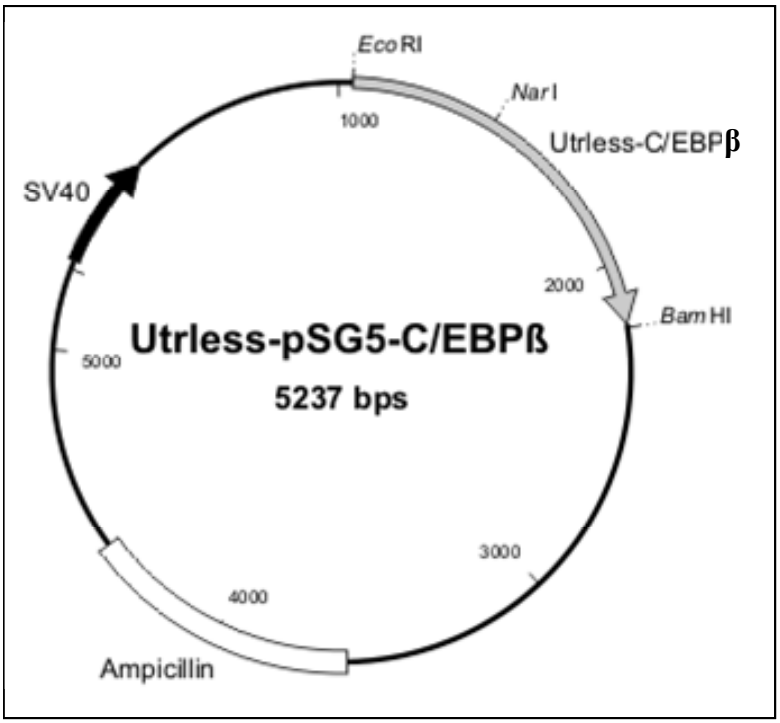

Clone Chart	pTER+-siRNA A
Description	Eucaryotic expression vector codes for the siRNA A directed against Hpdcd4 mRNA at position 603
Size	~5.3 Kb
Vector	~5.3 Kb
Insert	~60 bp
Promoter	Modified H1 promoter (Inserted with tetracycline operator region)
Resistance	Ampicillin and zeocin
Construction	The siRNA oligos (siRNAhumpdcd4_603s and siRNAhumpdcd4_603as) were annealed and cloned into the *BamH1/HindIII* restriction sites of the pTER+ vector (van de Watering et al., 2003). Later the sequence was confirmed by sequencing, using BGH reverse primer.

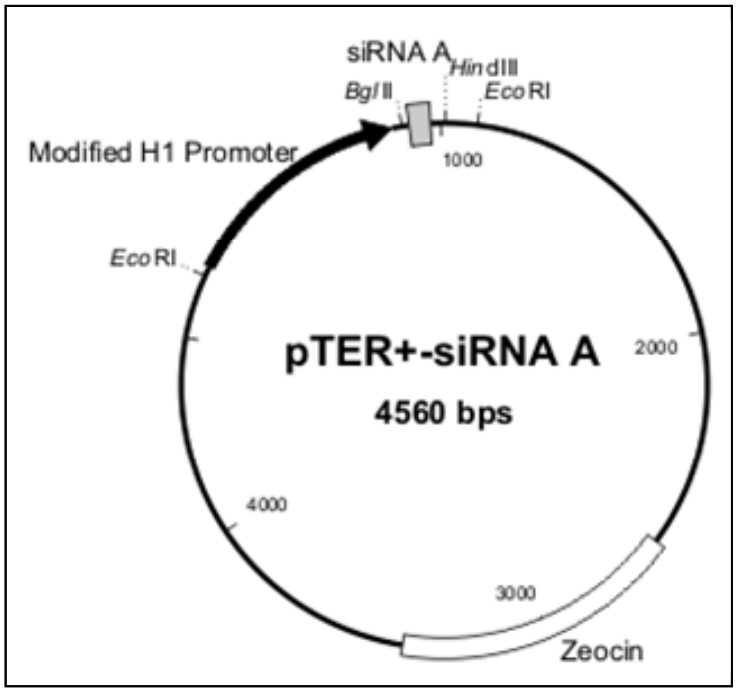

Clone Chart	pTER+-siRNA B
Description	Eucaryotic expression vector codes for siRNA B directed against Hpdcd4 at position 1260
Size	~5.3 Kb
Vector	~5.3 Kb
Insert	~60 bp
Promoter	Modified H1 promoter (Inserted with tetracycline operator region)
Resistance	Ampicillin and Zeocin
Construction	The siRNA oligos (siRNAhumpdcd4_1260s and siRNAhumpdcd4_1260as) were annealed and cloned into the *BamH1/HindIII* restriction sites of the pTER+ vector (van de Watering et al., 2003). Later the sequence was confirmed by sequencing, using BGH reverse primer.

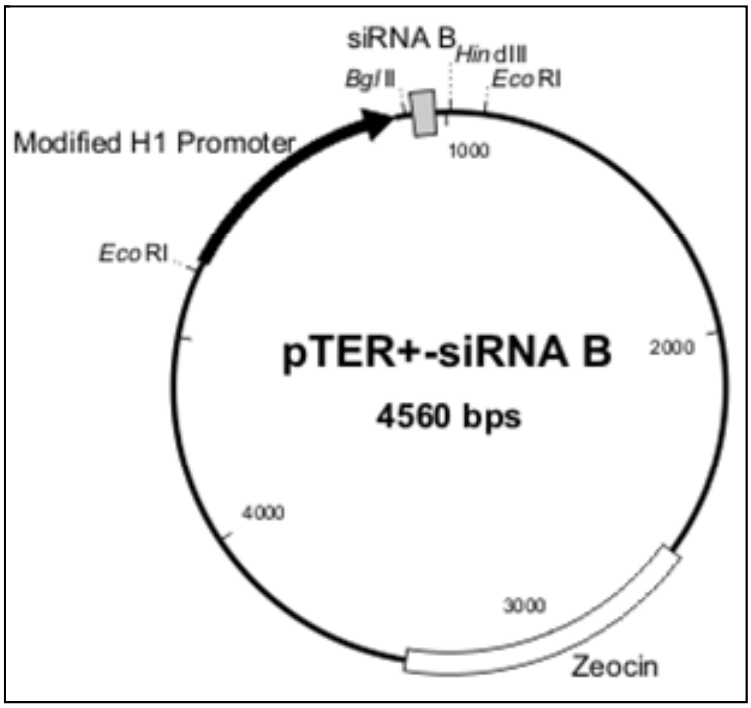

Clone Chart	pUC18#141
Description	A cloning vector has the ~2.2 Kb fragment of the chicken Pdcd4 exonss 7-9
Size	~4.9 Kb
Vector	~2.7 Kb
Insert	~2.2 Kb
Promoter	*LacZ* Promoter
Resistance	Ampicillin
Construction	The *KpnI/SalI* restricted fragment (~2.2 Kb) from the p15-1.6x vector was cloned into the *KpnI/XbaI* sites of the pUC18 vector (~2.7) to construct the pUC18#141 construct.

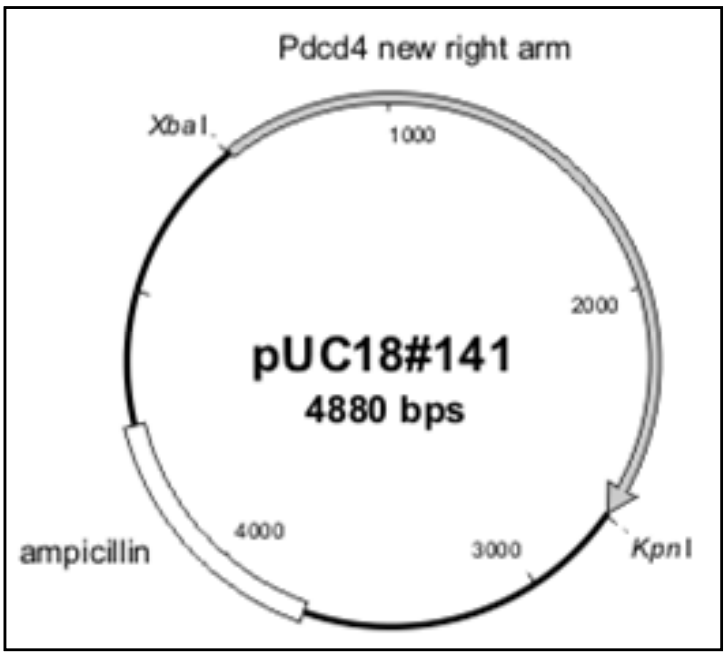

8.2 Sequence

The sequence of the human Pdcd4 in the pCR2.1-TOPO clone5 and the restriction map are given below.

The Sequence

```
   1  gaattcgccc ttctggatcc gccacaatgg atgtagttta tgagcatgag
  51  cagatactga atgtaaaccc tgcagatcct gataacttaa gtgactctct
 101  cttttccggt gatgaagaaa atgctgggac tgaggaagta aagaatgaaa
 151  taaatggaaa ttggatttca gcatactcca ttaacgaagc tagaattaat
 201  gccaaggcaa aaaggcgact aaggaaaaac tcatcccggg actctggcag
 251  aggcgattcg gtcagcgaca gtgggagtga cgcccttaga agtggattaa
 301  ctgtgccaac cagtccaaag ggaaggttgc tggataggcg atccagatct
 351  gggaaaggaa ggggactacc aaagaaaggt ggtgcaggag gcaaaggtgt
 401  ctggggtaca cctggacagg tgtatgatgt ggaggaggtg gatgtgaaag
 451  atcctaacta tgatgatgac caggagaact gtgtttatga aactgtagtt
 501  ttgcctttgg atgaaagggc atttgagaag actttaacac caatcataca
 551  ggaatatttt gagcatggag atactaatga agttgcggaa atgttaagag
 601  atttaaatct tggtgaaatg aaaagtggag taccagtgtt ggcagtatcc
 651  ttagcattgg aggggaaggc tagtcataga gagatgacat ctaagcttct
 701  ttctgacctt tgtgggacag taatgagcac aactgatgtg gaaaaatcat
 751  ttgataaatt gttgaaagat ctacctgaat tagcactgga tactcctaga
 801  gcaccacagt tggtgggcca gtttattgct agagctgttg gagatggaat
 851  tttatgtaat acctatattg atagttacaa aggaactgta gattgtgtgc
 901  aggctagagc tgctctggat aaggctaccg tgcttctgag tatgtctaaa
 951  ggtggaaagc gtaaagatag tgtgtggggc tctggaggtg ggcagcaatc
1001  tgtcaatcac cttgttaaag agattgatat gctgctgaaa gaatatttac
1051  tctctggaga catatctgaa gctgaacatt gccttaagga actggaagta
1101  cctcattttc accatgagct tgtatatgaa gctattataa tggttttaga
1151  gtcaactgga gaaagtacat ttaagatgat tttggattta ttaaagtccc
1201  tttggaagtc ttctaccatt actgtagacc aaatgaaaag aggttatgag
1251  agaatttaca atgaaattcc ggacattaat ctggatgtcc cacattcata
1301  ctctgtgctg gagcggtttg tagaagaatg ttttcaggct ggaataattt
1351  ccaaacaact cagagatctt tgtccttcaa ggggcagaaa gcgttttgta
1401  agcgaaggag atggaggtcg tcttaaacca gagagctact acccctacga
1451  cgtgcccgac tacgcctaac tcgaggaaag ggcgaattc
```

The Restriction Map

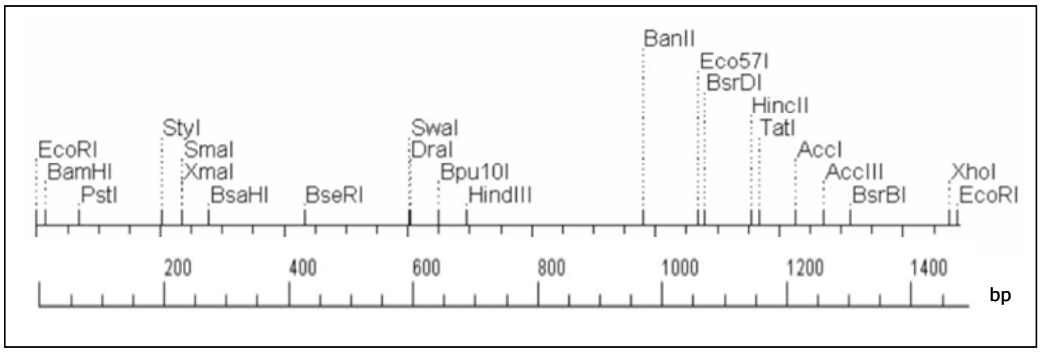

8.3 Zusammenfassung

Krebs ist eine der Haupttodesursachen beim Menschen und seine Bekämpfung ist seit Jahrzehnten eine große Herausforderung. Krebs ist eine Krankheit, die dynamische Veränderungen im Genom hervorruft. Dabei wird das Genom der Zellen ständig an verschiedenen Stellen verändert. Zwei Arten von Genen sind während der Tumorentwicklung entscheidend involviert, die Onkogene und die Tumorsuppressorgene.
Das Pdcd4-Gen („Programmed Cell Death 4") ist ein neues Tumorsupressorgen, das ursprünglich als ein Gen identifiziert wurde, das während der Apoptose aktiviert wird. Es konnte gezeigt werden, dass Pdcd4 die durch den Tumorpromotor TPA induzierte Transformation von Keratinozyten unterdrückt. Da Pdcd4 mit dem eucaryontischen Translations-Initiationsfaktor eIF4A interagiert, wurde vermutet, dass Pdcd4 in der Regulation der Translation von einigen, bisher unbekannten Proteinen involviert sein könnte. Das Fehlen eines gut charakterisierten Zellsystems jedoch erschwerte bis jetzt die Analyse der molekularen Funktionen von Pdcd4.

Um die molekularen Funktionen des Pdcd4 Tumorsuppressorgens durch einen reversen genetischen Versuchsansatz studieren zu können, wurde ein Knock-Down-System entwickelt. Das System wurde unter Verwendung der RNAi Technologie hergestellt, bei der siRNA gegen das humane Pdcd4-Gen (Hpdcd4) in Hela-Zellen eingesetzt wurden. Zur Analyse des Pdcd4-Einflusses auf die Cap-unabhängige Translation und der möglichen Funktion als Regulator des Zellwachstums/ Zelltodes, wurden Luciferase-Reportergenanalysen durchgeführt. Diese Luciferase-Doppelkonstrukte enthielten interne Ribosomen-Eintrittstellen (IRES) von unterschiedlichen Genen, die am Zellwachstum, der Zellzykluskontrolle und an der Apoptose beteiligt sind. Die Ergebnisse zeigten, dass Pdcd4 unter normalen physiologischen Bedingungen inhibierend auf einige IRES-Elemente wirkten.

Durch 1D-SDS-PAGE-Analyse konnte gezeigt werden, dass die Expression einiger Transkriptionsfaktoren durch Hpdcd4 beeinflusst wird. Während die Expression von c-Myc in der Abwesenheit von Hpdcd4 niedriger war als in seiner Anwesenheit, wurden für c-Jun und C/EBPβ höhere Expressionen registriert. Weiterhin zeigten die Hpdcd4-Knock-Down-Zellen eine geringere Phosphorylierung von ATF-2 und c-Jun als die HeLa-Wildtypzellen. Um neue molekulare Ziele von Hpdcd4 in seiner Gesamtheit zu identifizieren, wurde eine Proteom-Analyse der HeLa-Wildtypzellen und der Hpdcd4-Knock-Down-Zellen mittels 2D-SDS-PAGE und anschließender Massenspektroskopie durchgeführt. Hierbei konnten einige neue Zielproteine von Hpdcd4 ermittelt werden.

In der Abwesenheit von Hpdcd4 wurde sowohl Cytokeratin 17 (CK 17) als auch C2 und C3 überexprimiert, die zur Familie der Aldo-Keton-Reduktase 1 (AKR1) gehören. Zusätzlich scheinen Cytokeratin 8 (CK 8) und die Glutamyl-Prolyl-Bifunktionale tRNA Synthetase (GluProRS) im Gegensatz zu den HeLa-Wildtypzellen in den Pdcd4-Knock-Down-Zellen biochemisch modifiziert zu sein. Die differentielle Expression dieser Zielproteine wurde durch 1D/2D-SDS-PAGE mit anschließendem Immunoblotting unter Verwendung von spezifischen Antikörpern bestätigt. Die Überexpression von CK 17 und die biochemische Modifikation von CK 8 in der Abwesenheit von Hpdcd4 waren reproduzierbar. Die Identität von AKR1-C2 und von -C3 sowie GluProRS als mögliche Ziele von HPdcd4 muß in weiteren Versuchen festgestellt werden.

Es wurde auch untersucht, ob Hpdcd4 einen Effekt auf die mRNA-Menge von CK 17, c-Myc und c-Jun hat. Das mRNA-Expressions-Niveau dieser Gene war mit der jeweiligen Proteinexpression vergleichbar; außer bei c-Jun. Weiterhin wurde analysiert, ob Hpdcd4 die Transkription oder die Stabilität der mRNA-Transkripte beeinflusst. Um den Effekt von Hpdcd4 auf den Turn-Over der CK 17- und der c-Myc-mRNA zu analysieren, wurden die Zellen mit dem Transkriptionsinhibitor Aktinomycin D behandelt und die mRNA-Menge mittels Northern-Blot in einer zeitabhängigen Weise detektiert. Es scheint, dass Hpdcd4 die Degradation der CK 17- und c-Myc-mRNA-Transkripte erhöht. Zusätzlich scheint es, dass Hpdcd4 in Nonsense-vermittelten mRNA-Abbau (NMD) involviert ist.

Neben dem HeLa-Knock-Down-System wurde auch ein Knock-Out-System in der Hühner B-Zell-Linie DT40 entwickelt, in der beide funktionierende Kopien des Pdcd4-Gens durch homologe Rekombination entfernt wurden. Es zeigte sich, dass die Hühner-Pdcd4-Knock-Out-Zellen lebensfähig waren und mit der gleichen Teilungszeit wie DT40-Wildtypzellen wachsen. Es konnte jedoch kein Unterschied bezüglich der gesamten Rate der Proteinsynthese zwischen den Knock-Out-Zellen und den Wildtypzellen festgestellt werden. Diese beiden Systeme könnten weiterhin einen wesentlichen Beitrag zur Klärung der molekularen Funktionen des Tumorsuppressor Pdcd4 leisten. Auch die weitere Analyse der hier identifizierten molekularen Zielproteine von Pdcd4 werden zum besseren Verständnis seiner Funktion beitragen.

LEBENSLAUF

Persönliche Daten

Name	Rajeshwari Marikkannu
Geburtsdatum	5. April 1976
Familienstand	Ledig
Eltern	Frau Mahalakshmi Marikkannu
	Herr Marikkannu Muthuswamy

Schulausbildung

1980 - 86	Grundschule, Eriyodu, Tamil Nadu, Indien
1986 - 91	Government High School, Gymnasium
	Board of High School Examination, Tamil Nadu, Indien
	Annamalaiyar Girls Higher Secondary School, Gymnasium
	Board of Higher Secondary Examination, Tamil Nadu, Indien

Studium

1994 - 98	Bachelor of Pharmacy
	Tamil Nadu The Dr. M.G.R. Medical University, Tamil Nadu, Indien
1998 - 99	Master of Science in Pharmacy (Biotechnology)
	National Institute of Pharmaceutical Education & Research (NIPER), Punjab, Indien

Dissertation

Seit Okt 2003	Institut für Biochemie der WWU, Münster, Deutschland
	Betreuer: Prof. Dr. Karl-Heinz Klempnauer

Berufserfahrung

Mai 2002 - Sep 03	Wissenschaftliche Angestellte, Madurai Kamaraj University, Madurai, Indien. Betreuer: Prof. Dr. S. Krishnaswamy
Jun 2001 - Mai 02	Advanced Diploma in Bioinformatics, Madurai Kamaraj University, Madurai, Indien. Betreuer: Prof. Dr. P. Palanivelu
Apr 2000 - Mär 01	Wissenschaftliche Angestellte, National Institute of Immunology, New Delhi, Indien. Betreuer: Prof. Dr. Chandrima Shaha
Feb 2000 - Apr 00	Dozentin, Sri Ramachandra Medical College & Research Institute (SRMC & RI), Chennai, Indien
Mai 1997 - Jun 97	Industriepraktikum, Pharmafabrikon, Madurai, Indien

Stipendien

Okt 2003 - Sep 06	Stipendium der International NRW Graduate School of Chemistry, Münster, Deutschland

BIO-DATA

Personal Details

Name	Rajeshwari Marikkannu
Date of Birth	5th April 1976
Marital Status	Single
Parents	Mrs. Mahalakshmi Marikkannu
	Mr. Marikkannu Muthuswamy

School

1980 - 86	Primary School, Eriyodu, Tamil Nadu, India
1986 - 91	Government High School, SSLC
	Board of High School Examination, Tamil Nadu, India
1991-93	Annamalaiyar Girls Higher Secondary School, HSc Academic
	Board of Higher Secondary Examination, Tamil Nadu, India

Graduation

1994 - 98	Bachelor of Pharmacy
	Tamil Nadu The Dr.M.G.R. Medical University, Tamil Nadu, India
1998 - 99	Master of Science in Pharmacy (Biotechnology)
	National Institute of Pharmaceutical Education & Research (NIPER), Punjab, India

Dissertation

Since Oct 2003	Institute of Biochemistry, University of Muenster, Muenster, Deutschland Adviser: Prof. Dr. Karl-Heinz Klempnauer

Activities

May 2002 - Sep 03	Research Assistant, Madurai Kamaraj University, Madurai, India Advisor: Prof. Dr. Sankaran Krishnaswamy
Jun 2001 - May 02	Advanced Diploma in Bioinformatics , Madurai Kamaraj University, Madurai, India Advisor: Porf. Dr. P. Palanivelu
Apr 2000 - Mar 01	Research Assistant, National Institute of Immunology, New Delhi, India Advisor: Prof. Dr. Chandrima Shaha
Feb 2000 - Apr 00	Lecturer, Sri Ramachandra Medical College & Research Institute (SRMC & RI), Tamil Nadu, India
May 1997 - Jun 97	Pharmaceutical Industrial Training, Pharmafabrikon, Madurai, Tamil Nadu, India

Stipend

Oct 2003 - Sep 06	Stipend from the International NRW Graduate School of Chemistry, Muenster, Deutschland

ACKNOWLEDGEMENT

Although a pharmacist working on molecular biology was a daunting undertaking, it is greatly facilitated and succeeded by constructive and stimulatory criticisms from Prof. Dr. Karl-Heinz Klempnauer during these three years. I gained the molecular biology sense here. Visualizing 10µg of DNA by naked eyes started in Room No 107. I express my gratitude to him ever.

I would like to thank Prof. Dr. Hans-Joachim Galla for reviewing my dissertation and writing the report and Prof. Dr. Hellmut Eckert for being a member of my PhD review and examination committee. I would like to express my additional thanks to the International Graduate School of Chemistry for the professional and financial support and many scientific and cultural opportunities provided during my PhD study.

My thanks are addressed to Anne Brehmer-Fastnacht and Bianca Michaelis for their professional help in the laboratory and Nadja Bitomsky for aiding me in learning the techniques initially.

I acknowledge Dr. Detlaf Lang and and Dr. Simone Koenig for availing us the FACS facility and the proteomic facility, respectively. I am grateful to Prof. Dr. Horst Bürger for their generous offerering of the CK-8/18 antibody.

I thank the members of the research group of Prof KHK for their friendliness and cooperation in our laboratory: Anke Brüggemann, Annette Plachetka, Benjamin Hirschi, Carola Wilczek, Carolin Nordhoff, Dörthe Ahlbory, Daniel Kammer, Heike Most, Holger Gundelach, Jörg Kintscher, Kirsten Schulte, Monika Dzuganova, Olesya Chayka, Olga Ivanova, Sonia Chachara, Thorsten Bartusel, Thore Schmedt, and all the other colleagues including Poonam Balani and the official staffs from the institute of biochemistry.

I am grateful to Prof KHK, Mr. Vinaykumar Kontham and the following colleagues for their critical reading, extensive suggestion and stimulatory discussion of my thesis: Dr. Nils Wethkamp, Dr. Stephan Schubert and Dr. Tuyen Tran.

The 4Ms (Me, Marc, Marius and the Movie club) for their elegant company during the leisure time in Muenster and the movies followed by thoughtful discussion. Andrea for taking me out and Nuray for making our trip dreams come true.

Dr. Radha Banhatti and her family for their support during my stay in Muenster.

My batchmates Mr Dnyaneshwar Gawas, Mr Surajit Jana, Mr Saroj Kumar Panda, Mr Geo Paul and Mr Sebastian C. Peter for their finest coordination and friendship. I thank all the other members, including indians of the GSC-MS.

To my friends, Annalakshmi Subramanian, Manikandan Ramalingam, Mohammed Hareef, Senthilkumar Shanmugam and all my other friends.

To My teacher Mr. Nagendran Nagarajan and his family for their love and support.

I wish to honor my mother, brothers, sister, and Vinay by dedicating my every, the most precious feelings, which I preserved and cherished in my heart and mind, to them. Everything is possible only because of them including you read th(es)is.